# IDENTIFICATION OF SYNERGISTIC DRUG COMBINATIONS AGAINST CYSTIC FIBROSIS PATHOGENS

A Dissertation

by

QINGQUAN CHEN

Submitted to the Office of Graduate and Professional Studies of
Texas A&M University
in partial fulfillment of the requirements for the degree of

DOCTOR OF PHILOSOPHY

| | |
|---|---|
| Chair of Committee, | Carolyn L. Cannon |
| Committee Members, | Helene Andrews-Polymenis |
| | Jeffrey Cirillo |
| | Richard Gomer |
| | Thomas Meek |
| Head of Department, | Warren Zimmer |

August 2019

Major Subject: Medical Science

# ABSTRACT

Cystic fibrosis (CF) is a common, fatal, genetic disease caused by mutations in the cystic fibrosis transmembrane conductance regulator (CFTR) gene. CF has many clinical manifestations. The most important site of disease is the lung, where often colonized or infected in infancy or early childhood with microorganisms. The chronic bacterial infections, often with *Pseudomonas aeruginosa*, and concomitant airway inflammation damage the lung and lead to respiratory failure. The chronic use of multiple antibiotics increases the possibility of multidrug resistant (MDR) bacteria, and limits the treatment options. Therefore, there is a need to identify alternative antimicrobial strategies to optimize treatment of infections. Studies have demonstrated that synergy results in superior antimicrobial activity, while avoiding potential side-effects of both therapeutics. Hence, we hypothesize that by using drug combinations with an efficient delivery system, we could achieve improved antimicrobial efficacy against MDR bacteria.

Studies have demonstrated that high-dose ibuprofen (peak serum concentrations of 50-100 μg/mL) can improve the outcomes in CF patients. This beneficial effect has been attributed to the anti-inflammatory properties of ibuprofen. Our group demonstrated that high-dose ibuprofen has antimicrobial activity both *in vitro* and *in vivo*. Despite silver has been used as a antimicrobial agent with a low incidence of resistance, poor availability mandates a high dosage to effectively eradicate infections.

A silver carbene complex, SCC1, was conjugated with ibuprofen, SCC1-IBU. Compared with SCC1, SCC1-IBU demonstrated improved antimicrobial activity against CF pathogens while preserving the anti-inflammatory activity of ibuprofen. Then, checkerboard assays and end-point

colony forming unit (CFU) assays demonstrated synergistic combination of silver/minocycline against *P. aeruginosa* isolates. Furthermore, the synergistic combination can be co-loaded into nanoparticles as a next-generation antibiotic to combat MDR bacteria.

Lastly, disc diffusion assay demonstrated that FDA approved antibiotics have a significant increased zone of inhibition in the presence of ibuprofen. In a 24-hour endpoint CFU assay, amikacin, aztreonam and ceftazidime demonstrated synergy in combination with either ibuprofen or naproxen. Finally, mice treated with ceftazidime/ibuprofen demonstrated a significant survival advantage compared to the individually treated groups. Thus, therapy with high-dose ibuprofen in combination with antibiotics may improve outcomes in patients infected with MDR bacteria.

ACKNOWLEDGEMENTS

To my committee chair Dr. Cannon, and my committee members, Dr. Andrews-Polymenis, Dr. Cirillo, Dr. Gomer, and Dr. Meek, thank you for your guidance and assistant throughout my Ph.D program at Texas A&M. Special appreciation and thanks to Dr. Cannon, thank you for taking me on as your graduate student when I was at a crossroads during my graduate school. You have been a tremendous mentor to me, thanks for encouraging and challenging me during my research as well as giving me the flexibility that allowed me to explore science. Without the direction and support from my committee every step along the way, I would never have made it this far.

To my fellow colleagues and former colleagues, thank you for assistance and friendship. Special thanks to Dr. Parth Shah and Dr. Kush Shah for all the guidance and support; Bhagath Chirra and Sabona Simbassa for all the help during my mouse experiments; Marleni Illanga, Jeremiah Alexander, and Chelsea Ebert for all the assistance to complete the work in a speedy way.

To my family, words cannot express my gratitude. Thank you for your encouragement and support in all my pursuits. To my parents, it was always you who believed in me. I am grateful for your continuous and unparalleal love, help, and support. To my friends, thanks for your support and encouragement.

Last, to my beloved wife, Season (Yicheng Xie), this journey would never have been possible without you. Thank you for making this journey fun and joyful. Thank you for all of the support and love throughout ups and downs.

## CONTRIBUTORS AND FUNDING SOURCES

This work was supported by a dissertation committee consisting of Drs. Carolyn Cannon (chair), Helene Andrews-Polymenis, Jeffrey Cirillo of the Department of Microbioal Pathogenesis and Immunology, Dr. Richard Gomer of the Department of Biology, and Dr. Thomas Meek of the Department of Biochemistry.

SCC1-IBU used in this research was synthesized and characterized by Dr. Matthew Panzer in Dr. Wiley Young's laboratory in University of Akron. SCKs nanoparticles used in this research were provided and characterized by Dr. Fuwu Zhang in Dr. Karen Wooley's laboratory in Texas A&M University. Murine experiments were supported by the Texas A&M University comparative medical program.

Graduate research was financially supported by Texas A&M University of Health Science Center and Men of Distinction.

TABLE OF CONTENTS

Page

LIST OF FIGURES

Page

LIST OF TABLES

Page

# CHAPTER I

# INTRODUCTION AND LITERATURE REVIEW

## Cystic Fibrosis Is Genetic Disease

Cystic fibrosis is a common fatal genetic disease, predominantly occuring in Caucasians. An autosomal recessive disease, it is caused by mutations in the cystic fibrosis transmembrane conductance regulator (CFTR) gene. More than 2,000 mutations in the CFTR gene have been identified, with an incidence of clinical disease of 1 in 2,500 live births in the Caucasian population (1). The wild type CFTR gene encodes a cyclic AMP-regulated chloride ion transporter CFTR channel (2) that usually resides at the apical surface of many epithelial cell types. The CFTR protein is a member of ATP binding cassette (ABC) family of transporters. The CFTR contains highly conserved motifs in the ABC family, including two membrane-spanning domains that have six membrane-spanning peptides, and two nucleotide binding domains (NBDs) responsible for ATP binding and hydrolysis to supply energy for opening and closing the ion channel. The function of the CFTR channel is to export chloride ions, followed by Na+ and water, from inside of epithelial cells to the outside of the cell. The ability of epithelial cells to release fluid relies on the energy provided by the ubiquitous, basolaterally located Na+/K+-ATPase. The Na+/K+-ATPase maintains a low intracellular concentration of Na+. This low Na+ concentration, coupled with negative transmembrane potential, drives the passive diffusion of Na+ into the cell, as well as the energetically unfavorable intracellular accumulation of Cl-, through a basolaterally located Na+/K+/2Cl- cotransporter. When the CFTR opens, Cl- exits down its electrochemical gradient. Na+ ions follow through a paracellular pathway, and water follows the salt due to the resulting osmotic gradient (3). CFTR mutations can be classified into six different categories: 1. no CFTR protein production; 2. CFTR protein fails to reach the apical membrane due to defective

processing; 3. CFTR channel fails to open in response to cyclic adenosine monophosphate; 4. CFTR channel has a reduced conductance; 5. splicing inefficiency reduces CFTR protein synthesis; and 6. CFTR protein has less stability at the apical membrane (4; 5).

The defective epithelial transport of Na+, Cl- and fluid secretion results in the many clinical manifestations of CF (6; 7). The decreased fluid flow from the pancreatic acinar cells results in plugging of the pancreatic ducts that further leads to destruction of the exocrine pancreas. In older patients, the destruction of the pancrease leads to an increasing incidence of diabetes mellitus. About 5-10% of patients with CF present as neonates with a gastrointestinal blockage known as meconium ileus caused by accumulation of fecal material. In infants and children, the decrease in pancreatic enzyme production results in malabsorption, especially of fats and proteins. Abnormal fluid secretion that reduces the airway surface fluid and impairs the activity of the mucociliary escalator, contributes to the cardinal respiratory features of CF, such as pansinusitis. Dehydration, particularly during the summer months, caused by loss of sodium may result in hyponatremic dehydration and metabolic alkalosis due to electrolyte losses in sweat.

However, the most important site of disease is the lung. The normal lung airway surface has a thin layer of fluid to maintain mucociliary movement. With poorly functional mutated CFTR, the impaired secretion of fluid to the lung epithelial surface results in dehydration of lung airway surface. The decreased volume of periciliary fluid in the lower respiratory tract interferes with mucociliary clearance of inhaled microorganisms (2). The impaired periciliary movement results in mucus accumulation, leading to chronic lung infections. About 80-95% of patients with CF succumb to respiratory failure caused by chronic bacterial infection and concomitant airway inflammation (8). The infections in the respiratory tract incite secrection of pro-inflammatory cytokines, early recruitment of inflammatory cells, including polymorphonuclear leukocytes

(PMNs), and eventual production of antibodies (9-11). If not treated, most CF patients die at a young age due to airway infections. In 1974, the international median age at death for CF was 8 years old (12). Intensive treatment with antibiotics has extended the median expected lifetime dramatically. In 2017, the predicted median survival age has increased to 43.6 years old compared to the median survival age of 32.7 years old in 2002 (12).

**Common Microorganisms Result in Infections in CF Patients**

The respiratory tract in CF patients is a complex and diverse ecosystem where multispecies communities coexist (13). The majority of studies of CF-associated lung infections have focused on *Pseudomonas aeruginosa*, *Staphylococcus aureus*, *Haemophilus influenzae*, and on the *Burkholderia cepacia* complex species group (14). Lungs of CF patients are often colonized or infected in infancy or early childhood with microorganisms, such as *Staphylococcus aureus* and *Haemophilus influenzae*. The early bacterial infections damage the lung epithelial surfaces, leading to increasing attachment of, and eventual replacement by *Pseudomonas aeruginosa* (15) (**Figure 1**).

***Staphylococcus aureus***

*Staphylococcus aureus* are Gram-positive bacteria that are commonly found on the skin, hair, as well as in the nose and throat of healthy people. *S. aureus* is a member of the Micrococcaceae family with an appearance of gold pigmentation of colonies and positive coagulase, mannitol-fermentation, and deoxyribonuclease tests (16). *S. aureus* appear in coccoid clusters upon microscopic examination. Thirty to fifty percent of healthy adults are colonized with *S. aureus*, and ten to twenty percent of individuals are persistently colonized (17; 18). *S. aureus* is a facultative anaerobes. *S. aureus* is a notorious and opportunistic pathogen causing a wide range

of diseases, including bacteremia, pneumonia, cellulitis, osteomyelitis and skin/soft tissue infections (16).

**Figure 1. Prevalence of respiratory microogranisms isolated from cystic fibrosis patients by age cohort.**

(MDR-PA: multi-drug resistant *Pseudomonas aeruginosa*; MRSA: methecillin resistant *staphylococcus aureus*; Data modified from Cystic Fibrosis Patient Registry, 2017)

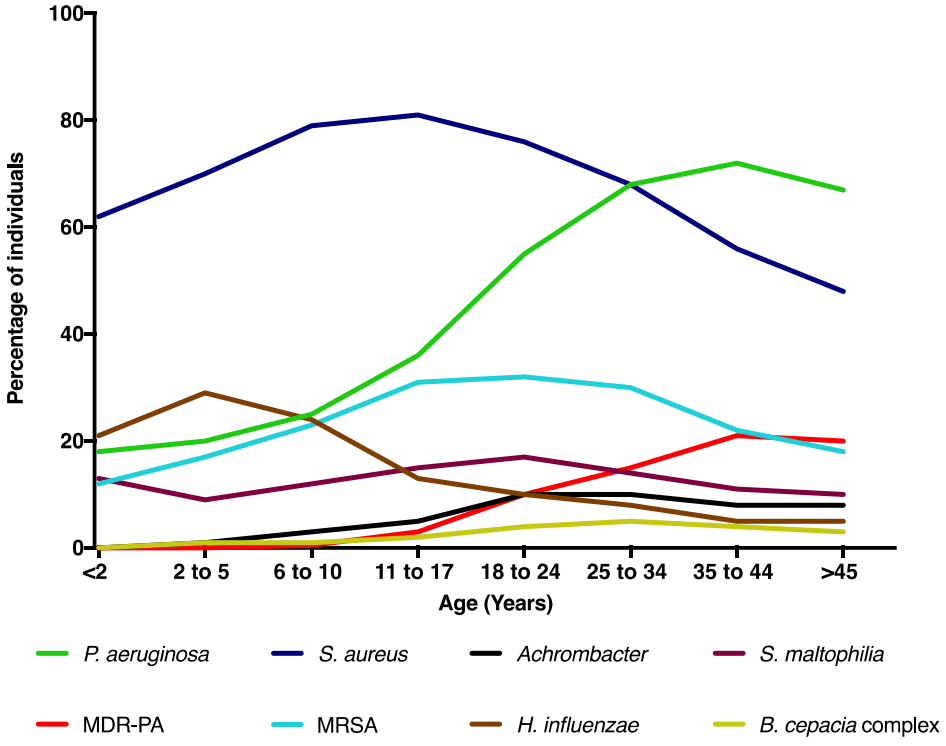


In addition, *S. aureus* is well known for its ability to acquire antibiotic resistance. Since 1960, about eighty percent of all *S. aureus* isolates have been resistant to penicillin (19). Shortly after introduction of methicillin, the first case of *S. aureus* resistant to methicillin was reported in 1961 (20). Although the first reported case of methicillin-resistant *S. aureus* (MRSA) was in 1961,

studies have suggested that *S. aureus* harbored *mecA*, a gene that encodes an alternative penicillian-binding protein resulting in drug resistance, prior to the introduction of methicillin (21). MRSA is one of the most serious threat-level pathogens that has developed multi-drug resistance (22).

Early MRSA isolates were only associated with hospital acquisition (HA); however, after the 1990s, community associated (CA) MRSA emerged (23). CA-MRSA is resistance to fewer classes of antibiotics. However, as CA-MRSA has caused outbreaks in hospitals and HA-MRSA can spread into the community, the distinction between CA-MRSA and HA-MRSA has blurred (24). Although the genetic interchange between CA-MRSA and HA-MRSA makes molecular classification difficult, HA-MRSA does carry a larger staphylococcal chromosomal cassette *mec* (SCC*mec*) compared to the size of SCC*mec* in CA-MRSA (24).

In the U.S., the most prevalent strain is the CA-MRSA strain, USA300 (25). MRSA can be spread by person to person or person to object contact, tiny drops of liquid caused by coughs, sneezes or laughs, and skin-to-skin contact. Penicillin is the drug of choice if the isolate is sensitive to it (25). However, for MRSA, vancomycin is the drug of choice. Sulfamethoxazole-trimethoprim (TMP-SMZ), minocycline, ciprofloxacin, levofloxacin, and carbapenem are alternative choices for treatment of patients who are infected with MRSA (16).

*S. aureu*s is generally cultured only from the nose of healthy individuals, not the throat or respiratory secretions. However, it is often considered to be among the first pathogenic organisms in a throat culture when isolated from the CF respiratory tract (26). In the 1940s and 1950s, *S. aureus* was the most prevalent bacteria cultured from the respiratory tracts of CF patients (27; 28), and is still the most common microorganism reported among individuals with CF, particularly younger patients (29). An estimated 71 percent of CF patients are colonized with *Staphylococcus aureus* including sixty to seventy percent of CF patients up to the age of 18 (12). After patients

reach ages between 25-34 years, *P. aeruginosa* surpasses *S. aureus* as the most prevalent bacteria in CF patients (12).

*S. aureus* colonizes and infects CF patients at an early age. Abman and colleagues conducted a neonatal screening with a cohort of 42 CF children. The mean age of CF patient with an oropharyngeal swab culture positive for *S. aureus* is 12.4 months (30). In another study, Rosenfeld et al. found that fifty percent of 141 infants with CF cultured positive with *S. aureus* from brnonchalveolar (BAL) fluid during their first 6 months of life (31). Despite the apparent increase in prevalence of *S. aureus* in CF patients over the past decade (32-34), this increase could just reflect more sensitive culturing protocols (35; 36).

*S. aureus* may result in chronic infection and contribute to chronic *P. aeruginosa* infections. A study using pulsed-field gel electrophoresis showed that *S. aureus* persisted for an average of 37 months (37) indicating that infections in CF patients maybe intermittent or chronic (38; 39). Burns et al. studied 40 CF children and found a ninty-seven percent *S. aureus* infection rate in the first 3 years of life suggesting that there might be a progression from *S. aureus* to *P. aeruginosa* infection (40). Abman et al. examined 42 CF infants between 0-48 months; 18 infants were cultured positive with *S. aureus*, and 11 infants cultured positive with *P. aeruginosa*. Eighty percent of CF infants infected with *S. aureus* were between 0-24 months, and eighty percent of CF infants infected with *P. aeruginosa* were between 13-48 months. Nine of 11 *P. aeruginosa* infected CF infants were previously infected with *S. aureus* and had received treatment with antibiotics (30). A proposed mechanism suggested that early *S. aureus* infections may trigger or amplify an inflammatory cascade and lead to subsequent tissue damage. Damaged tissue may increase attachment of other bacterial pathogens, such as *P. aeruginosa*, hence, contribute to worse outcomes (41).

Although MRSA emerged in CF patients in the 1980s (42), MRSA has only recerntly been designated as a "serious" threat (22), and is another cause of deterioration of the CF lung. Twenty-six percent of CF patients with *S. aureus* infections are colonized with MRSA. Several studies have demonstrated that MRSA is associated with poor outcomes in CF patients. A small study conducted between 1992 and 1998 showed that 10 CF patients with MRSA in their respiratory tract showed a worsening in chest X-ray scores, as well as an increasing number of courses of intravenous (i.v.) antibiotics compared to non-infected CF patients (29). Furthermore, in a large North American observational study, a cohort of 1,834 patients was examined with respiratory cultures positive for MRSA only versus MSSA only (43). In comparison with MSSA, CF patients with MRSA had decreased lung function both in children less than 18 years of age (80.7 versus 89.4% predicted; $P < 0.001$) and in adults (60.9 versus 70.4% predicted; $P < 0.001$). Similarly, patients infected with MRSA had an increased frequency of hospitalizations and administration of i.v. antibiotics (29). Later, in a cohort study from 1996 to 2005, 17,357 individuals from the CFF Patient Registry were studied. In patients Aged 8 to 21 years, new onset of persistent MRSA infection, defined as ≥3 MRSA positive cultures in a year, was associated with a difference in the average FEV1 decline of -0.62 percent ($P < 0.001$), compared to those without MRSA (39). MRSA infection was also associated with a higher risk of death in a follow-up study (44). Thus, studies indicate that chronic infection with MRSA worsens the clinical outcomes of CF patients.

***Haemophilus influenzae***

*Haemophilus influenzae* is the third most common microorganism cultured from the respiratory tracts of individuals with CF with a prevalence about fifteen percent in the United States (12). *H. influenzae* most frequently infects CF patients early in childhood. Because *H. influenzae* identified from respiratory cultures of CF patients are usually unencapsulated

(nontypeable), CF patients are not protectecd by the *Haemophilus influenzae* type b (Hib) vaccine (45-47). A study from Spain examined the *H. influenzae* colonization in a cohort of 30 patients from three different hospitals. They noted that *H. influenzae* could generally persist for an average of 2 1/2 months; but in some cases, *H. influenzae* can persist as long as 6 1/2 years (46). Ninety percent of CF patients were infected with two or more distinct clones over a 7-year period (46). In BAL fluid from 75 CF infants in Australia with an average age of 17 months, and eight percent of infants cultured positive for *H. influenzae* (48). Sampling the lungs of 40 CF infants, thirty-eight percent of infants cultured positive for *H. influenzae*, which was the most commonly isolated pathogen at 1 year of age in that study (49). In 2017, 20 percent of CF infants and toddlers were colonized with *H. influenzae* (12). As their age increased to 5 years old, the colonization rate increased ~30 percent, making *H. influenzae* the second most prevalent microorganism in CF patients after *S. aureus* (12). Thus, *H. influenzae* is one of the first organisms to infect the airways of individuals with CF.

Whether *H. influenzae* is pathogenic in CF remains controversial (3) and complicated by the fact that *H. influenzae* commonly colonizes the respiratory tracts of healthy children (50). Although a study of 7,010 patients from the European Epidemiologic Registry of Cystic Fibrosis (EERCF) found that isolation of *H. influenzae* from the respiratory tract was not associated with decreased lung function (51), this cross-sectional analysis only examined CF children over 6 years old, the age period that other traditional CF pathogens, such as MRSA, and *P. aeruginosa* increase in prevalence.

Several other studies, suggest that *H. influenzae* plays a role in CF disease progression. *H. influenzae* can be isolated from 30 percent of sputa samples collected from clinically stable CF patients. 27 percent of those sputa samples also demonstrated additional CF pathogens, such as *S.*

*aureus* or *P. aeruginosa* (52). *H. influenzae* is capable of inducing inflammation that may contribute to tissue injury. For example, when $>10^5$ CFU/mL of *H. influenzae* were present in BAL fluid from CF infants, the total leukocyte and neutrophil counts were higher than when there were no identifiable pathogens (49). A more recent study examined 56 CF children; 12 percent of them cultured positive for *H. influenzae* and demonstarted a >15% reduction in lung function compared to the children who were culture negative (53). Rayner et al. observed an increased rate of isolation of *H. influenzae* prior to and during acute exacerbations in CF patients, indicating that *H. influenzae* also plays a role during acute pulmonary exacerbations (54). After antibiotic therapy, a reduced rate of isolation of *H. influenzae* was observed, as well as clinical improvement, which concurs with the conclusions of other studies that *H. influenzae* is capable of causing exacerbations and should be treated with appropriate antibiotics (55; 56).

***Burkholderia* subspecies**

Members of the *Burkholderia cepacia* complex (BCC) were first recognized as opportunistic pathogens of cystic fibrosis patients in the 1980s (57). Pulmonary infection caused by *B. cepacia* was associated with increased rates of morbidity and mortality. The infection could lead to cepacia syndrome, characterized by fulminating pneumonia, high temperatures, respiratory failure and may progress to septicemia (57). Certain species within the BCC, such as *Burkholderia cenocepacia* and *Burkholderia dolosa*, are capable of patient-to-patient transmission causing epidemics in CF patients (58). *B. cenocepacia* is the most prevalent of the *Burkholderia* subspecies in CF patients in the USA and Canada, as well as Europe, such as France, the Czech Republic, Italy, and Portugal (59). *B. cenocepacia* is considered one of the most serious pathogens; not only is it frequently associated with low survival and a high risk of causing cepacia syndrome, but it also encompasses the majority of epidemic strains (60).

Virulence factors are important to BCC pathogenesis in CF patients. The BCC members have intrinsic antimicrobial resistance (61-63), the ability to form biofilms (64; 65), catalase and superoxide dismutase (66), the ability to invade and intracellularly survive within host cells (67; 68), siderophores for nutrient scavenging (69-72), and type III secretion systems (73-75).

A cohort of CF patients from the Manchester adult CF center were retrospectively reviewed and the survival of patients with BCC infection were compared with matched controls with *P. aeruginosa* infection. Since the referral to the adult CF center, 49 CF patients had become infected with *B. multivorans* (n=16) or *B. cenocepacia* (n=33). Another six patients had developed infection with *B. gladioli*. Ten patients had transient infection: 8/16 and 2/33 with *B. multivorans* and *B. cenocepacia*, respectively. Patients infected with *B. cenocepacia* and *B. multivorans* experienced a decline in pulmonary function. Nineteen out of 31 patients with *B. cenocepacia* were dead with 1-year survival rate of 80.2% and 5-year survival rate of 66.6%. Five of 8 patients infected with *B. multivorans* were dead with 1-year survival rate of 100% and 5-year survival rate of 75%. *B. cenocepacia* demonstrated worse survival rate compared to the controls with *P. aeruginosa* infections (76). Further, *B. dolosa* caused an outbreak at the Boston Children's Hospital from 1998 to 2005. Over 40 patients were infected with *B. dolosa* through patient-to-patient spread via the first patient who came from Salt Lake City, UT. The chronic infection with *B. dolosa* was associated with five deaths and an accelerated decline in pulmonary function in the other patients (77).

***Stenotrophomonas maltophilia***

*S. maltophilia* was first isolated in 1943, classified as a member of the genus *Pseudomonas* in 1961, then reclassified as *Xanthomonas* in 1983, and finally classified as *Stenotrophomonas* in 1993 (78). The genus *Stenotrophomonas* consists of 4 subspecies, and only *S. maltophilia* is known

as a human pathogen. *S. maltophilia* can cause various diseases, such as respiratory tract infections, acute exacerbations of chronic obstructive pulmonary disease, and bacteremia (79), complicated by the pathogen's accompanying resistance to commonly used antibiotics, such as carbapenems (80), co-trimoxazole and ciprofloxacin (81). Risk factors for *S. maltophilia* colonization and infection are attributed to mechanical ventilation, previous exposure to antibiotics, prolonged hospitalization, and use of medical equipment in contact with the respiratory tract, such as nebulizers (82).

*S. maltophilia* has been recognized as an emerging nosocomial pathogen, especially in immunocompromised patients (83). 56-69 percent of *S. maltophilia* clinical isolates originated from the respiratory tract of hospitalized patients (84-87). *S. maltophilia* can occur in any aquatic or humid environment, including the drinking water supply (80), and nebulizers (88). Frederiksen et al. reported the first isolated *S. maltophilia* in a cystic fibrosis patient in 1975 in Denmark (80), and the first to cause infection in a CF patient reported in 1979 (89). The prevalence of colonization of the respiratory tract of CF patients by *S. maltophilia* has increased (12), with some CF clinics reporting colonization rates over 30 percent (90). By 2017, the overall prevalence of *S. maltophilia* is about 13% in CF patients in the United States (12). Studies have associated this increase with extensive use of anti-pseudomonal antibiotics for early treatment of *P. aeruginosa* colonization and control of chronic *P. aeruginosa* repiratory tract infections (91). *S. maltophilia* infections occur in CF patients of all ages (12), and infections are frequently chronic (92; 93). In particular, Goss et al. observed that older CF patients have a higher rate of *S. maltophilia* infection, and a high rate of prior co-infection with *P. aeruginosa* and *B. cepacia* (94). A single cohort analysis observed that CF patient with *S. maltophilia* have increased lung function decline, as well as increased rates of hospitalization (95). In a 12-year study, a total 687 CF patients infected

chronically with *S. maltophilia* were followed for their progression. Ninety-five patients underwent a lung transplantation. Twenty-six of transplanted patients, along with an additional 49 patients, died. The study suggested that chronic *S. maltophilia* infection is associated with three-fold higher risk of death or lung transplant in CF patients (96).

***Achromobacter xylosoxidans***

*Achromobacter* spp. are Gram-negative bacilli, aerobic, and nonfermenters of glucose. *Achromobacter xylosoxidans* are the most common bacillus and is recognized as an emerging multi-drug resistant microorganism. *A. xylosoxidans* is increasingly cultured from CF sputum. The infection or colonization rate of *A. xylosoxidans* in CF patients varies between 2 percent and 17.9 percent (97; 98). *A. xylosoxidans* colonized patients are mostly older with lower lung function with greater need for intravenous antibiotic treatments (97). In 2016, a retrospective study evaluated the clinical impact of *A. xylosoxidans* colonization/infection in CF patients. There was an increase in infection or colonization in children, and lung function was worse in chronically colonized patients compared to other *A. xylosoxidans* infected CF patients (99). Hansen et al. noted that *A. xylosoxidans* infected CF patients have lower lung function and similar inflammation levels compared with *P. aeruginosa* chronically infected patients (100).

***Elizabethkingia meningoseptica***

*Elizabethkingia meningoseptica* are Gram-negative bacillus, non-motile, non-fastidious, and catalase and oxidase positive (101; 102). *E. meningoseptica* was firstly identified by King in 1959 (102). *E. meningoseptica* is frequently isolated from soil, saltwater, freshwater, dry and moist clinical environmental and equipment surfaces, intravenous lipid solutions, and municipal water even if adequately chlorinated (103). *E. meningoseptica* infections have high mortality rates, between 23-52 percent, partly due to multi-drug resistance (104-106). Until 2018, the Clinical and

Laboratory Standards Institute had not established interpretive breakpoints for minimum inhibitory concentrations (MICs) for *E. meningoseptica*. Most reports used MIC breakpoints for *P. aeruginosa* or non-Enterobacteriaceae spp. Interestingly, *E. meningoseptica* exhibits susceptibility to many antibiotocs used to treat Gram-positive cocci (105; 107; 108). However, SENTRY and other surveys suggest that vancomycin and other anti-Gram-positive antibiotics, including teicoplanin, linezolid and quinupristin-dalfopristin cannot be considered as optimal treatment options for *E. meningoseptica* infection (109-111). Studies show that *E. meningoseptica* are susceptible to minocycline; however, bacteria could quickly develop resistance to minocycline, a bacteriostatic agent (104; 109; 112). Despite studies demonstrating that levofloxacin and newer quinolones could be promising therapeutics against *E. meningoseptica*, anecdotal studies suggested that *E. meningoseptica* infections only respond when combination therapies are used, such as vancomycin combined with rifampicin (108; 113-115). Preterm neonates, immunocompromised patients, patients with multiple or prolonged hospital admissions, or patients heavily exposed to broad-spectrum antibiotics are at high risk of acquiring *E. meningoseptica* infections (103). The intrinsic drug resistance complicates the management of invasive infections caused by *E. meningoseptica*, that may result in serious consequences.

***Pseudomonas aeruginosa***

*Pseudomonas aeruginosa* is an opportunistic pathogen that causes complicated disease states such as bacteremia, otitis, and soft tissue, urinary tract, and respiratory infections. The over-use of antimicrobials and the lack of effective antibiotic stewardship programs has led to development of resistance against several FDA-approved standard-of-care (SoC) therapeutics, including ciprofloxacin, levofloxacin, cefepime, and gentamicin (116). Multi-drug resistant (MDR) *P. aeruginosa* has been designated as a "serious" threat by the Centers for Disease Control

and Prevention (CDC) (22). With over 51,000 health-care associated infections including 6,700 MDR *P. aeruginosa* infections annually in the United States, *P. aeruginosa* is the leading cause of nosocomial infections and the second most common pathogen associated with ventilator-associated pneumonia (VAP) (117). *P. aeruginosa* infections are particularly challenging to manage and often result in poor prognosis for immunocompromised patients and CF patients. An estimated 47.5% of CF patients harbor *P. aeruginosa* in their lungs, including 9.2% of them with MDR *P. aeruginosa* (12). In CF patients, the presence of sticky dehydrated mucus in the airways provides ideal conditions for the colonization of such opportunistic pathogens (3; 12). These pathogens in the accumulated mucus also form biofilms (3), creating unique conditions resulting in poor drug penetration, ultimately leading to treatment failure despite the use of aggressive antibiotics (118; 119). Consequently, these chronic pulmonary infections result in declining lung function, the leading cause of mortality in CF patients (6). Moreover, repeated intravenous (i.v.) administration of high-dose antibiotics may result in severe side effects and increased propensity of resistance acquisition (120; 121).

**Multi-drug Resistant Bacterial Infection**

There is a continuous arms race between the antimicrobial treatments devised by humans and the microorganisms that cause infection and disease. Around the middle of the 20$^{th}$ century, with the discovery of penicillin and subsequently other antibiotics, humans turned the tide in their favor. However, soon after antibiotics were marketed, microorganisms responded with various mechanisms of resistance. Today, antibiotic resistance is a worldwide problem. In 2013, at least 2 million people in the United States acquired serious infections with bacteria that are resistant to one or more antibiotics, and 23,000 individuals die each year due to drug resistant infections (22).

Antibiotic resistance adds a great burden to U.S. healthcare system. Drug resistant bacterial infections require prolonged hospitalization, extensive treatments, additional doctor visits, and cause treatment failures, and increased mortality. In addition, it has been estimated that drug resistant infections result in as high as 20 billion additional U.S. dollars in healthcare costs, with estimated extra costs to society as much as 35 billion U.S. dollars a year (22; 122). Drug resistant bacteria have become a particular concern for hospitalists and intensivists, due to identification of various resistant bacteria in healthcare institutions. Some of the bacteria, however, such as MRSA and extended-spectrum beta-lactamase (ESBL)-producing *E. coli*, are present in the community. The spread of resistant bacteria in the community could pose serious problems for infection control in long-term care facilities, sport teams, military recruits, as well as children attending day care centers. Epidemiological studies have demonstrated a direct relationship between the emergence and dissemination of drug resistance bacteria and consumption of antibiotics (123). The overuses of antibiotics clearly drives the evoluction of resistance.

Most antimicrobials can be categorized based on their mechanisms of action. There are five major mode of actions: 1. Interference with cell wall synthesis, including beta-lactams and

glycopeptides; 2. Inhibition of protein synthesis, including inhibition of 50s or 30s ribosomal subunits, and bacterial isoleucyl-tRNA synthetase; 3. Interference with DNA or RNA synthesis; 4. Inhibition of a metabolic pathway; and 5. Disruption of bacterial membrane structure. Bacteria may develop resistance to antimicrobials through different mechanisms, including 1. The organisms may acquire genes encoding enzymes, such as beta-lactamases; 2. Bacteria may acquire efflux pumps that extrude the antimicrobials before they reach target sites; 3. Bacteria may alter metabolic pathways or target sites (124). Hence, bacteria can become resistant to antimicrobial agents through mutation, selection, and acquiring genes that encode resistance. Microorganisms that have acquired non-susceptibility to at least one agent in three or more antimicrobial categories are defined as multi-drug resistant (MDR) (125).

**Silver as an Antimicrobial Agent**

Silver has a long history of medicinal use in humans. The human body contains less than 2.3 µg/L of silver (126; 127). The use of silver can be traced to ancient times, as a disinfectant to store and purify water. For example, Alexander the Great (335 BC) drank water stored in silver vessels (128). Silver has also been used for storing and purifying water in Apollo spacecraft (129), and the MIR space station (130). Silver has been used as an antiseptic in wound care before the 1800s. Silver nitrate was used for various medical treatment and infectious diseases (131). For example, 2 percent silver nitrate solution was used by Crede in 1881 to prevent ophthalmia neonatorum in newborn children (132). Due to the side effects of silver nitrate, including irritation, blackening of skin, and electrolyte imbalance, colloidal silver was introduced for medical use in late 19th century (131). Colloidal silver contains silver particles in suspension with less than 10 percent ionized silver. Currently in Mexico, colloidal silver is marketed as any fluid containing silver used to disinfect vegetables and drinking water (131). Colloidal silver remained popular

until the 1940s, when the discovery and use of penicillin, sulfonamide and mafenide antibiotics displaced it as an antimicrobial (131-133). However, the emergence of bacteria, such as MDR *P. aeruginosa* and MRSA, resistant to commonly used antibiotics, including penicillin and sulfonamide, led to the need for new antibiotics. In the 1960s, Moyer *et al.* proposed the use of 0.5 percent silver nitrate solution for the treatment of burn wounds (134). Moyer rekindled interest in silver as an antimicrobial. Following Moyer, Fox *et al.* discovered silver sulfadiazine, which is still used for the treatment of burn wounds (135). Silver sulfadiazine has broad-spectrum antimicrobial effects by combining the broad-spectrum activity of silver with a sulfonamide, sulfadiazine. Silver sulfadiazine is marketed as a water-soluble cream, Silvadene Cream 1%, and demonstrates potent antimicrobial effects against a number of Gram-positive and Gram-negative bacteria. Silver has also been introduced into wound dressings in the nanocrystalline form. The nanocrystalline silver formulation not only gives a slow release of silver to create a barrier for infection at the wound site, but also helps manage the wound site healing. In addition to the nanocrystalline formulation, silver has been impregnated into different dressing materials, such as nylon fabrics, meshes, biodegradable collagens, carbon fibers, and hydrofiber alginates (131; 136).

Silver ($Ag^{+}$) is a broad-spectrum antimicrobial. The silver metal ($Ag^{0}$) is inactive; however, in the presence of moisture, it readily ionizes to become silver cations that have antimicrobial activity (133). Nageli reported that only $10^{-5}$ to $10^{-8}$ M of silver cations derived from silver metal are required to inhibit the growth of fungal spores (131). Silver cations exhibt multiple mechanisms of action, including an ability to condense bacterial DNA and disrupt bacterial cell membranes by interacting with enzymes and proteins important to cell wall synthesis (137). Silver can also affect cell respiration, transport and metabolism, and subcellular organelle structure (131). Studies of the mechanism of action of silver on the yeast *C. albicans* showed that silver cations

bind to the cysteine residues of phosphomannose isomerase, an essential cell wall synthesis enzyme, and result in loss of cell wall integrity (131). Silver cations can also block matrix metalloproteinases, enzymes that delay chronic wound healing, and thus, speed the healing process (138). These diverse mechanisms provide potent antimicrobial activity (139) and may explain the paucity of reported cases of resistance (140-143) despite its widespread use to treat burn and wound infections (134; 136; 144-146). Although silver sulfadiazine resistant strains of *P. aeruginosa* have been isolated in burn units, the mechanism of resistance is unknown (147-149). In contrast, the mechanism of resistance of a *Salmonella* strain that resulted in patient deaths and the temporary closing of a burn unit has been well characterized (150). This particular *Salmonella* strain carries a plasmid, pMG 101 that encodes a peri-plasmic silver binding protein (SilE) and two parallel efflux pumps (SilCBA and SilP) (143; 151).

Silver antimicrobials have been known to cause a rarely seen cosmetic side effect, argyria. Argyria is a gray to blue discoloration of the skin due to deposition of silver sulfide in the dermis or eyes after long term silver exposure (131). Systemic silver is excreted in the urine, and burn patients treated with silver have shown elevated levels of urinary silver (152; 153). Some studies showed that, by inhibiting cellular respiration (154), silver salts affect the growth of keratin producing epidermal cells (155), bone marrow (156), connective tissue cells (154), hepatocytes (131) and lymphocytes (157). However, other studies have reported no observed cytotoxicity of silver. Potent antimicrobial activity coupled with low toxicity to human tissues (158) has led to several FDA approved antimicrobial dressings such as, Acticoat absorbent, Actisorb Silver 220, and Aquacel AG with ionic silver as the active antimicrobial agent (159). Recent studies have suggested that in the presence of high concentrations of chloride anions, silver forms soluble anionic $AgCl^{2-}$ compounds rather than precipitating as AgCl (160). Both sensitive and resistant

bacteria have increased susceptibility to silver in the presence of high concentrations of chloride anions, perhaps due to increased access of silver cations to the cell membranes (160). The activity of silver cations depend on their bioavailability, which can be affected by delivery methods, solubility and ionization of the silver source, and the presence of biological ligands, such as proteins, chloride, and sulfides. Although $AgCl^{2-}$ improves the bioavailability of silver, due to the affinity of silver cations for thiolated proteins and the relatively low physiological concentration of chloride ions (161; 162), the bioavailability of silver is poor, which suppresses the antimicrobial activity of silver ions (161), necessitating an increased dosage to effectively eradicate infections.

**The Use of Ibuprofen for CF Lung Disease.**

Ibuprofen is a commonly used nonsteroidal anti-inflammatory drug (NSAID) for pain, fever, and inflammation. The lungs of CF patients are characterized by persistent neutrophilic inflammation partly due to chronic bacterial infections. The exuberant inflammation contributes to lung destruction prompting the need for anti-inflammatory therapeutics. However, adverse effects, such as growth retardation and cataracts, limits the ability to use systemic corticosteroids for prolonged periods (163). Several NSAIDs including aspirin, ibuprofen, naproxen, and diclofenac are routinely used for the treatment of acute or chronic conditions involving pain and inflammation (164-171). High-dose ibuprofen (peak serum concentration > 50 μg/mL) inhibits the migration, adherence, swelling, and aggregation of neutrophils, as well as the release of lysosomal enzymes. Several animal models of pulmonary infection and inflammation have shown that high-dose ibuprofen reduces neutrophil influx (172). For instance, the use of ibuprofen for the treatment of inflammation associated with chronic pulmonary infection in CF has been shown to significantly decrease the rate of lung function decline, a benefit that has been attributed to the anti-inflammatory effects of the drug (171). The evaluation of high-dose ibuprofen to alleviate

inflammation associated with CF lung disease has been ongoing for more than two decades (96; 163; 167; 168; 173). In the early 1990's a 4-year, randomized, double blind, placebo-controlled trial demonstrated that CF patients treated with high-dose ibuprofen had a 40 percent slower rate of lung function decline compared with CF patients treated with placebo (167; 168). These significant improvements were recently affirmed following the completion of a two-year, multiple CF center, randomized, placebo-controlled trial conducted in Canada (163). Both trials were able to demonstrate the benefits and relative safety of long-term use of high-dose ibuprofen for treating CF lung disease. Despite its proven efficacy and relative safety, high-dose ibuprofen is used by only a minority of CF patients in the United States, primarily due to the inconvenience of required pharmacokinetic studies and the concern regarding the risk of gastrointestinal bleeding.

**Combinational Therapy as an Alternative Antimicrobial Strategy**

In addition to *P. aeruginosa*, several other pathogens reside in the CF lung including *S. aureus*, *S. maltophilia*, and *B. cepacia* complex species. Thus, to address the polymicrobial infection affecting this disease state, it is imperative to develop broad-spectrum therapeutics with potent antimicrobial activity against both Gram-positive and Gram-negative pathogens. Thus, a combinatorial antimicrobial approach is particularly attractive to address polymicrobial infections. Many studies have demonstrated the effectiveness of combinational therapy. Synergy between antimicrobials *in vitro* is defined as antimicrobial effects of a combinational therapy greater than the sum of the independent activities when measured separately (174). Certain beta-lactams and aminoglycosides demonstrated synergistic activity against various Gram-positive and Gram-negative bacteria (175). In addition, combination therapy can also extend the antimicrobial spectrum beyond the spectrum of single antimicrobials, which is especially useful for patients with polymicrobial infections. Finally, the emergence of antimicrobial resistance is generally generated

by selective pressure from antimicrobial therapy. The chance that a bacteria can generate mutations to resist antimicrobials with different mechanisms of action is much lower than the chance of generating resistance to either one (176). Hence, combination therapy could prevent the emergence of resistant bacteria that cause therapeutic failures. This rationale underpins the wide use of combination therapy for treatment of tuberculosis and AIDS (177).

**Lung Physiology and the Fate of Particles**

The main function of the lungs is to facilitate gas exchange between the blood and the gaseous external environment and in the process, maintain homeostatic systemic pH (178). The thoracic cavity houses the majority of the respiratory system, the principal anatomical features of which include airways, lungs, and the respiratory muscles. The upper conducting airways are comprised of the nasopharynx, oropharynx, and the trachea, which bifurcates into the bronchi and subsequently branches into smaller bronchioles. These bronchioles ultimately divide into terminal bronchioles that end with the alveolar sacs (lower airways). The upper conducting airways are lined with ciliated columnar epithelium (50-60 μm thick) that gradually transitions to a cuboidal shape towards the distal end of the airways with a subsequent reduction in thickness to 0.1 – 0.2 μm at the alveoli (178; 179). The thickness of the epithelium in the upper airway poses as a barrier to absorption (178); however, in the distal airways within the lungs, the extremely thin barrier between the pulmonary lumen and the underlying capillaries, combined with the large surface area of over 100 $m^2$ (presented by the existence of approximately 300 million alveoli), create excellent conditions for efficient mass transfer (180; 181). The alveolar surface is comprised of three main types of cells, of which, type I pneumocytes are the most abundant (178). These cells share a basement membrane with the pulmonary capillaries (178). The other two cell types include the type II pneumocytes that are responsible for secretion of lung surfactants to prevent alveolar

collapse (178), and alveolar macrophages belonging to the immune system that scavenge foreign material from the lung surface (178; 182). Apart from these cell types, the distal airway also hosts other cells such as progenitor cells for the type I pneumocytes (181) and cells of the immune system, such as dendritic cells that sample for foreign substances and pathogens (183).

Particles entering the lung are deposited by inertial impaction, sedimentation, and diffusion (180). The fate of these particles is primarily determined by their diameter. Large particles ($d > 5$ μm) deposit by inertial impaction in the oropharyngeal region or sedimentation in the bronchial region. In the oropharyngeal region, these particles get entrapped in the mucous layer and are subsequently moved to the proximal airway by the rhythmic, coordinated beating of the cilia, where they are expectorated or swallowed and metabolized (mucociliary clearance) (178; 179). On the other hand, small particles ($d < 1$ μm) are driven by diffusion and more likely to reach the alveolar region (184).

Once deposited inside the lung, the particles and the encapsulated drug are subjected to a variety of barriers. As previously described, inhaled particles deposited in the upper airway get rapidly cleared by the mucociliary escalator (181; 185). Furthermore, the presence of catabolic enzymes in the tracheobronchial region also poses as a deterrent to efficient drug delivery. However, the particles deposited in the peripheral lung are reported to have an approximate residence time of 24 hours (181; 185). These particles must then release the therapeutic agent via dissolution, degradation, diffusion or a combination of these mechanisms. Following deposition in the peripheral lung, the larger particles are subject to phagocytosis by the alveolar macrophages. Particles that are either too large or too small may be able to escape phagocytosis by the alveolar macrophages (186; 187). Released drug must subsequently diffuse through the lung epithelium and into the bloodstream, whereupon it encounters majority of the resistance in the form of plasma

membrane of the lung epithelium (188; 189). Usually, small molecule drugs rapidly permeate through the lungs and are absorbed systemically. For instance, small hydrophobic molecules are thought to pass through the epithelial barrier by passive diffusion; whereas, small hydrophilic molecules can be absorbed via the tight junctions or through specific transporters (190). Therefore, it is important to determine the site of delivery within the lung depending on the type of therapeutic molecule administered.

**Drug Delivery Approaches**

The three main types of technologies to deliver therapeutic agents to the lungs are nebulizers, dry powder inhalers (DPIs), and metered dose inhalers (MDIs). All three types of devices use different delivery mechanisms and require different types of drug formulations (178). Nebulizers have been in use the longest, with the first documented use dating back to the mid-1800s (179). Devices in this class belong either to the air-jet-type or ultrasonic-type nebulizers. Using high velocity air, a liquid or a bulk suspension is sheared into a liquid film at the spray nozzle that subsequently collapses under surface tension into aerosol droplets in an air-jet nebulizer (191). Ultrasonic nebulizers utilize a vibrating piezoelectric crystal, which causes bubble formation at the liquid surface via cavitation (191). Droplets effervescing from the turbulent medium create a dense mist that is inhaled by the patient (191). While nebulizers produce ultra-fine droplets (~ 1 μm), the degree of polydispersity of the aerosolized droplets is high, and particles larger than the aerosol droplet cannot be nebulized (191). Furthermore, many of these devices tend to be limited to home or hospital use due to their bulk and therefore lack of portability (179).

Advances in medical aerosol development in the 1950s focused on delivering asthma drugs directly to the lung to significantly reduce the amount of systemic drug and, thereby, adverse reactions led to the development of metered dose inhalers (MDIs). MDIs are hand-held, portable

systems that contain drug that is either dissolved or suspended in a compressed liquid propellant (initially chlorofluorocarbons (CFCs) later replaced by hydrofluoroalkanes (HFAs)) (179; 192). Upon actuation, the device releases a metered volume of drug and propellant through a valve system (193). The resulting aerosol droplets are in the correct size range for deposition in the lung (179). However, the performance and efficiency of MDIs is largely patient-dependent, since it requires coordination between actuation and inhalation to achieve optimal deposition of the drug in the lungs (192; 194). A further disadvantage of these types of devices is the presence of surfactants within the formulation that may impact lung performance (192).

Dry powder inhalers (DPIs) were developed as an alternative to MDIs because of the disadvantages of MDIs. DPIs are breath-actuated devices that utilize shear-induced aerosolization of a dry powder drug to deliver the therapeutic agent to a patient's lung (193). Potential advantages associated with DPIs include their ease of use compared with other types of inhalers since they do not require coordination of actuation and inhalation and the lack of liquid propellant in the drug formulation (192; 195). Furthermore, DPIs store drug in a dry state, which could confer long-term stability and sterility (179). However, the particles within a DPI tend to aggregate due to electrostatic interactions and/or hygroscopic phenomena that can interfere with their aerosolization (178). Additionally, the actual dose delivered from a DPI is a function of the inspiratory flow rate, and therefore can be difficult to replicate (192; 196; 197). Numerous advances have been made in the field of DPIs to improve performance, primarily in the engineering of particles that are easily respirable and have improved aerodynamic properties as well as in the methods used to disperse the particles such as compressed air or electric motors (196). For instance, an advance in particle engineering is represented by formulations comprising of "porous particles" that are ideally suited for delivery to the peripheral lung. These particles possess a low mass density, thus resulting in a

low aerodynamic diameter (1 to 5 μm) even though the geometrical diameters are larger (5 to 30 μm) (189). The small aerodynamic diameter of the particles enables their deposition in the alveolar region; however, the large geometric diameter prevents phagocytosis by alveolar macrophages (198) and improves dispersion properties of the particles (188).

**Nanotechnology in Medicine**

Nanotechnology encompasses the understanding and control of matter, generally in the 1-100 nm dimension range (199). Manipulation of materials at the nano-scale provides access to unique physico-chemical properties such as ultra small size, large surface area to mass ratio, high reactivity, and unique interactions with biological systems (199; 200). Furthermore, the use of materials at this scale provides unparalleled freedom to modify fundamental material properties including solubility, diffusivity, drug release characteristics, blood-circulation half-life, and immunogenicity (199). The application of nanotechnology to medicine, known as nanomedicine, relates to the use of nanostructured materials for the development of novel therapeutic and diagnostic modalities (201; 202). However, these unique medical effects are not strictly restricted to objects with dimensions below a 100 nm, and therefore, structures and objects with dimensions up to 1000 nm in size are included (179; 203). Over the last two decades, nanomedicine has seen a huge surge with research activities occurring in the fields of drug delivery, *in vitro* and *in vivo* diagnostics, *in vivo* imaging, biomaterials, and active implants (203). Of these, the application of nanomedicine to drug delivery is the dominating field based on parameters such as publications, patent filings, number of companies, clinically approved products, as well as and sales and revenue (203). Even within the realm of drug delivery, applications of nanomedicine include treatment of cancer, infections, diabetes, immune diseases, and so on (203-205).

**Nanoparticle Formulations for Pulmonary Drug Delivery: Advantages**

Numerous advantages of nanoparticle drug delivery have been recognized (206; 207). In a general sense, incorporation of a drug within nanoparticles through physical encapsulation, chemical conjugation or adsorption improves the pharmacokinetics and therapeutic index of the drug compared with its free drug counterpart (200). Such drug delivery systems improve the serum solubility of poorly water-soluble therapeutic agents, prolong their systemic circulation half-life, reduce immunogenicity, and offer the possibility of concurrently delivering multiple therapeutic agents at a sustained or controlled rate to target organs and/or tissues of interest (208-210). Furthermore, the controlled release aspect of nanoparticulate drug delivery formulations lower the frequency of drug administration thus affording improved patient adherence (199).

Specifically, in case of pulmonary formulations, a fast release of the drug from the particle following deposition in peripheral airways is desired due to the short residence time of the particles. Nanoparticles possess a larger surface area to volume ratio compared with larger particles (179). Therefore, a greater number of its molecules will be present at the surface rather than within the core of the particle (211), thus leading to an increase in the dissolution velocity (212). Additionally, the saturation solubility of a particle increases with a decrease in the particle size (212). The dependence of these properties on particle size is unique to particles with dimensions approximately under 1 μm (212). Consequently, nanoparticulate formulations provide a highly effective means to improve mass transfer from the particle into the surrounding medium (212), and thus improve the bioavailability of insoluble or poorly soluble hydrophobic drugs (211). Furthermore, with solution-based formulations, the dose of the drug is thermodynamically limited by the aqueous solubility of the drug, which can be enhanced by the use of nanoparticle-based drug formulations (179). For instance, prodrugs with increased hydrophobicity have been

formulated to enhance their permeability through biological barriers (213-217). Nanoparticle formulations can be developed in these instances to mitigate the decreased solubility of such compounds and increase their local bioavailability (178).

Additionally, current therapeutic regimens for the treatment of pulmonary infections utilize frequent dosing of intravenous antibiotics at high doses to achieve significant serum concentration of the drug to eradicate disease-causing pathogens. Although this strategy is the current gold standard for the treatment of pulmonary infections, it can result in serious side effects due to the high dose of antimicrobials administered. For example, in the case of aminoglycosides, high dose administration can result in nephrotoxicity and ototoxicity (200; 218). Along with the potential of reducing toxicity, direct administration of antimicrobials to the lungs as nanoparticle formulations can aid in reducing the problem of antimicrobial resistance, since a high localized concentration of the drug can be maintained while overcoming the rapid clearance of the drug from the lungs (219; 220). Finally, numerous intracellular infections remain difficult to treat due to the poor ability of many antimicrobials to traverse cell membranes and their subsequent low intracellular activity (200). In such instances, nanoparticle formulations can be used to improve the performance of the antimicrobial agent, since several studies have demonstrated the ability of nanoparticles to be internalized by a variety of cell types (221-225). As an example, pulmonary epithelial cells internalize particles in a size-dependent fashion with particles 0.5 μm or smaller being internalized 10 times more than 1 μm particles and 100 times more than 2 to 3 μm particles (178). Such a strategy can also be used to passively target cells of the respiratory tract along with other strategies to actively target cells and pathogens of interest within the respiratory system.

Nanoparticles for inhalation have been studied by various research groups. Suk *et al* demonstrated that the average mesh spacing in CF sputum was $140 \pm 50$ nm (226), which was

supported by a later study that showed that polystyrene particles less than 200 nm in diameter have faster transport through CF sputum (227). Hence, particles sizes less than 200 nm have a higher chance of reaching deeper into the thick mucus and the site of infections. Biodegradable polymers are preferred over non-degradable polymers for fabrication of drug delivery systems, because, by definition, these materials can be degraded and metabolized by the body.

In the studies presented here, a mixture of two biodegradable polymer systems: poly (lactide-co-glycolide) (PLGA) and a copolymer of PLGA and poly (ethylene glycol) (PEG) (PLGA-PEG) will be used for nanoparticle formulation. PLGA will be used to formulate the core of the nanoparticles. PLGA is biodegradable, and FDA-approved for human therapy. It has extended release rates from days to months, mechanical properties that are amenable to forming nanoparticles, and been extensively used for intravenous administration of therapeutic agents (228; 229). However, nanoparticles comprised of only PLGA have a tendency to be rapidly shuttled to the liver and spleen by macrophages in the mononuclear phagocyte system (230), limiting their circulation time and thus, the effectiveness of the encapsulated drug. This effect can be reduced by incorporation of PEG on the nanoparticle surface. PEG is an FDA-approved polymer that has no known debilitating effects, and is widely known as a biological 'stealth' agent that protects a particle's surface from non-specific opsonization by certain plasma components, inhibiting recognition by phagocytes of the reticuloendothelial system (RES) (231). PEG is extensively used in the formulation of drug delivery devices, especially for the purpose of surface modification (232; 233). The reduction in immune recognition by PEGylation leads to longer circulation times, thus increasing drug effectiveness. Furthermore, PEG has been shown to increase nanoparticle diffusion through human mucoid surfaces (234), increasing their ability to penetrate into the deep mucus layers, and thus bypassing one of the protective barriers bacteria utilize against

antimicrobials in the CF lung. I hypothesize that encapsulating antimicrobials into PLGA/PLGA-PEG nano-delivery systems will result in enhanced antimicrobial efficacy through both controlled and sustained delivery of drugs, and penetration into the thick mucus and MDR *P. aeruginosa* biofilms found in CF lungs.

# CHAPTER II

# DEVELOPMENT OF A MULTIFUNCTIONAL SILVER CARBENE THERAPEUTIC BEARING IBUPROFEN FUNCTIONALITY AS A TREATMENT FOR CYSTIC FIBROSIS LUNG DISEASE

## Introduction

Silver (Ag) has gained great interest as an antimicrobial candidate because of its excellent potency, broad spectrum activity, and low toxicity towards eukaryotic cells (156; 235; 236). Despite the widespread and continuous use of silver, few cases of silver resistance have been reported and, in most cases, including *P. aeruginosa*, resistance is transient and unstable (237-239). Although stable silver resistance by acquisition of plasmids or transposons has been documented in *Salmonella Typhimurium* and *Escherichia coli* (150; 240; 241), there are no reports of transfer of these components to *P. aeruginosa* (242). However, the poor bioavailability of silver cations, poses a challenge, because silver cations, the bioactive state of silver, react with physiological substrates and become inactive (237).

Youngs et al. have synthesized N-heterocyclic silver carbene complexes (SCCs) to overcome this challenge (131; 243-245). The use of N-heterocyclic carbenes (NHCs) as an innovative class of metal chelates for metallopharmaceutical synthesis has garnered interest in recent years (246-249), due in part to the excellent stability of NHC metal complexes and their vast potential for chemical modification. These chemical alterations can serve to tailor the solubility, toxicity, and electronic properties of the resulting complexes for medicinal applications (250-253). These SCCs provide gradual release of bioactive silver cations from a stable silver complex, sustaining silver cation bioavailability, as well as providing prolonged antimicrobial activity (131; 250). At the forefront of medicinal NHC research are studies involving the use of

silver carbene complexes (SCCs) as a new class of broad-spectrum antimicrobials. Within the past several years, significant strides have been made in the design of stable SCCs for the nebulized treatment of virulent and multi-drug resistant pathogens causing cystic fibrosis lung (CF) infections (254-256). For example, the methylated caffeine-based SCC1 has served as one of the best candidates of interest because of its moderate aqueous solubility and low toxicity.

The clinical implementation of NSAIDs, such as ibuprofen, for the treatment of CF associated pulmonary inflammation has remained sporadic despite several large multi-year studies demonstrating the positive impact such regimens have on reducing lung function decline (163; 257). Studies have shown that, in addition to their anti-inflammatory effects, NSAIDs may increase mucociliary clearance through combating the capacity of quorum sensing molecules produced by bacteria to down regulate P2Y2 receptors on airway epithelia, as well as through direct enhancement of the activity of the protein that malfunctions in CF, namely CFTR (163; 257).

We previously demonstrated a dose-dependent reduction in bacterial colony forming units (CFU) of *P. aeruginosa*, both *in vitro* and during infection, after ibuprofen treatment (258). Next, we evaluated the survival advantage of IBU treatment in an acute *P. aeruginosa* pneumonia model. Mice treated with high-dose ibuprofen had a survival advantage compared to sham treated mice. Thus, the combination of anti-inflammatory and antimicrobial properties of IBU results in a lower bacterial burden and a significant survival advantage over the sham-treatment group (258). Apart from CF, ibuprofen has also been shown to improve outcomes in pneumococcal infection models when combined with antibiotics suggesting synergistic antimicrobial effects (259). We have synthesized and characterized new multifunctional silver NHCs through direct chemical modification with nonsteroidal anti-inflammatory drugs (NSAIDs). Here, we report *in vitro* testing

of a silver carbene therapeutic bearing an ibuprofen substituent as a first approach towards a multifunctional treatment for CF lung disease.

## Materials and Methods

### Bacteria

The laboratory strain PAO1-V was provided by Dr. Maynard Olson (University of Washington, Seattle). The mucoid clinical isolate of *P. aeruginosa* PA M57-15 was provided by Dr. Thomas Ferkol (Washington University, St. Louis, MO). The *P. aeruginosa* PA HP3, PA RR05, PA LF05, *A. xylosoxidans* AX RE05, AX22, *S. maltophilia* SM AH06, and *S. aureus* SA EH05, and SA LL06 strains were cultured from the sputum of cystic fibrosis patients at St. Louis Children's Hospital. The silver sensitive and silver resistant *E. coli* strains J53 and J53+pMG101, were provided by Dr. Simon Silver (University of Chicago, Chicago, IL). The J53 strain is known to be sensitive to killing by silver cations and serves as a positive control. In contrast, the J53+pMG101 is a J53 derivative that harbors the pMG101 plasmid originally conferring silver resistance to a burn ward isolate of *Salmonella* and serves as a negative control. All bacterial strains were maintained as glycerol stocks at -80 °C.

### *In vitro* antimicrobial activity

Minimal inhibitory concentrations (MICs) were determined by broth microdilution method as previously described by a standard Clinical and Laboratory Standards Institute (CLSI) protocol. Briefly, bacteria were streaked from frozen glycerol stocks onto TSA or blood agar plates and incubated overnight at 37 °C. Colonies from the fresh plates were suspended in the Miller Hinton (MH) broth and grown at 37 °C in a shaking incubator at 200 rpm to an $OD_{650}$ of 0.4, which corresponds to ~5 x $10^8$ colony forming units (CFU)/mL. The bacteria were diluted in the broth to a concentration of $10^5$ in 100 µL, added to triplicate wells of a 96-well plate, containing 100 µL of

SCC1, SCC1-IBU, ibuprofen or tobramycin diluted in sterile water to various concentrations from a 10 mg/mL stock. The final concentrations of SCC1, SCC1-IBU, or tobramycin tested were 0.125, 0.25, 0.5, 1, 2, 4, 6, 8, 10, 15, and 20 μg/mL. The final concentrations of ibuprofen tested were 1, 2, 4, 8, 16, 32, 64, 128, 256, 512, and 1024 μg/mL. The plates were incubated overnight at 37 °C. The MIC was the lowest of these concentrations, at which each of the triplicate wells in each 96-well plate was clear after 18-24 h incubation. Each triplicate measurement was performed at least in duplicate for a minimum of 6 separate measurements. The MBC of SCC1, SCC1-IBU, ibuprofen and tobramycin was determined by plating the wells with growth inhibition (clear) on TSA plates and noting the lowest concentration that resulted in no growth after an overnight incubation at 37 °C.

**Determination of synergistic drug combinations**

All the strains except *E. coli* J53 and J53+pMG 101 were used to determine potential synergistic drug combinations between SCC1 and ibuprofen by checkerboard assay. The final drug concentrations of ibuprofen were 0, 50, 75, and 100 μg/mL. Based on the MIC values of SCC1 and SCC1-IBU, the final drug concentrations of SCC1 for checkerboard assay were 0.0625, 0.125, 0.25, 0.5, 1, and 2 μg/mL. The final solutions were comprised of 95% MH broth and 5% DMSO. A 100 μL working stock of bacterial suspension was incubated with a 100 μL solution of therapeutic agents (n = 3) for 18 hours at 37 °C. Wells demonstrating bacterial growth inhibition were identified visually to determine a synergistic MIC. All experiments were performed in duplicate. To evaluate for potential synergy, the fractional inhibitory concentration (FIC) was calculated as shown in **Equation 1** and defined in **Table 1**.

**Equation 1. The fractional inhibitory concentration (FIC) was calculated by comparing the MIC of each agent to the MIC of that agent in combination.**

$$FIC = \frac{\text{MIC A combined}}{\text{MIC A}} + \frac{\text{MIC B combined}}{\text{MIC B}}$$

**Table 1. Interpretation of FIC values to define synergy based on the checkerboard assay.**

| Definition | FIC |
|---|---|
| Synergistic | FIC ≤ 0.5 |
| Additive | 0.5< FIC ≤1 |
| Indifferent | 1< FIC ≤4 |
| Antagonistic | 4<FIC |

**Determination of bacterial burden for synergistic drug combinations**

Potential synergy between combinations of SCC1 and ibuprofen against *P. aeruginosa* isolate PAHP3 at a final concentration of $10^6$ CFU/mL were determined using a 24-hour end point CFU study performed in triplicate. The concentrations of ibuprofen tested against PAHP3 were 0, 50, 75, 100 μg/mL. The concentrations of SCC1 in combination with ibuprofen against PAHP3 were 0.0625, 0.125, 0.25, and 0.5 μg/mL. A 100 μL working stock of bacterial suspension was incubated with 100 μL drug solution (n = 3) in each well of a 96 well plate at 37 °C for 24 hours with constant shaking at 100 RPM. The final solutions were comprised of 97.5% MH broth and 2.5% (v/v) DMSO. Finally, a 10-fold serial dilution was performed in MH broth with the bacterial suspension from each well and 50 μL of each dilution was plated onto a blood agar plate. Plates were incubated for 18-24 hours and colonies counted to determine the CFU for each condition.

Synergy was defined as ≥2 $\log_{10}$ CFU/mL reduction between combined agents and the most effective individual agent at 24 hours. All experiments were performed in duplicate.

**Cell culture**

Human bronchial epithelial cell line (16HBE14o-) obtained by transformation of normal bronchial epithelial cells with SV40 large T antigen using the replication defective pSVori-plasmid were used between passages of 20 and 40 for all experiments. 16HBE cells were cultured in Minimum Essential Medium (MEM) with Earle's Balanced Salts and non-essential amino acids supplemented with 10% fetal bovine serum (FBS), 1% L-glutamine, and 1% penicillin-streptomycin (P/S) solution at 37°C in an incubator (5% $CO_2$, 100% RH). When the cells reached 90-95% confluency, they were harvested by trypsinizing and sub-cultured.

***In vitro* anti-inflammatory properties**

The ability of SCC1-IBU to act as an anti-inflammatory agent was also evaluated using 16HBE cells. Cells were seeded at a density of 100,000 cells/well in 24 well plates, the total volume adjusted to 1 mL per well, and the plates were incubated at 37 °C (5% $CO_2$, 100% RH). The cells were monitored daily for confluency and the feeding media was exchanged on alternate days. When the cells were found to be approximately 90% confluent, the feeding media was aspirated and the cells were washed twice with 1 mL phosphate buffered saline (PBS, 1X). The cells were stimulated by addition of 500µl of a lipopolysaccharide (LPS) solution (20 µg/mL) in 16HBE feeding media, and the plates were re-incubated at 37 °C for 2 hours. Subsequently, 500 µL of a 120 µM solution of SCC1-IBU was added to the wells of the plate. 120µM solutions of Ibuprofen as well as untreated cells were used as the corresponding controls. The final concentration of each compound was 60 µM and the final DMSO concentration in each well was 5% (v/v). The plates were re-incubated at 37 °C for 6 hours, following which; the supernatant from

each well was collected, aliquoted into micro-centrifuge tubes, and frozen at -20 °C till analysis. At the time of analysis, the supernatant was thawed and the IL-8 concentration in each sample was probed using IL-8 Human ELISA kit (Life Technologies) according to the manufacturer's instructions. A total of 7 replicates were analyzed for each treatment and the data has been presented as the mean ± standard error of the mean.

**Toxicity comparison of SCC1 and SCC1-IBU**

*In vitro* cytotoxicity of SCC1 and SCC1-IBU was determined using an alamarBlue® cell viability assay (Life Technologies) on 16HBE cells. Cells were seeded at a density of 25,000 cells/well in clear 96-well plates, the volume adjusted to 100 µL per well using feeding media, and the plates incubated overnight at 37 °C (5% $CO_2$, 100% RH). The following day, the media from each well was aspirated and the cells were washed with 1X PBS. Subsequently, 100 µL of drug solution (SCC1 or SCC1-IBU) in Opti-MEM® was added to the designated wells. The concentrations of the drug used were 20, 30, 50, 75, 100, 125, and 150 µg/mL. Each well, including the no-drug control wells, contained 3.3% (v/v) DMSO, which was used to solubilize SCC1-IBU. At this time, 10 µL of alamarBlue® solution was added to each well, and the plates were re-incubated at 37 °C (5% $CO_2$, 100% RH) for 24 hours. At the end of 24 hours, the plates were read for absorbance at 570 and 600 nm using a spectrophotometer. Cell viability was calculated based on the optical density data according to the manufacturer's instructions. A total of 8 replicates were analyzed for each treatment and the $IC_{50}$ data for each compound was determined using GraphPad Prism by plotting the cell viability versus the log of the molar concentration of the drug and applying a non-linear curve fit.

**Acute Murine-P. aeruginosa lung infection model**

Male C57BL/6J mice (The Jackson Laboratory, Bar Harbor, ME) aged 5 weeks were used for all acute lung infection studies [34, 35], approved by the Texas A&M University Institutional Animal Care and Use Committee (IACUC). Mice were weighed and randomly assigned into four groups and were housed in a barrier facility under pathogen-free conditions until bacterial inoculation. When necessary, animals were euthanized with an overdose of ketamine:xylazine followed by cardiac puncture for exsanguination, a method approved by our IACUC (TAMU) and are consistent with the recommendations of the Panel on Euthanasia of the American Veterinary Medical Association.

*P. aeruginosa* PA HP3 was grown in LB (LB), pelleted, washed with phosphate buffered saline (PBS), and resuspended to an $OD_{650}$ of 2.4 in LB (corresponding ~1.3 x $10^{10}$ CFU/mL, as determined by serial dilution and plating). Following anesthesia via intraperitoneal injection of ketamine (60 mg/kg) and xylazine (8 mg/kg) cocktail, mice were intranasally inoculated with 75 µL of bacteria inoculum in LB broth at an $LD_{100}$ of ~7.5 x $10^8$ CFU per mouse. To test the efficacy of combinational therapy against PA HP3, at 2 h post infection, treatment was administrated every 12 hours subsequently for a maximum of 5 doses via nebulization of 5 mL of control, ibuprofen, SCC1, SCC1-IBU solutions with 5% DMSO (containing 25 µmol total $Ag^+$ cation per dose for each SCC). Mice survival were monitored up to 48 hours.

**Statistical analysis**

All statistics were calculated using JMP pro 13 for Macintosh (SAS Institute, Cary, North Carolina, USA, www.jmp.com) and GraphPad Prism 7.0 (GraphPad Software, San Diego, CA). Differences between the treatments were investigated by one-way ANOVA followed by Tukey's multiple comparison test (95% confidence intervals). For the analysis of IL-8 release data, a one-way

ANOVA was performed followed by Tukey's multiple comparison post-hoc test. The *in vivo* survival curves in the infection model were compared using a Log-rank Mantel-Cox test. * indicates $p \leq 0.05$, ** indicates $p \leq 0.01$, *** indicates $p \leq 0.001$, and **** indicates $p \leq 0.0001$. Data were deemed to be significantly different for $p \leq 0.05$.

**Results and Discussion**

***In vitro* MIC and MBC determinations for SCC1, SCC1-IBU, ibuprofen, and tobramycin**

The minimum inhibitory concentration (MIC) of SCC1, SCC1-IBU, and tobramycin against strains of *Pseudomonas aeruginosa, Achromobacter xylosoxidans, Stenotrophomonas maltophilia, Staphylococcus aureus, and Escherichia coli* species was determined by broth microdilution (**Table 2**). The MICs of ibuprofen suggested that it is a mild antimicrobial agent that has MIC 512 µg/mL against PAHP3 and >1024 µg/mL against other strains we tested. The MBCs of ibuprofen against all the strains were above our detection limit. The MICs of SCC1 and SCC1-IBU against PA O1-V, PA M57-15, PA RR05, PA LF05 were not significantly different from the MICs of tobramycin. Interestingly, the MICs of SCC1 and SCC1-IBU against PA HP3 were 4 and 8 µg/mL, respectively, significantly lower than the MIC of tobramycin against PA HP3, 15 µg/mL. The MIC for J53 lacking the silver-resistant plasmid was 0.5 µg/mL for both SCC1 and SCC1-IBU and 1 µg/mL for tobramycin. In contrast, the MIC of SCC1 and SCC1-IBU for J53 containing pMG101 was greater than 20 µg/mL while the MIC of tobramycin remained unchanged, demonstrating that the antimicrobial activity of both SCC's is primarily due to the silver functionality. In 7 out of 10 isolates we tested, the MICs of SCC1-IBU were lower compared to the parent compound SCC1, suggesting that the incorporation of IBU moiety confers additional antimicrobial activity to the SCC1-IBU compound. Furthermore, in several instances, particularly against *Achromobacter xylosoxidans*, *Stenotrophomonas maltophilia,* and *Staphylococcus aureus*

bacterial strains, the MICs of both SCC1 and SCC1-IBU were improved compared with the MICs of tobramycin, a commonly used antibiotic for the treatment of cystic fibrosis patients. Additionally, determination of the minimum bactericidal concentration (MBC) of SCC1, SCC1-IBU, and Tobramycin against the tested strains was performed. With the exception of the silver resistant *E. coli* strain, SCC1 and SCC1-IBU appeared to be bactericidal for all of the strains tested, which indicate that both SCCs are capable of killing numerous bacterial strains at clinically achievable concentrations.

**Synergistic effect of ibuprofen and SCC1 against CF pathogens demonstrated by checkerboard assay.**

To explore the potential synergistic antimicrobial effects between SCC1 and ibuprofen, we tested SCC1 in combination with high-dose ibuprofen (50-100 µg/mL) against all the tested strains except *E. coli* J53 and J53+pMG 101 using a checkerboard assay. The MICs of SCC1 were reduced with the presence of 100 µg/mL ibuprofen (**Table 3**). Then, we used the fractional inhibitory concentration to interpret potential drug combination effects. Based on the FIC calculation performed using **Equation 1** and FIC interpretation in **Table 1**, we determined that SCC1 is synergistic with ibuprofen against all the test strains except PA RR05 and AX 22.

**Synergistic effects of ibuprofen and SCC1 demonstrated by endpoint CFU studies.**

Even though we observe a synergistic effect between SCC1 and ibuprofen against 9 out of 11 tested strains using a checkerboard assay, we further performed an end-point CFU study to investigate the effect of the combination therapeutic on CFU. The concentrations used in 24-hour end point CFU study were selected based on the checkerboard assay result. For the 24-hour end point CFU study, we selected SCC1 and ibuprofen concentrations at sub- or at individual MIC concentrations, but included the combinational MIC within the testing range. When we

supplemented with 50, 75 or 100 μg/mL ibuprofen to various concentrations of SCC1, the combination treatment achieved significant reduction in bacterial burden (**Figure 2A, B, and C**). The bacterial concentration of PA HP3 is ~$2.2\times10^9$ CFU/mL when treated with 0.5 μg/mL SCC1 alone. However, following supplementation with100 μg/mL naproxen, the bacterial numbers of PA HP3 were reduced to $1.9\times10^7$ CFU/mL (**Figure 2D**). Since a synergistic effect in an endpoint CFU study is defined as a $\geq$ 2-$\log_{10}$ reduction in bacterial burden compared with the most efficacious individual treatment, the aforementioned combination of aztreonam and naproxen demonstrated synergy in our endpoint CFU study.

***In vitro* anti-inflammatory properties of SCC1-IBU**

The goal of this work was to synthesize a nebulizable therapeutic capable of combining the potent antimicrobial properties of the silver carbene complex with the anti-inflammatory properties of ibuprofen. The MIC and MBC studies unequivocally demonstrate that the antimicrobial properties of the SCCs are retained, and in certain instances, enhanced by the conjugation of an ibuprofen moiety to SCC1. To demonstrate that the anti-inflammatory properties of ibuprofen are conserved following conjugation with SCC1, the release of IL-8 from a human bronchial epithelial cell line 16HBE was investigated (**Figure 3**). Following stimulation by 10 μg/mL LPS, an increase in IL-8 release was observed in the case of control (untreated) cells. However, upon treatment with 60 μM ibuprofen or SCC1-IBU, these effects were mitigated and a decline in IL-8 concentration in the supernatant was observed ($p\leq0.0001$ for comparison between control and ibuprofen or control and SCC1-IBU). Treatment with 60 μM SCC1 also led to a reduction in the release of the pro-inflammatory cytokine IL-8 from 16 HBE cells ($p\leq0.0001$ for comparison with control). While both SCC1 and ibuprofen appeared to be equally effective in attenuating the release of IL-8 following LPS stimulation ($p = 0.9513$ for comparison between SCC1 and ibuprofen), SCC1-IBU

further reduced the quantity of IL-8 released from 16 HBE cells following LPS stimulation ($p = 0.0213$ for comparison between ibuprofen and SCC1-IBU and $p = 0.0061$ for comparison between SCC1 and SCC1-IBU). The inflammation in CF airways is dominated by neutrophils, and IL-8 is a potent neutrophil chemoattractant that drives this inflammatory response inside lung (260). Stimulation of IL-8 secretion can occur through multiple pathways including NF-kB dependent and NF-kB independent prostaglandin E2 (PEG-2) receptor pathway (261). Down-regulation of IL-8 production in the CF respiratory epithelium may be beneficial, because it would attenuate neutrophil-dominated inflammation and its negative consequence in the CF lung (262). Mechanistically, ibuprofen is conventionally known to act on cyclooxygenase (COX) resulting in suppression of prostaglandin synthesis and more recently, it has been demonstrated to down-regulate leukotriene 4 (unknown mechanism) (263), and suppress activity of NF-kB (264). By demonstrating that SCC1-IBU has further reduced levels of IL-8 secretion compared with either SCC1 or IBU, we have shown that SCC1-IBU has superior anti-inflammatory activity, in addition to its superior antimicrobial against CF pathogens.

***In vitro* toxicity of SCC1-IBU**

As a final measure, preliminary *in vitro* cytotoxicity of SCC1 and SCC1-IBU was evaluated in order to establish the safety profile for both drug candidates (**Figure 4**). Studies performed with 16HBE cells demonstrate an $IC_{50}$ of 170.3 μM (63.9 μg/mL) for SCC1 and 170.7 μM (88.9 μg/mL) for SCC1-IBU, respectively. Therefore, the incorporation of an ibuprofen moiety on the SCC1 molecule does not appreciably change the $IC_{50}$ compared with the parent molecule (SCC1). The $MIC_{90}$ of SCC1, SCC1-IBU, and tobramycin were 6 μg/mL, 2 μg/mL, and >20 μg/mL, respectively for non-silver resistant organisms tested. Furthermore, there exists at least an order of magnitude difference between the $MIC_{90}$ and $IC_{50}$ of SCC1-IBU, suggesting the

availability of a broad window over which the therapeutic agent may be employed. Previous studies performed with murine tracheal epithelial cells (MTEC) exposed to SCC1 demonstrated no significant consistent transcriptional change at any concentration tested (255). Furthermore, no dose responsive genes among the small, likely insignificant, number that did appear to be > 2-fold altered were found (255). Additional studies performed with MTECs using SCC1 demonstrated toxicity to ciliated epithelial cells at concentrations exceeding 50 μg/mL and to all epithelial cell types at concentrations of 500 μg/mL (265). While such detailed studies with SCC1-IBU are currently underway, preliminary results similar to SCC1 are suggestive of a favourable safety profile.

One possible explanation for these enhanced anti-inflammatory effects may stem from the caffeine base. Xanthines other than caffeine has been used medicinally as central nervous stimulants, diuretics, and as inhibitors of cyclic adenosine monophosphate (cAMP) phosphodiesterase resulting in smooth muscle relaxation of the airway (266). Several xanthine derivatives have been shown to have anti-inflammatory effects in the airways including aminophylline, theophylline, and pentoxifylline (267-269). Use of caffeine as a central nervous stimulant to treat apnea of prematurity is associated with a decreased risk of bronchopulmonary dysplasia (BPD) (270). A very recent publication by Weichelt et al. has shown that caffeine prevents hyperoxia-mediated pulmonary inflammation in neonatal rats suggesting that the caffeine related reduction in BPD may be due, in part, to anti-inflammatory effects (271). However, other reported inflammation models have demonstrated a lack of inflammation attenuation by caffeine at physiologically relevant doses (272). To date, no studies have linked the anti-inflammatory properties of SCC1 to the xanthine portion of the molecule. However, from these data it is clear

that further studies are needed to fully investigate the role that NSAIDs can serve in enhancing the anti-inflammatory and antimicrobial properties of this new class of metallopharmaceuticals.

**SCC1-IBU extended mice survival length significantly in an acute pneumonia infection.**

We have demonstrated that SCC1-IBU has both anti-inflammatory and antimicrobial properties. Hence, we decided to test the efficacy of SCC1-IBU in a murine pneumonia model. Mice were intranasally infected with PAHP3 and treated with either 1) sham, 2) ibuprofen, 3) SCC1, or 4) SCC1-IBU via nebulization and monitored for survival. Infected mice were treated every 12 hours for up to 5 doses. The experiment lasted 48 hours. At 48 hours, infected mice treated with SCC1-IBU demonstrated a significantly longer survival time over the groups of mice treated with individual drugs or sham (**Figure 5**).

**Conclusions**

In conclusion, the antimicrobial, anti-inflammatory, and cytotoxicity properties of SCC1-IBU were tested and compared to the well-studied caffeine derived silver carbene complex SCC1. It was demonstrated that SCC1-IBU exhibits enhanced antimicrobial and anti-inflammatory activity compared to SCC1 while demonstrating slightly lower toxicity against human bronchial epithelial cells. In addition, these studies also revealed the unexpected anti-inflammatory properties of SCC1.

**Table 2. MICs and MBCs of selected CF strains with treatment of SCC1, SCC1-IBU, ibuprofen, and tobramycin (Unit: μg/mL).**

| Strains | SCC1 | | SCC1-IBU | | Tobramycin | | Ibuprofen | |
|---|---|---|---|---|---|---|---|---|
| | MIC | MBC | MIC | MBC | MIC | MBC | MIC | MBC |
| PA O1-V | 1 | 2 | 2 | 6 | 4 | 8 | >1024 | >1024 |
| PA M57-15 | 2 | 4 | 1 | 2 | 0.5 | 1 | >1024 | >1024 |
| PA RR05 | 0.5 | 1 | 0.25 | 2 | 0.5 | 1 | >1024 | >1024 |
| PA HP3 | 4 | 8 | 0.25 | 2 | 15 | >20 | 512 | >1024 |
| AX 22 | 0.5 | 2 | 0.5 | 2 | 20 | >20 | >1024 | >1024 |
| AX RE05 | 4 | 8 | 1 | 2 | >20 | >20 | >1024 | >1024 |
| SM AH06 | 4 | 8 | 1 | 2 | 8 | 20 | >1024 | >1024 |
| SA LL06 | 8 | 10 | 2 | 6 | >20 | >20 | >1024 | >1024 |
| SA EH05 | 6 | 20 | 2 | 4 | >20 | >20 | >1024 | >1024 |
| J53 | 0.5 | 1 | 0.5 | 0.5 | 1 | 1 | >1024 | >1024 |
| J53+pMG101 | >20 | >20 | >20 | >20 | 1 | 1 | >1024 | >1024 |

**Table 3. The MICs of combining SCC1 and ibuprofen against selected CF strains.**

| Strain | SCC1+IBU | FIC | FIC interpretation |
|---|---|---|---|
| PA O1-V | 0.25/100 | 0.35 | Synergy |
| PA M57-15 | 0.25/100 | 0.22 | Synergy |
| PA RR05 | 0.25/100 | 0.59 | Additive |
| PA HP3 | 0.25/100 | 0.26 | Synergy |
| AX 22 | 0.25/100 | 0.59 | Additive |
| AX RE05 | 0.25/100 | 0.16 | Synergy |
| SM AH06 | 0.25/100 | 0.16 | Synergy |
| SA LL06 | 1/100 | 0.22 | Synergy |
| SA EH05 | 1/100 | 0.36 | Synergy |

**Figure 2. Synergy demonstrated between SCC1 and ibuprofen against *P. aeruginosa* isolate PAHP3.**

Synergy demonstrated between SCC1 at A) 0.0625 µg/mL, B) 0.125 µg/mL, C) 0.25 µg/mL, and D) 0.5 µg/mL and ibuprofen against *Pseudomonsa aeruginosa* (PA) HP3 by endpoint colony forming unit (CFU) study after 24-hour incubation with the drug concentration ratios (in µg/mL) indicated under each panel. 0: bacterial CFU without drug treatment; S: bacterial CFU treated with SCC1; I: bacterial CFU treated with ibuprofen (IBU); C: bacterial CFU treated with SCC1 in combination with ibuprofen at the ratio indicated. Data are shown as mean and standard deviation (n = 6). Statistical significance determined by one-way ANOVA followed by Tukey's multiple comparison test (**** $p \leq 0.0001$).

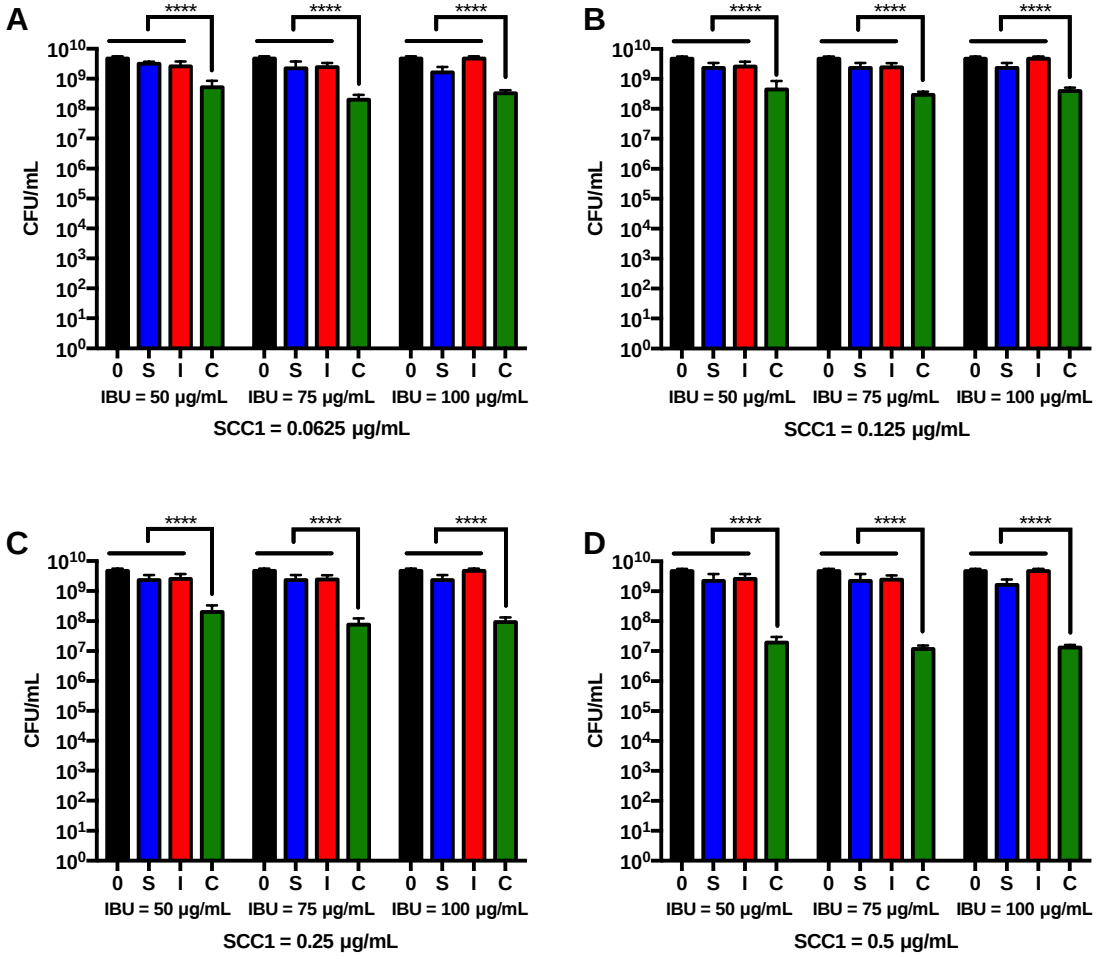

**Figure 3. IL-8 levels in supernatants following stimulation of human bronchial epithelial cells, 16HBE.**

IL-8 levels in supernatants following stimulation of human bronchial epithelial cells (16HBE) with LPS (10 μg/mL) and subsequent treatment with 60 μM ibuprofen or SCC1-IBU. (* $p \leq 0.05$). (Experiment was performed by Parth Shah and Justin Smolen.)

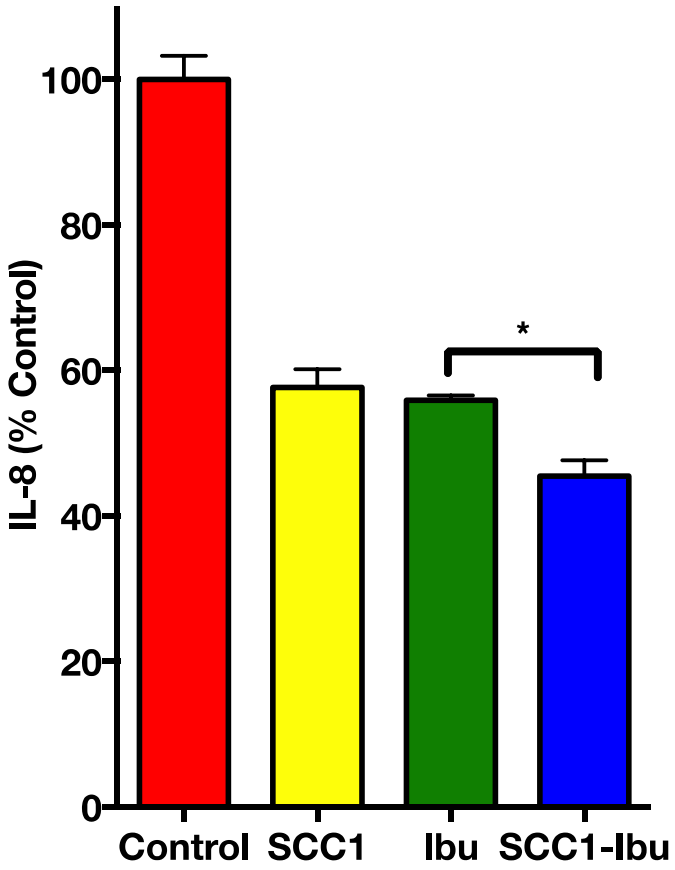

**Figure 4. Cytotoxicity of SCC1-IBU compared with SCC1.** $IC_{50}$ determination of SCC1 and SCC1-IBU on 16HEB cells using alamarBlue®. (Experiment was performed by Parth Shah and Justin Smolen.)

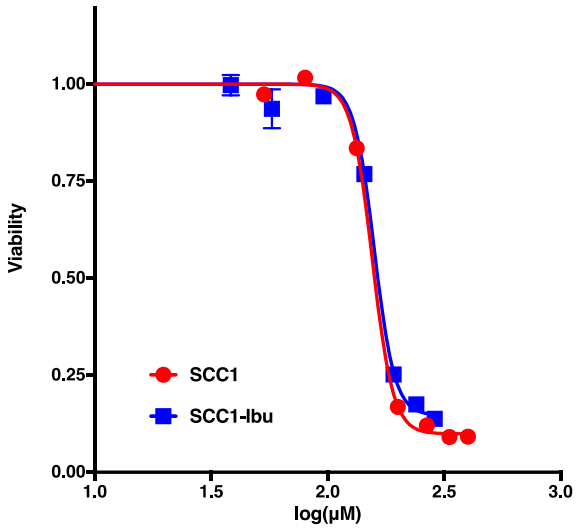


**Figure 5. The survival curve of mice treated SCC1-IBU.** SCC1-IBU demonstrated a significant survival advantage in a murine pneumonia model (n=6). Statistical significance determined by Mantel-Cox test (** indicates $p \leq 0.01$).

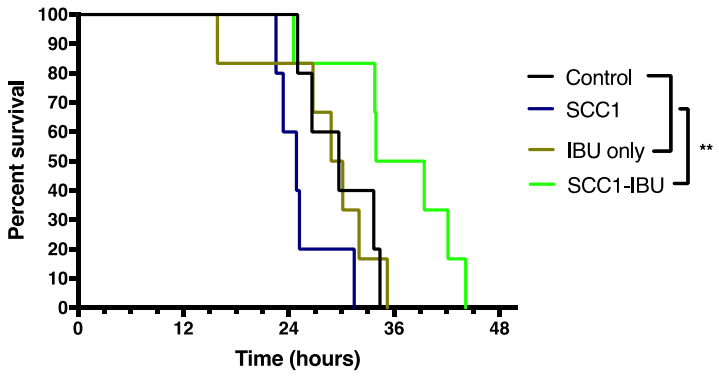

# CHAPTER III[1]

# MINOCYCLINE AND SILVER DUAL-LOADED POLYPHOSPHOESTER-BASED NANOPARTICLES FOR TREATMENT OF RESISTANT *Pseudomonas aeruginosa*

## Introduction

Several reports, including those by our research group, have demonstrated improved clinical outcomes when infections are treated with nanoparticle devices (273). These improvements in treatment outcomes are often achieved with reduced drug dosages and fewer side effects compared with unencapsulated drug treatments. The high localized therapeutic concentrations achieved by nanoparticles often overwhelm drug resistance mechanisms in pathogens, thereby improving the antimicrobial efficacy against drug resistant pathogens (274). Through the use of engineered nanoparticles, many antimicrobial agents with poor solubility, unfavorable pharmacokinetics, or poor penetration into diseased tissues can be successfully delivered at optimal therapeutic concentrations to eradicate MDR pathogens (275; 276).

We have previously demonstrated the ability of non-degradable and degradable nanoparticle formulations to shield silver from biological inactivation (276; 277). For example, shell crosslinked knedel-like (SCK) nanoparticles exhibit comparable antimicrobial efficacy to silver-based small molecules *in vitro* and superior *in vivo* efficacy in a murine *P. aeruginosa* acute lung infection model (276; 278). We first introduced SCKs in the 1990s to overcome the micellar dissociation and enhance structural stability (279). The crosslinking provides structural stability to polymeric micelles, maintains its size and shape, and improves the ability for chemical

[1] Reprinted with permission from "Minocycline and Silver Dual-loaded Polyphosphoester-Based Nanoparticles for Treatment of Resistant *Pseudomonas aeruginosa*" Qingquan Chen, Kush N. Shah, Fuwu Zhang, Adam J. Salazar, Parth N. Shah, Richen Li, James C. Sacchettini, Karen L. Wooley, and Carolyn L. Cannon. *Molecular Pharmaceutics* 2019 16 (4), 1606-1619, Copyright 2019 American Chemical Society.

modification. The SCK nanoparticles offer a versatile platform for efficient delivery of antimicrobials. The unique micellar structure comprising of a hydrophobic core and hydrophilic shell allows for co-delivery of two unique therapeutics (280) . Further, the physico-chemical properties and surface characteristics of SCK nanoparticles, including hydrophilicity, density and porosity of the core and shell, can also be easily customized. For instance, the molecular weight and length of the amphiphilic polymeric chain is directly linked to the nanoparticle size and can be utilized to precisely tune the nanoparticle size (281). The amphiphilic block terpolymer comprising the SCKs was designed and synthesized to provide unique characteristics, such as efficient loading of silver ions by reversible interactions to alkyne side chain moieties, as well as ability to penetrate the thick mucus encountered in the lungs of CF patients (277). These nanoparticles provide sustained release, shield the therapeutic from biological interactions, and can be localized at the infection site (282) resulting in a reduction in number of doses, as well as propensity of resistance acquisition.

Several groups have reported synergy with antimicrobials when used in combination with silver (283). A tobramycin/silver combination at specific concentrations exerts synergistic antimicrobial activity against *P. aeruginosa* biofilms (284). Thus, combination therapeutic strategies demonstrate tremendous potential and have been employed with FDA approved SoC antibiotics. However, such combinations need careful dose calibrations, as well as efficient delivery systems to eliminate potential pitfalls of both therapeutics. To enhance the efficacy of silver, we performed a high-throughput screen to identify potential antimicrobials with activity against *P. aeruginosa* that may synergize with silver. We identified 4-epi-minocycline, previously considered an inactive metabolite of minocycline (285; 286), as a molecule with antimicrobial activity against *P. aeruginosa*. Minocycline is a broad-spectrum bacteriostatic agent that inhibits

protein synthesis and demonstrates potent antimicrobial activity (287; 288). In addition, minocycline also exhibits favorable absorption and pharmacokinetic properties upon oral or intravenous administration (289). Because of these favorable characteristics and potent antimicrobial activity against Gram-positive and Gram-negative bacteria, i.v. minocycline was reintroduced in 2009 as an alternative therapy to treat MDR bacterial infections (290). Minocycline, including its i.v. formulation, has also been used as an alternative therapeutic against *Staphylococcus aureus* and methicillin resistant *Staphylococcus aureus* (MRSA) (290) that are commonly found bacteria in CF lungs. We have evaluated the antimicrobial activity of 4-epi-minocycline against clinical isolates of *P. aeruginosa* and MRSA obtained from CF patients. Further, we evaluated the efficacy of the parent drug, minocycline, and have demonstrated comparable antimicrobial activity to 4-epi-minocycline. Next, we investigated the potential synergistic activity of the silver/minocycline combination against *P. aeruginosa* and MRSA using checkerboard and end-point colony forming unit (CFU) determination assays. Finally, we expand upon previously reported nanoparticle formulations loaded with silver cations[29]. We have taken advantage of the unique design of these nanoparticles and leveraged our expertise to incorporate both minocycline (core) and silver (shell) with the goal of developing novel formulations that provide sustained release of two therapeutics and shield them from biological interactions. Thus, we have investigated the potential of a silver/minocycline combination as a next-generation antibiotic to combat the threats presented by MDR pathogens.

## Materials and Methods

### Materials

4-epi-minocycline (Chemos GMBH, Germany), minocycline hydrochloride (Sigma-Aldrich), silver acetate (Sigma-Aldrich), dimethyl sulfoxide (DMSO) (Sigma-Aldrich), Mueller

Hinton (MH) broth (BD Difco), tryptic soy agar plates (BD BBL), sheep blood agar plates (BD), 2,2'-(ethylenedioxy)bis(ethylamine) (Sigma-Aldrich), 1-[3'-(dimethylamino)propyl]-3-ethylcarbodiimide methiodide (Sigma-Aldrich). The Spectra/Por dialysis membranes (MWCO 6-8 kDa) were purchased from Spectrum Laboratories, Inc (Rancho Dominguez, CA). Nanopure water (18 MΩ•cm) was acquired by means of a Milli-Q water filtration system, Millipore Corp. (Bedford, MA).

**Preparation of drug solutions**

4-epi-minocycline was dissolved in DMSO and minocycline hydrochloride was dissolved in autoclaved water (Milli-Q synthesis system; Millipore Corp., Billerica, MA) to prepare stock solutions at a final concentration of 1.0 mg/mL and stored at -80 °C until use. A fresh stock solution of 1.0 mg/mL silver acetate was reconstituted in autoclaved water before each experiment.

**Preparation and characterization of aSCKs**

Briefly, a polyphosphoester-based anionic amphiphilic diblock copolymer was synthesized from poly(2-ethylbutyl phospholane)-*block*-poly(butynyl phospholane) by a "click" type thiol-yne reaction with 3-mercaptopropanoic acid (291; 292). Then, the anionic diblock copolymers (623 mg, 2.08 mmol of acrylic acid) were suspended into nanopure water (60.0 mL) and sonicated for 10 min. The clear solution was stirred for another 1 h to obtain well dispersed micelles, followed by the addition of a solution of 2,2'-(ethylenedioxy)bis(ethylamine) (EDDA, 46.1 mg, 0.311 mmol) dropwise in nanopure water (10.0 mL). The solution was allowed to stir for 1 h at room temperature. To this reaction mixture was added dropwise a solution of 1-[3'-(Dimethylamino)propyl]-3-ethylcarbodiimide methiodide (EDCI, 204 mg, 0.687 mmol) in nanopure water (10.0 mL) via a syringe pump over 1 h. The reaction mixture was allowed to stir overnight at room temperature and was then transferred to presoaked dialysis membrane tubes

(MWCO ca. 12–14 kDa), and dialyzed against nanopure water for 36 h in the cold room (4–8 ºC) to remove small molecules. The purified anionic SCK (aSCK) solution was lyophilized into powder and kept in the freezer at -20 ºC.

**Silver loading into aSCKs**

In a typical experiment, aSCKs (250 mg) were dissolved in 25.0 mL of nanopure water and sonicated for 5 min. Silver acetate (100 mg) in 20.0 mL of nanopure water was added, and the mixture solution was shaded with aluminum foil and stirred overnight. The solution was transferred to a centrifugal filter device (100 kDa MWCO), and washed extensively for several cycles (n>3) with nanopure water to remove free small molecules. The purified samples were lyophilized and stored at -20 ºC. The amount of silver loaded into the micelles was quantified by ICP-MS using rhodium as an internal standard. The drug loading efficiency was determined to be 28%, with a 10.1% silver loading (mass of silver / total mass of drug-loaded aSCKs).

**Minocycline loading into aSCKs**

In a typical experiment, aSCKs (5.0 mg) were dissolved in 3.0 mL of nanopure water and sonicated for 5 min. Minocycline hydrochloride (1.5 mg) in 1.0 mL of nanopure water was added, and the mixture solution was shaded with aluminum foil and stirred overnight. The solution was transferred to a centrifugal filter device (100 kDa MWCO), and washed extensively for several cycles (n>3) with nanopure water to remove free small molecules. The purified samples were lyophilized and stored at -20 ºC. The amount of minocycline hydrochloride loaded into the micelles was quantified by UV-Vis using absorbance at 345 nm. The drug loading efficiency was determined to be 40%, with a 10.8% minocycline hydrochloride loading (mass of minocycline hydrochloride / total mass of drug-loaded aSCKs).

**Dual loading into aSCKs**

In a typical experiment, Ag-loaded aSCKs (9.2 mg, containing 0.92 mg silver) were dissolved in 5.0 mL of nanopure water and sonicated for 5 min. Minocycline hydrochloride (2.8 mg) in 1.8 mL of nanopure water was added, and the mixture solution was shaded with aluminum foil and stirred overnight. The solution was transferred to a centrifugal filter device (100 kDa MWCO), and washed extensively for several cycles (n>3) with nanopure water to remove free small molecules. The purified samples were lyophilized and stored at -20 ºC. The amount of minocycline hydrochloride loaded into the micelles was quantified by UV-Vis using absorbance at 345 nm, while the amount of silver loaded into the micelles was quantified by ICP-MS using rhodium as an internal standard. The drug loading efficiency for minocycline hydrochloride was determined to be 51%, with a 13.4% minocycline hydrochloride loading (mass of minocycline hydrochloride / total mass of drug-loaded aSCKs).

**Release of drugs from nanoparticles**

The release profiles of the drug-loaded aSCKs were studied by monitoring the decrease of drug concentration over time in dialysis cassettes by ICP-MS or UV-Vis. In a typical procedure, drug-loaded aSCKs (3.0 mL) were transferred into a presoaked dialysis cassette. The cassette was allowed to stir in a beaker containing 3000 mL nanopure water at 37 ºC. Aliquots (*ca*. 0.05 mL) were taken at pre-determined timepoints up to 50 hours. Silver and minocycline hydrochloride concentrations were determined by ICP-MS and UV-Vis, respectively. The release experiments were conducted in triplicate.

**Bacterial culture**

Clinical isolates of *P. aeruginosa* (PA 0531, PA 0540, PA 0545, PA 0551, PA 0552, PA 0554, PA 0557, PA 0561, PA HP3, PA M57-15, and PA O1) were streaked from frozen stocks

onto tryptic soy agar (TSA) plates and incubated overnight at 37 °C. A single bacterial colony was then suspended in MH broth and allowed to grow at 37 °C in a shaking incubator at 200 rpm to an $OD_{650}$ of 0.4, which corresponds to ~5 $\times 10^8$ CFU/mL. Bacterial cultures were adjusted to 5 $\times$ $10^8$ CFU/mL to prepare a working stock for all experiments.

**High-throughput screen**

*P. aeruginosa* strain PA O1 was streaked onto LB agar plates and incubated overnight at 37 °C. A single bacterial colony was re-suspended in LB broth and grown overnight at 37 °C in a shaking incubator at 200 rpm. Compounds from the "SAC1" Sacchettini lab diversity library (~50,000 unique compounds assembled in house; 1mM in 100% DMSO) were transferred to clear 384-well assay plates (1.5 µL). The overnight culture was then diluted to an $OD_{600}$ of 0.005 in fresh LB and aliquoted to assay plates (60 µL). Following a 2-hour incubation at 37 °C, 0.2 mM filtered resazurin dye (0.05% w/v) was added (3 µL). After an additional hour of incubation, the absorbance at 573 nm and 605 nm was measured on a POLARstar Omega plate reader. Percent inhibition of each compound was calculated according to the following equation: % Growth = ($\omega$ - $\bar{x}p$)/($\bar{x}n$ - $\bar{x}p$) x 100%, where values of $\omega$ (sample), p (positive control), and n (negative control) were determined by the difference between sample absorbance values ($OD_{573}$-$OD_{605}$). Trimethoprim (100 µM) and DMSO were used as positive and negative controls, respectively.

***In vitro* antimicrobial activity**

Minimum inhibitory and bactericidal concentrations (MIC and MBC) were determined according to the standard Clinical and Laboratory Standards Institute (CLSI) broth-microdilution method. Briefly, 100 µL working stock of bacterial suspension was added to each well (n=3) containing 100 µL silver acetate, 4-epi-minocycline, or minocycline solution in a 96 well plate. All solutions were comprised of 95% MH broth and 5% (v/v) DMSO. Bacteria were incubated

with 0.06, 0.13, 0.25, 0.5, 1, 2, 4, 8, 16, 32, 64, 128 μg/mL minocycline or 4-epi minocycline, or 0.13, 0.25, 0.5, 1, 2, 4, 8, 16, 32 μg/ml silver acetate at 37 °C for 18 - 24 hours under static conditions. The final concentration of DMSO in the assay was 2.5% (v/v). The MIC was determined as the lowest concentration that did not show any signs of bacterial growth upon visual inspection. Finally, the MBC was determined by plating the bacterial solutions demonstrating growth inhibition on blood agar plates and recording the lowest concentration that resulted in no growth after an 18 – 24 hour incubation at 37 °C. All experiments were performed in triplicate. The color codes indicate the drug resistance cutoffs for minocycline against *S. aureus* as published by CLSI. Green, yellow, and red indicate if a particular *S. aureus* isolate is susceptible, intermediate susceptible, or resistant to minocycline, respectively. A similar scale was adopted for *P. aeruginosa.*

**Determination of synergistic drug combinations**

Four *P. aeruginosa* isolates (PA 0540, PA 0557, PA HP3, and PA O1) were selected based on their sensitivity to silver acetate and minocycline. The selection criteria included one strain from each of the following categories; sensitive to both drugs, resistant to both drugs, or sensitive to one drug and resistant to the other drug. Hence, we selected PA O1, which is sensitive to both drugs; PA 0540, which is sensitive to silver acetate and resistant to minocycline; PA HP3, which is sensitive to minocycline and resistant to silver acetate; and, PA 0557, which is resistant to both drugs. A dynamic concentration scale based on the MIC and MBC values was used to determine the optimal ratio of synergistic concentrations between the two therapeutic agents. The final solutions were comprised of 95% MH broth and 5% DMSO. A 100 μL working stock of bacterial suspension was incubated with a 100 μL solution of therapeutic agents (n = 3) for 18 hours at 37 °C. Final drug concentrations incubated with each bacterial isolate is mentioned in **Table 4**. Wells

demonstrating bacterial growth inhibition were identified visually to determine a synergistic MIC. All experiments were performed in duplicate. To evaluate for potential synergy, the fractional inhibitory concentration (FIC) was calculated as shown in **Equation 1** and defined in **Table 1**.

Four MRSA bacterial strains (SA LL06, SA EH05, MRSA 0608, and MRSA 0631) were selected based on their sensitivity to silver acetate and minocycline. The criterion for selection included one strain from each of the following categories; sensitive to both drugs, resistant to both drugs, or sensitive to one drug and resistant to the other drug. SA LL06 is sensitive to both drugs. SA EH05 is sensitive to silver and resistant to minocycline. MRSA 0631 is resistant to silver and sensitive to minocycline. MRSA 0608 is resistant to both drugs. A dynamic concentration scale based on the MIC and MBC values was used to determine the optimal ratio of synergistic concentrations between the two therapeutic agents. The final solutions were comprised of 95% MH broth and 5% DMSO. A 100 μL working stock of bacterial suspension was incubated statically with a 100 μL solution of therapeutic agents (n = 3) for 18 hours at 37 °C. Final drug concentrations for each bacterial strain are mentioned in **Table 5**. Wells demonstrating bacterial growth inhibition were identified visually to determine a synergistic MIC. All experiments were performed in duplicate.

**Table 4. Concentrations of silver acetate and minocycline hydrochloride incubated with select *P. aeruginosa* isolates to determine synergistic activity.**

Bacteria were incubated with a combination of each of the drugs at the following concentrations. **(**Reprinted with permission from "Minocycline and Silver Dual-loaded Polyphosphoester-Based Nanoparticles for Treatment of Resistant *Pseudomonas aeruginosa*" Qingquan Chen, Kush N. Shah, Fuwu Zhang, Adam J. Salazar, Parth N. Shah, Richen Li, James C. Sacchettini, Karen L. Wooley, and Carolyn L. Cannon. *Molecular Pharmaceutics* 2019 16 (4), 1606-1619, Copyright 2019 American Chemical Society.)

| **Strain** | **Silver Acetate Concentration (µg/mL)** | **Minocycline.HCl Concentration (µg/mL)** |
|---|---|---|
| PA O1 | 1, 2, 3, 4, and 6 | 1, 2, 4, 8, 16, and 32 |
| PA HP3 | 2, 4, 6, 8, and 16 | 1, 2, 4, 8, 16, and 32 |
| PA 0540 | 1, 2, 3, 4, and 6 | 4, 8, 16, 32, 64, and 128 |
| PA 0557 | 2, 4, 6, 8, and 16 | 2, 4, 8, 16, 32, and 64 |

**Table 5. Concentrations of silver acetate and minocycline hydrochloride incubated with select MRSA strains to determine synergistic activity.**

Bacteria were incubated with a combination of each of the following concentrations. **(**Reprinted with permission from "Minocycline and Silver Dual-loaded Polyphosphoester-Based Nanoparticles for Treatment of Resistant *Pseudomonas aeruginosa*" Qingquan Chen, Kush N. Shah, Fuwu Zhang, Adam J. Salazar, Parth N. Shah, Richen Li, James C. Sacchettini, Karen L. Wooley, and Carolyn L. Cannon. *Molecular Pharmaceutics* 2019 16 (4), 1606-1619, Copyright 2019 American Chemical Society.)

| **Strain** | **Silver Acetate Concentration (µg/mL)** | **Minocycline.HCl Concentration (µg/mL)** |
|---|---|---|
| SA LL06 | 4, 8, 16, 32, and 64 | 0.06, 0.13, 0.5, 1, 2, and 4 |
| SA EH05 | 2, 4, 8, 16, and 32 | 0.13, 0.5, 1, 4, 32, and 128 |
| MRSA 0608 | 4, 8, 16, 32, and 64 | 1, 2, 8, 32, 64, and 128 |
| MRSA 0631 | 4, 8, 16, 32, and 64 | 0.06, 0.13, 0.5, 1, 2, and 4 |

**Determination of bacterial burden for synergistic drug combinations**

Potential synergy between combinations of silver acetate and minocycline against *P. aeruginosa* isolates PA 0557 and PA 0540 at a final concentration of $10^6$ CFU/mL were determined using a 24-hour end point CFU study performed in triplicate. The concentrations of silver acetate tested against PA 0557 were 1, 2, and 4 μg/mL and the concentrations of minocycline tested were 2, 4, 8, and 16 μg/mL. Individual drugs served as controls. The concentrations of silver acetate tested individually against PA 0557 were 1, 2, 4, 6, and 8 μg/mL and the tested concentrations of minocycline alone were 4, 8, 16, 32, and 64 μg/mL. The concentrations of silver acetate tested against PA 0540 were 0.13, 0.25, 0.5 and 1 μg/mL and the concentrations of minocycline tested were 16, 32, and 64 μg/mL. Individual drugs served as controls. The concentrations of silver acetate tested individually against PA 0540 were 0.13, 0.25, 0.5, and 1 μg/mL and the tested concentrations of minocycline alone were 16, 32, and 64 μg/mL. Synergy was defined as $\geq$2 $\log_{10}$ CFU/mL reduction between combined agents and the most effective individual agent at 24 hours (293).

The bacterial concentrations (CFU) of PA 0557 were also determined after incubation with combinations of free drugs, as well as dual-loaded nanoparticles. Individual drugs at concentrations corresponding to those tested in combination, as well as blank nanoparticles, served as controls. The ratio of silver acetate to minocycline was maintained at 1:0.87 (w/w) for all combinations to mirror the drug loading in the dual-loaded nanoparticles. The tested concentrations of silver acetate and minocycline were 1, 2, 4, 6, and 8 μg/mL and 0.87, 1.74, 3.48, 5.22, 6.96 μg/mL, respectively. A 100 μL working stock of bacterial suspension was incubated with 100 μL drug solution (n = 4) in each well of a 96 well plate at 37 °C for 24 hours with constant shaking at 100 RPM. The final solutions were comprised of 97.5% MH broth and 2.5% (v/v)

DMSO. Finally, a 10-fold serial dilution was performed in MH broth with the bacterial suspension from each well and 50 μL of each dilution was plated onto a blood agar plate. Plates were incubated for 18 hours and colonies counted to determine the CFU for each condition. The potential synergistic effects between silver acetate and minocycline were determined as described above. All experiments were performed in duplicate.

Potential synergy between combinations of silver acetate and minocycline against MRSA strains SA EH05 and MRSA 0608 at a final concentration of $10^6$ CFU/mL were determined through a 24-hour end point CFU study performed in triplicate. The concentrations of silver acetate tested against SA EH05 were 1, 2, and 4 μg/mL and the concentrations of minocycline tested were 0.06, 0.13, 0.5 and 1 μg/mL. The concentrations of silver acetate tested individually against SA EH05 were 2, 4, 8, 12, and 16 μg/mL and minocycline alone were 0.13, 0.25, 0.5, 1 and 2 μg/mL. The concentrations of silver acetate tested against MRSA 0608 were 0, 1, and 2 μg/mL. The concentrations of minocycline tested against MRSA 0608 were 0, 0.25, 0.5, and 1 μg/mL. Individual drugs served as controls.

The bacterial concentrations (CFU) of SA EH05 were determined after incubation with combinations of free drugs, as well as dual-loaded nanoparticles. Individual drugs at concentrations corresponding to those tested in combination, as well as blank nanoparticles, served as controls. The ratio of silver acetate to minocycline was maintained at 1:0.87 (w/w) for all combinations to mirror the drug loading in the dual-loaded nanoparticles. The tested concentrations of silver acetate and minocycline were 0.5, 1, 2, 8, and 12 μg/mL and 0.44, 0.87, 1.74, 6.96, 10.43 μg/mL, respectively. A 100 μL working stock of bacterial suspension was incubated with 100 μL drug solution (n = 3) in each well of a 96 well plate at 37 °C for 24 hours with constant shaking at 100 RPM. The final solutions were comprised of 97.5% MH broth and

2.5% (v/v) DMSO. Finally, a 10-fold serial dilution was performed in MH broth with the bacterial suspension from each well and 50 μL of each dilution was plated onto a blood agar plate. Plates were incubated for 18 hours and colonies enumerated to determine the CFU for each condition. The potential synergistic effects between silver acetate and minocycline were determined as described above.

**Transmission electron microscopy (TEM)**

The drug loaded nanoparticles suspended in aqueous solutions (4 μL) were deposited onto carbon-coated copper grids for 1 min and excess solution was wicked away with a piece of filter paper. For minocycline-loaded SCKs, a drop of 1 wt% uranyl acetate was then added and allowed to stand for 30 seconds before the excess stain was wicked away. No stain was used for silver-loaded SCKs and dual loaded SCKs. The grids were allowed to dry in air overnight. TEM images were collected using a JEOL 1200EX operating at 100 kV and micrographs were recorded at calibrated magnifications using a SIA-15C CCD camera.

Untreated bacteria, and bacteria treated with silver acetate, minocycline or both drugs, to be examined by transmission electron microscopy were pelleted and fixed in 2.5% glutaraldehyde and 1% acrolein in 0.2 M Sorensons Phosphate Buffer for 1 hour at room temperature. The fixed samples were stained with 1% aqueous osmium tetroxide overnight at 4 ℃. Samples were dehydrated with acetone and then infiltrated with resin. Subsequently, the samples were thin-sectioned in a microtome (Boeckeler MTX), post-stained in uranyl acetate and lead citrate, and then visualized on a JEOL 1200 EX electron microscope.

**Statistical analysis**

All statistics were calculated using JMP pro 13 for Macintosh (SAS Institute, Cary, North Carolina, USA, www.jmp.com). Differences between the treatments were investigated by one-

way ANOVA followed by Tukey's multiple comparison test (95% confidence intervals). * indicates $p \leq 0.05$, ** indicates $p \leq 0.01$, *** indicates $p \leq 0.001$, and **** indicates $p \leq 0.0001$.

**Results and Discussion**

The high rates of morbidity and mortality associated with MDR pathogens, particularly, MDR *P. aeruginosa*, pose a serious threat to the public health and call for accelerated development of novel treatment strategies. Several new antimicrobial strategies are being evaluated by research laboratories across the world. However, to expedite the regulatory approval processes, we have focused on the development of combination therapies that utilize existing SoC antimicrobials. We have established antimicrobial efficacy of several silver based small molecules (131; 243; 250; 276; 294). Moreover, silver, incorporated into bandages or creams, has been widely used for treatment of bacterial infections in burn and wound patients. However, the poor stability of these silver cations has limited its use to these topical applications. We have previously demonstrated the ability of nanoparticles to shield silver cations from such external factors and improve their bioavailability to address this limitation (276). To further enhance the antimicrobial efficacy of silver against MDR pathogens, as well as realize the full potential of SCK nanoparticles, we selected 4-epi-minocycline as the candidate for combination therapy identified from high throughput screening of a diverse compound library. The hydrophobic nature of 4-epi-minocycline allows us to incorporate it in the core-shell interfaces of the SCK nanoparticles *via* hydrophobic interaction & electrostatic interaction between amino groups of the drug and carboxylate groups in the hydrophilic shells, in conjunction with the silver cations loaded into the shell *via* electrostatic interaction with carboxylate groups & coordination with two sulfur atoms (28; 295-297). In addition, minocycline, an isomer of 4-epi-minocycline is an SoC antimicrobial with potent

antimicrobial activity against Gram-positive pathogens including MRSA. Thus, minocycline and its isomers, including 4-epi-minocycline, are ideal candidates for use as combination therapeutics.

High throughput screening identified 4-epi-minocycline as a potent inhibitor of *Pseudomonas aeruginosa*. In order to identify novel compounds with anti-pseudomonal activity for loading into aSCK nanoparticles, we screened a high diversity library of small molecules (SAC1) for inhibition of the clinical *P. aeruginosa* isolate, PA O1. Plates with high control variability, as indicated by control z' scores > 0.4, were removed from the resulting dataset. Of the remaining 39,340 compounds, nine hits were identified with > 90% growth inhibition (**Figure 6**). The properties of 4-epi-minocycline, including its high antimicrobial activity against PA O1 (98% inhibition) and hydrophobicity known to enhance loading into the core-shell interface of the aSCK nanoparticles (28; 295; 296), prompted the use of this inhibitor for further efficacy studies.

***In vitro* antimicrobial activity of silver acetate, 4-epi-minocycline, and minocycline against *Pseudomonas aeruginosa***

Minor structural differences between the parent compound, minocycline, and its isomer, 4-epi-minocycline, prompted further investigation into the activity of minocycline against these *P. aeruginosa* and MRSA isolates. We characterized the minimum inhibitory and bactericidal concentrations (MICs and MBCs) of 4-epi-minocycline, minocycline and silver acetate against 11 *P. aeruginosa* clinical isolates (**Table 3**). Silver acetate has consistent antimicrobial activity against *P. aeruginosa* with MICs between 4-6 μg/mL and MBCs between 4-8 μg/mL (**Table 3**). 4-epi-minocycline exhibits MICs similar to those of minocycline against eight of the eleven tested strains; whereas, it shows slightly lower MICs than minocycline against the remaining three strains (**Table 3**). With regards to MBCs, 4-epi-minocycline exhibits MBCs against PA 0554, PA 0557, and PA M57-15 that are lower than those of minocycline; whereas, the MBCs for 4-epi-

minocycline and minocycline are comparable for PA 0545 and PA 0551. In contrast, minocycline has lower MBCs against PA 0552, PA HP3, and PA O1 compared with 4-epi-minocycline. Finally, the MBCs of 4-epi-minocycline and minocycline are out of our detection range against PA 0531 and PA 0540 (Table 3). Minocycline and 4-epi-minocycline demonstrate comparable antimicrobial activity against the 11 *P. aeruginosa* strains tested (**Table 3**). In addition, minocycline demonstrates comparable or superior antimicrobial activity to 4-epi-minocycline against 11 MRSA strains tested (**Table 7**). This observed activity of minocycline is comparable to previously reported results (298), however, this is the first report of antimicrobial activity of 4-epi-minocycline, which is generally thought to be a pharmacologically inactive molecule (299-301). The tetracycline family, including minocycline, inhibits protein synthesis through binding via its hydrophilic surface to the 16S rRNA component of the 30S ribosomal subunit (302)s. A competition study has demonstrated that minocycline binds to the ribosomes in a fashion similar to tetracycline (303). Hence, owing to the structural similarities between minocycline and 4-epi-minocycline exerts, we believe that 4-epi-minocycline exerts antimicrobial activity via a mechanism similar to tetracycline and minocycline.

Silver, on the other hand, demonstrated lower MIC values, namely, 4 μg/mL for 7 of 8 strains and 6 μg/mL for another, compared with the MICs of both 4-epi-minocycline and minocycline, which were 4 μg/mL for only 3 of 8 strains, and ranged from 8 to 32 μg/mL for the remaining 5 *P. aeruginosa* strains (**Table 6**). Further, silver demonstrated relatively higher MIC values; MIC of 8 μg/mL against SAEH 05, MIC of 16 μg/mL against 4 of 11 tested MRSA strains and 24 μg/mL against 6 of 11 tested MRSA strains (**Table 7**). This antimicrobial activity of silver is in agreement with previous results (277; 304). These compounds have been evaluated individually as antimicrobial agents, however, their combinations with other antimicrobials have

yet to be explored as next-generation antimicrobials. Minocycline has been used by clinicians as a broad-spectrum antibiotic with well-established pharmacokinetics, pharmacodynamics, efficacy and safety profiles (305; 306). In addition, minocycline is known to epimerize into 4-epi-minocycline under mildly acidic conditions in the body and excreted as a metabolite (285; 286). Moreover, minocycline demonstrated similar or superior antimicrobial efficacy to 4-epi-minocycline against tested *P. aeruginosa* and MRSA isolates *in vitro*. Finally, 4-epi-minocycline is an impurity isolated during the synthesis of minocycline. Thus, the costs associated with synthesis, isolation, and purification of this epimer are significantly higher compared with minocycline. These parameters favored the use of minocycline over 4-epi-minocycline as the choice of drug for investigation in combination with silver.

**Additive effects of silver cations and minocycline demonstrated by checkerboard assay**

To explore the potential synergistic antimicrobial effects between silver cations and minocycline, we tested combined drugs against 4 *P. aeruginosa* and 4 MRSA isolates, selected based on the MICs of silver and minocycline, to identify the optimal ratio of the two drugs that delivers maximum therapeutic efficacy. The MICs of combined drugs summarized in **Table 8** are reduced compared with the MICs of silver cations or minocycline alone against PA 0540, PA 0557 and PA O1. FIC values were calculated[46] to identify synergistic and/or additive concentrations. However, based on the FIC calculations performed using **Equation 1**, we observe an additive effect for the combination of silver cations and minocycline, rather than a synergistic effect against PA 0540, PA 0557, PA O1, and all four tested MRSA isolates (**Table 8 and Table 9**). Combining silver cations and minocycline did not change the MIC of either drug tested alone against PA HP3 (**Table 8**). However, the poor sensitivity of the checkerboard assay, which relies on evaluating turbidity in each microdilution to detect bacteriostatic effects, is a major limitation of the assay.

**Synergistic effects of silver cations and minocycline demonstrated by endpoint CFU studies**

Even though we did not observe a synergistic effect between silver cations and minocycline against *P. aeruginosa* using a checkerboard assay, we performed an end-point CFU study to investigate the effect of the combination therapeutic on CFU. The concentrations used in 24-hour end point CFU study were selected based on the checkerboard assay result. For PA 0557, the combinational MIC of silver acetate and minocycline is 2 and 4 μg/mL. For PA 0540, the combinational MIC of silver acetate and minocycline is 1 and 32 μg/mL. Therefore, for 24-hour end point CFU study, we selected silver acetate and minocycline concentrations at sub or at individual MIC concentrations but including the combinational MIC within the testing range. The bacterial concentration of PA 0557 is ~$10^9$ CFU/mL when treated with 4 μg/mL silver acetate or minocycline alone. However, following exposure to a combination of 4 μg/mL silver acetate and 2 μg/mL minocycline, the bacterial burden of PA 0557 is reduced to less than $10^4$ CFU/mL (**Figure 7 A and B**). Since the synergistic effect in endpoint CFU study is defined as a $\geq$ 2-$\log_{10}$ reduction in bacterial burden compared with the most efficacious individual treatment, the aforementioned combination of silver cations and minocycline demonstrated synergy in our endpoint CFU study. We verified the synergy of this combination against an additional *P. aeruginosa* isolate, PA 0540. Upon treatment with a combination of 0.5 μg/mL silver acetate and 32 μg/mL minocycline, PA 0540 demonstrates a > 2-$\log_{10}$ reduction of bacterial burden, indicating synergy (**Figure 7C**). We have confirmed similar results with MRSA isolates SA EH05 and MRSA 0608 (**Figure 8)**. SAEH 05 upon treated with a combination of 4 μg/mL silver acetate and 0.13 μg/mL minocycline, demonstrates a >2-$\log_{10}$ reduction compared with individual drug treatments, indicating synergy (**Figure 8A**). Despite the significant reduction in the bacterial burden of MRSA 0608 treated with a combination of 2 μg/mL silver acetate and 0.5 μg/mL minocycline compared with individual

drug treatments, the reduction is less than 2-$\log_{10}$, which does not meet the synergy criterion established by CLSI (**Figure 8B**). Thus, although we observed a significant difference in the bacterial burden between the combination treated group and the individual drug treated groups, we did not identify synergistic effects between silver acetate in combination with minocycline against MRSA 0608 (**Figure 8B**). We speculate that, given the relatively higher MICs of silver acetate against MRSA, the potent activity of minocycline as an anti-staphylococcal drug eclipses the effect of the combination therapy.

**Transmission electron microscopy demonstrated the antimicrobial activity of silver cations and minocycline**

Transmission electron microscopy (TEM) was further used to confirm the morphological changes in *P. aeruginosa* after exposure to the silver/minocycline combination. In the absence of any treatment, *P. aeruignosa* showed typical cellular morphology with no damage to cellular components or membranes. When bacteria were exposed to silver cations at 4 μg/mL, electron-dense granules are observed along the bacterial membrane throughout the cross section of the samples at low and high magnifications. An irregular morphology and disintegration of the cellular components is also seen. DNA condensation is also observed in the center of bacteria. Gaps are observed between the cytoplasm membrane and the cell wall. In the presence of 2 μg/mL minocycline, membrane segmentation is observed in *P. aeruginosa* along with condensed and disintegrated cellular components. Leakage of the cellular components from the bacterial cells is also observed. The electron dense granule clusters likely represent deposition of silver at the outer bacterial membrane, as demonstrated by Sondi and Salopek-Sondi[65] and supported by Feng *et al.* (304). Similar to data reported by our group and others, silver-treated bacteria exhibit irregular cellular shape and ruptured membranes leading to leakage and efflux of cytoplasmic contents

(307). Gaps between the cytoplasm membrane and the cell wall is observed when bacteria are treated with minocycline. In addition to membrane rupture, minocycline-treated bacteria cells uniquely show spheroplasts in the lower magnification images, membrane segmentation, as well as condensation of the inner membrane and detachment from the outer membrane. Regardless of their targets, antibiotics that disrupt protein synthesis display unique cellular disruptions, which result in similar effects (308-310). Finally, following treatment of bacteria with both silver cations and minocycline, a combination of the previous observations, with silver deposition outside bacteria and segmentation of the bacterial membrane resulting in leakage of bacterial components is observed. In addition, electron-dense granules are seen in combination treated bacteria, but not with minocycline treated bacteria (**Figure 9**). As far as we are aware, we are the first group to document the effect of minocycline against *P. aeruginosa* through TEM images. The absence of such TEM images in the literature may be due to minocycline's common use as an anti-staphylococcal, but not as an anti-pseudomonal therapeutic.

The combination of silver and minocycline demonstrates tremendous potential as a combination therapy, however, low bioavailability of silver cations and the potential side effects of long-term minocycline dosing remain a concern (311). These pitfalls can be addressed by use of drug delivery devices such as nanoparticles. For instance, nanoparticles can be delivered directly to the lung, the site for *P. aeruginosa* infections in CF patients, minimizing interactions between the therapeutic and other organs (181). Previously, Shah *et al.* have demonstrated that silver loaded SCK nanoparticles achieve a 16-fold reduction in the amount of silver compared with free drug to attain a 60% survival advantage in an acute *P. aeruginosa* pneumonia model (276). Moreover, the silver loaded SCK nanoparticles were delivered in two doses compared with five doses required for free drug over a period of 72h. Thus, such localized drug administration into lung results in

lower systemic toxicity and adverse effects, reduction in the number of drug doses (276), as well as improved patient adherence (181). Nanoparticles with diameter less than 1 μm penetrate deeper into the alveolar region (178), while smaller particles with diameter less than 5 nm are typically cleared at a rapid pace from the lung by exhalation, as well as extravasation into the blood stream (312). Currently, the common nanoparticle drug formulations for lung therapeutics have diameters less than 500 nm to avoid alveolar macrophage uptake (312). We have engineered particles with diameters ranging between 12 and 22 nm. The average 3D mesh spacing in CF lung mucus is 230 ± 50 nm (313), while the pore size of *P. aeruginosa* biofilms has been found to be between 100 and 500 nm (314). The smaller NPs engineered here have the potential to overcome the mucus- and biofilm-associated obstruction in CF patients, as well as avoid opsonization by alveolar macrophages. Thus, by optimizing the nanoparticle size, we can achieve enhanced penetration into otherwise difficult to penetrate mucus and biofilm layers to achieve sustained release in close proximity to the bacteria hiding in these complex matrices.

**Table 6. MICs and MBCs of *Pseudomonas aeruginosa* strains with treatment of silver acetate, 4-epi- minocycline, and minocycline (Unit: μg/mL).**

(Reprinted with permission from "Minocycline and Silver Dual-loaded Polyphosphoester-Based Nanoparticles for Treatment of Resistant *Pseudomonas aeruginosa*" Qingquan Chen, Kush N. Shah, Fuwu Zhang, Adam J. Salazar, Parth N. Shah, Richen Li, James C. Sacchettini, Karen L. Wooley, and Carolyn L. Cannon. *Molecular Pharmaceutics* 2019 16 (4), 1606-1619, Copyright 2019 American Chemical Society.)

| **Drugs Names** / ***P.a.* Strains** | **Silver acetate** | | **4-epi-minocycline** | | **Minocycline** | |
|---|---|---|---|---|---|---|
| | **MIC** | **MBC** | **MIC** | **MBC** | **MIC** | **MBC** |
| PA O1 | 4 | 4 | 4 | 64 | 4 | 64 |
| PA 0531 | 4 | 6 | 32 | >128 | 32 | >128 |
| PA 0540 | 4 | 6 | 32 | >128 | 64 | >128 |
| PA 0545 | 4 | 6 | 4 | 64 | 4 | 64 |
| PA 0551 | 4 | 6 | 8 | 64 | 8 | 64 |
| PA 0552 | 4 | 4 | 8 | 128 | 16 | 64 |
| PA 0554 | 4 | 6 | 8 | 64 | 8 | 128 |
| PA 0557 | 6 | 6 | 8 | 32 | 8 | 64 |
| PA 0561 | 4 | 6 | 16 | >128 | 32 | >128 |
| PA HP3 | 4 | 8 | 8 | 32 | 8 | 32 |
| PA M57-15 | 4 | 6 | 4 | 32 | 4 | 32 |

| Drug Concentration | [drug]≤4 | 4<[drug]<16 | [drug]≥16 |
|---|---|---|---|

**Table 7. MIC and MBC of MRSA strains with treatment of 4-epi-minocycline, minocycline, and silver acetate (Unit: μg/mL).**

(Reprinted with permission from "Minocycline and Silver Dual-loaded Polyphosphoester-Based Nanoparticles for Treatment of Resistant *Pseudomonas aeruginosa*" Qingquan Chen, Kush N. Shah, Fuwu Zhang, Adam J. Salazar, Parth N. Shah, Richen Li, James C. Sacchettini, Karen L. Wooley, and Carolyn L. Cannon. *Molecular Pharmaceutics* 2019 16 (4), 1606-1619, Copyright 2019 American Chemical Society.)

| Drug Name / SA Strain | Silver Acetate | | 4-epi-minocycline | | Minocycline | |
|---|---|---|---|---|---|---|
| | MIC | MBC | MIC | MBC | MIC | MBC |
| MRSA 0606 | 24 | >32 | 0.13 | 128 | 0.13 | 128 |
| MRSA 0608 | 24 | >32 | 2 | 128 | 2 | 128 |
| MRSA 0611 | 24 | >32 | 2 | >128 | 2 | >128 |
| MRSA 0631 | 24 | >32 | 0.25 | 64 | 0.13 | 64 |
| MRSA 0633 | 24 | >32 | 0.13 | 128 | 0.13 | 64 |
| MRSA 0638 | 24 | >32 | 0.13 | 128 | 0.13 | 64 |
| MRSA 0641 | 16 | >32 | 4 | 64 | 4 | 64 |
| MRSA 0646 | 16 | >32 | 0.25 | 64 | 0.13 | 64 |
| SA EH05 | 8 | 12 | 1 | 64 | 1 | 128 |
| SA LL06 | 16 | >32 | 0.13 | 64 | 0.13 | 2 |
| USA 300-TCH1516 | 16 | >32 | 0.13 | 64 | 0.13 | 64 |

**Table 8. The MIC of combining silver acetate and minocycline against four selected strains of *P. aeruginosa*.**

(Reprinted with permission from "Minocycline and Silver Dual-loaded Polyphosphoester-Based Nanoparticles for Treatment of Resistant *Pseudomonas aeruginosa*" Qingquan Chen, Kush N. Shah, Fuwu Zhang, Adam J. Salazar, Parth N. Shah, Richen Li, James C. Sacchettini, Karen L. Wooley, and Carolyn L. Cannon. *Molecular Pharmaceutics* 2019 16 (4), 1606-1619, Copyright 2019 American Chemical Society.)

| **Drug** / **Strains** | **MIC (μg/mL)** **Silver acetate/minocycline** | **FIC** | **FIC Interpretation** |
|---|---|---|---|
| PA O1 | 1/2 | 0.75 | Additive |
| PA HP3 | 4/8 | 2 | Indifference |
| PA 0540 | 1/32 | 0.75 | Additive |
| PA 0557 | 2/4 | 0.58 | Additive |

**Table 9. The MIC of combining silver acetate and minocycline against four selected strains of MRSA.**

(Reprinted with permission from "Minocycline and Silver Dual-loaded Polyphosphoester-Based Nanoparticles for Treatment of Resistant *Pseudomonas aeruginosa*" Qingquan Chen, Kush N. Shah, Fuwu Zhang, Adam J. Salazar, Parth N. Shah, Richen Li, James C. Sacchettini, Karen L. Wooley, and Carolyn L. Cannon. *Molecular Pharmaceutics* 2019 16 (4), 1606-1619, Copyright 2019 American Chemical Society.)

| Drug / Strains | MIC (μg/mL) Silver acetate/minocycline | FIC | FIC Interpretation |
|---|---|---|---|
| SA LL06 | 4/0.06 | 0.75 | Additive |
| SA EH05 | 2/0.5 | 0.75 | Additive |
| MRSA 0608 | 4/1 | 0.67 | Additive |
| MRSA 0631 | 8/0.06 | 0.83 | Additive |

**Figure 6. High throughput bacterial inhibition screen.** A small molecule diversity library (SAC1) was screened for inhibition of *P. aeruginosa* strain, PA O1. Nine compounds with > 90% inhibition were identified. Of these potent inhibitors, 4-epi-minocycline was selected for characterization and downstream loading applications. 4-epi minocycline is highlighted in red. 10% growth (90% inhibition) cut off is indicated by dashed green line. (Experiment was performed by Adam Salazar.) (Reprinted with permission from "Minocycline and Silver Dual-loaded Polyphosphoester-Based Nanoparticles for Treatment of Resistant *Pseudomonas aeruginosa*" Qingquan Chen, Kush N. Shah, Fuwu Zhang, Adam J. Salazar, Parth N. Shah, Richen Li, James C. Sacchettini, Karen L. Wooley, and Carolyn L. Cannon. *Molecular Pharmaceutics* 2019 16 (4), 1606-1619, Copyright 2019 American Chemical Society.)

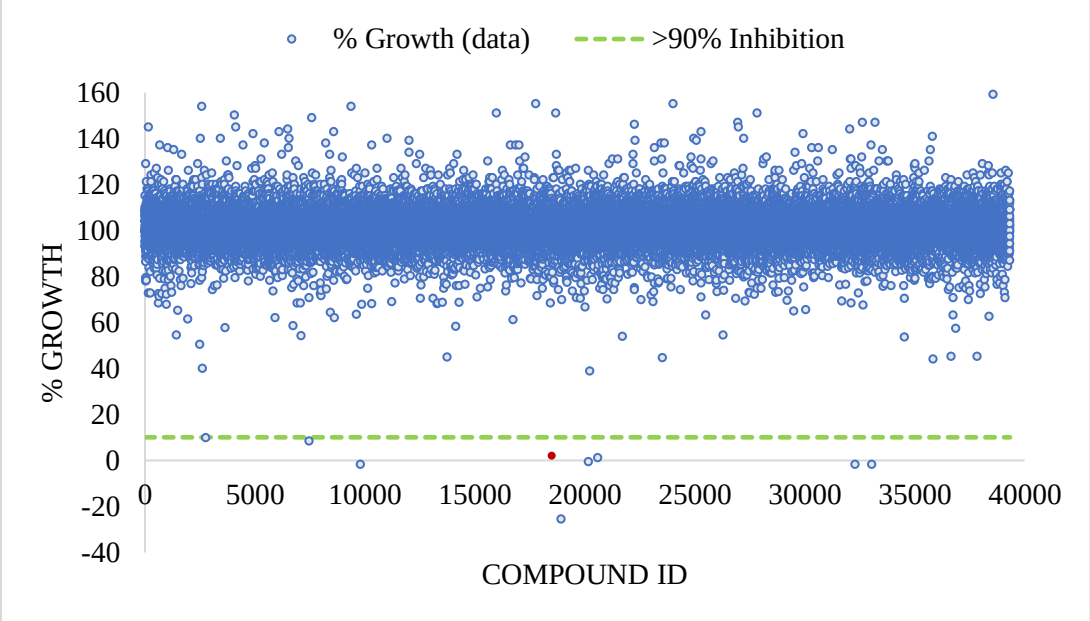

**Figure 7. Synergy demonstrated between silver and minocycline against *P. aeruginosa* isolates PA0557 and PA0540 by endpoint CFU study.**

Synergy demonstrated between silver and minocycline against A) and B) *P. aeruginosa* (PA) 0557 and C) PA 0540 by endpoint CFU study after 24-hour incubation with the drug concentration ratios (in mg/mL) indicated under each panel. 0: bacterial CFU without drug treatment; S: bacterial CFU treated with silver acetate; M: bacterial CFU treated with minocycline; C: bacterial CFU treated with silver acetate in combination with minocycline at the ratio indicated. Data are shown as mean and standard deviation (n = 6). Statistical significance determined by one-way ANOVA followed by Tukey's multiple comparison test (**** $p \leq 0.0001$). (Reprinted with permission from "Minocycline and Silver Dual-loaded Polyphosphoester-Based Nanoparticles for Treatment of Resistant *Pseudomonas aeruginosa*" Qingquan Chen, Kush N. Shah, Fuwu Zhang, Adam J. Salazar, Parth N. Shah, Richen Li, James C. Sacchettini, Karen L. Wooley, and Carolyn L. Cannon. *Molecular Pharmaceutics* 2019 16 (4), 1606-1619, Copyright 2019 American Chemical Society.)

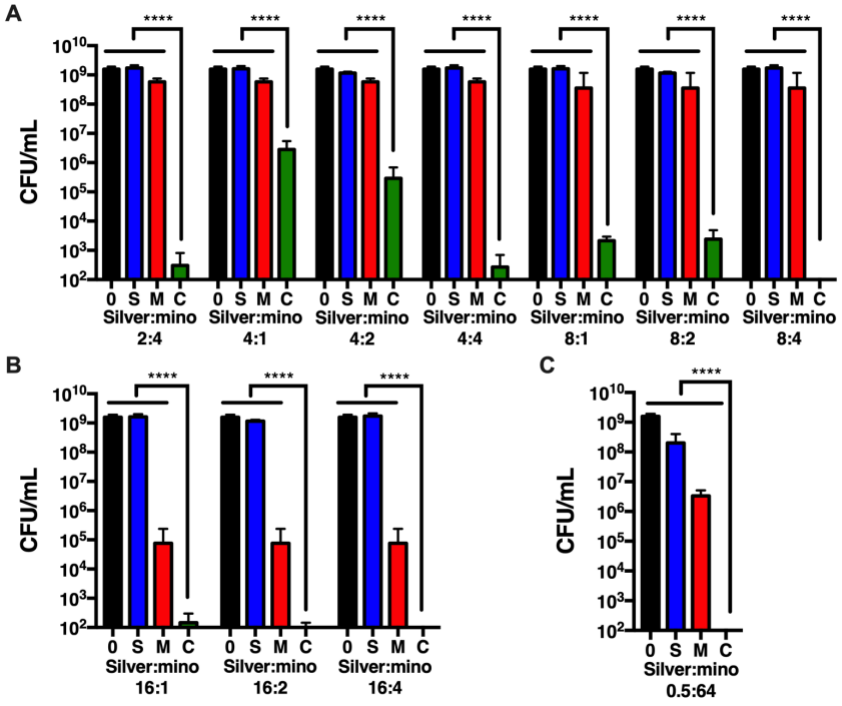

**Figure 8. Synergy demonstrated between different ratios of silver and minocycline against methicillin resistant *Staphylococcus aureus* (MRSA) isolates SAEH05 and MRSA0608 by endpoint CFU study.**

Synergy demonstrated between different ratios of silver and minocycline against A) *S. aureus* (SA) EH05 and B) methicillin resistant *S. aureus* (MRSA) 0608 by endpoint CFU study after 24-hour incubation with the drug concentration ratios (in μg/mL) indicated under each panel. 0: bacterial CFU without drug treatment; S: bacterial CFU treated with silver acetate; M: bacterial CFU treated with minocycline; C: bacterial CFU treated with silver acetate in combination with minocycline at the ratio indicated. Data are shown as mean and standard deviation (n = 6). Statistical significance determined by one-way ANOVA followed by Tukey's multiple comparison test (**** $p \leq 0.0001$). (Reprinted with permission from "Minocycline and Silver Dual-loaded Polyphosphoester-Based Nanoparticles for Treatment of Resistant *Pseudomonas aeruginosa*" Qingquan Chen, Kush N. Shah, Fuwu Zhang, Adam J. Salazar, Parth N. Shah, Richen Li, James C. Sacchettini, Karen L. Wooley, and Carolyn L. Cannon. *Molecular Pharmaceutics* 2019 16 (4), 1606-1619, Copyright 2019 American Chemical Society.)

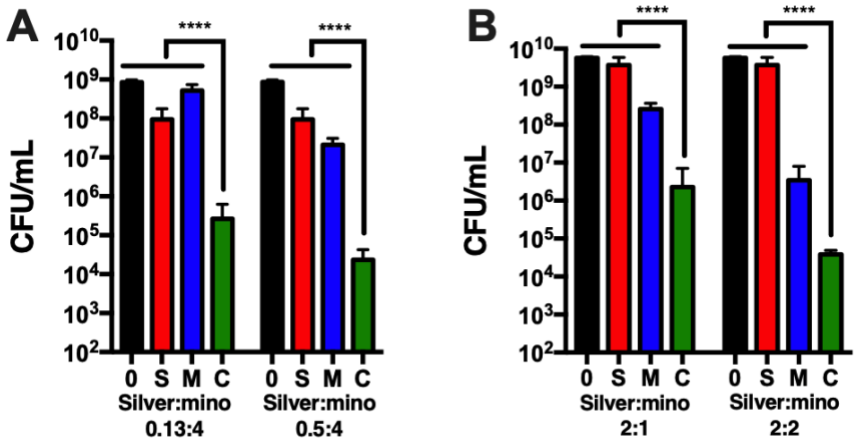

**Figure 9. TEM images of *P. aeruginosa* treated with silver acetate, minocycline or both.** TEM images of *P. aeruginosa* (PA) treated with silver acetate, minocycline or both. Top: PA 0557 at 7.5k magnification (scale bar: 1 μm); Bottom: PA 0557 at 20k magnification (scale bar: 0.5 μm). From left to right: without treatment; 4 μg/mL of silver acetate alone; 2 μg/mL of minocycline alone; 4 μg/mL of silver acetate combined with 2 μg/mL of minocycline. Arrows indicate electron-dense granules outside bacteria and segmentation of the bacterial membrane. (Reprinted with permission from "Minocycline and Silver Dual-loaded Polyphosphoester-Based Nanoparticles for Treatment of Resistant *Pseudomonas aeruginosa*" Qingquan Chen, Kush N. Shah, Fuwu Zhang, Adam J. Salazar, Parth N. Shah, Richen Li, James C. Sacchettini, Karen L. Wooley, and Carolyn L. Cannon. *Molecular Pharmaceutics* 2019 16 (4), 1606-1619, Copyright 2019 American Chemical Society.)

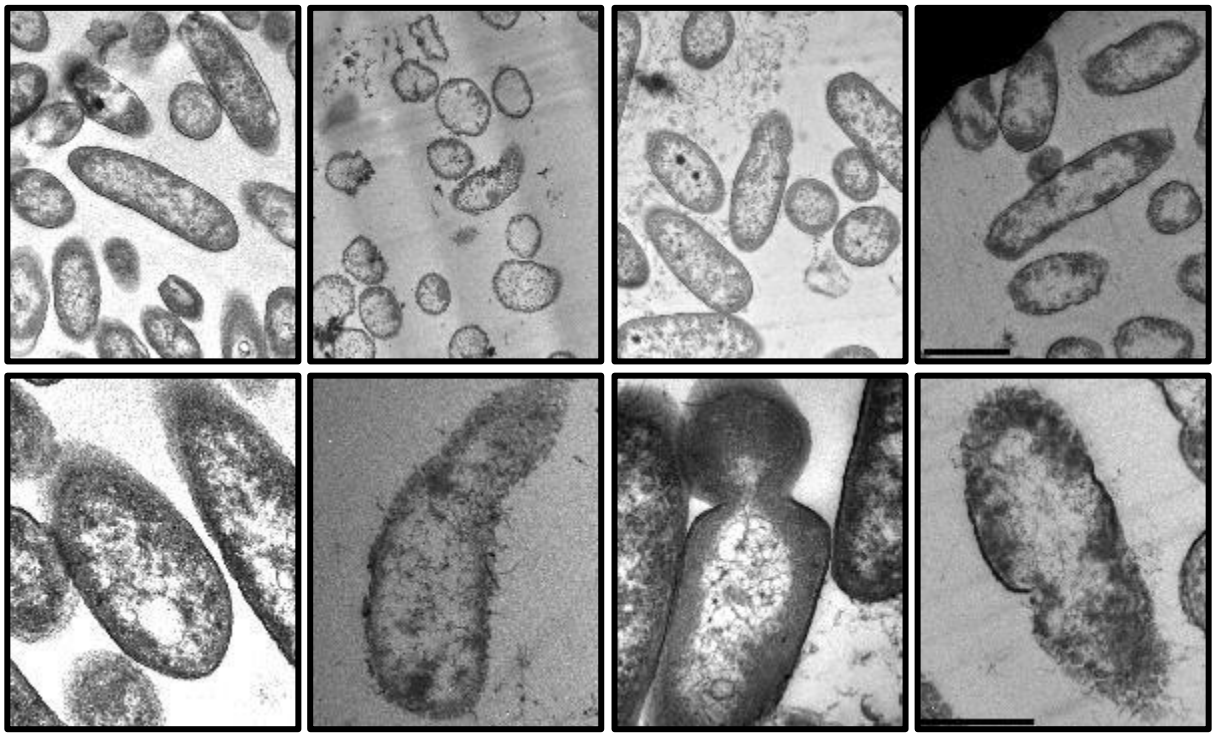

**Characterization of the Nanoparticles**

The anionic polymer was synthesized *via* thiol-yne reaction between 3-mercaptopropionic acid and diblock copolymer poly(2-ethylbutoxy phospholane)-block-poly(2-butynyl phospholane) (PEBP-b-PBYP). Then, aSCKs were prepared by self-assembly of the anionic polymer, followed by crosslinking using a diamine as a crosslinker. Silver cations and minocycline were loaded into the aSCKs by mixing for 3 h, and purified by centrifugal filter devices. The dual loaded aSCKs were obtained by stirring silver-loaded aSCKs with minocycline for 3 h, followed by purification. Both silver cations and minocycline could be loaded into the same aSCKs with *ca.* 10% loading (**Table 10**). Dual loaded aSCKs had a slightly higher minocycline loading, which might be due to potential interactions between the two drugs. The sizes and size distributions of these silver- and minocycline-loaded nanoparticles were characterized by DLS and TEM (**Figure 10**). These data suggest that minocycline loading had little effect on the number-averaged hydrodynamic diameter of the nanoparticles. Previous studies have shown that the average diameter of the anionic micelles prior to cross-linking was 15 nm (277)and after crosslinking, 16 nm ($D_{av}$ (TEM) = 16 ± 3 nm, $D_h$ (DLS, number) = 16 ± 4 nm; $D_h$ (DLS, volume) = 22 ± 14 nm; $D_h$ (DLS, intensity) = 25 ± 8 nm) (282). The diameter of the silver-loaded nanoparticles was similar to empty nanoparticles, namely, 15 nm (**Figure 10A**; $D_h$ (DLS, number) = 15 ± 4 nm; $D_h$ (DLS, volume) = 19 ± 6 nm; $D_h$ (DLS, intensity) = 175 ± 19 nm). The diameter of the minocycline-loaded nanoparticles was also similar to empty nanoparticles, namely, 12 nm (**Figure 10B**; $D_h$ (DLS, number) = 12 ± 3 nm; $D_h$ (DLS, volume) = 17 ± 9 nm; $D_h$ (DLS, intensity) = 42 ± 27 nm). In contrast, the dual-loaded nanoparticles were slightly larger than either of the single-loaded SCK nanoparticles at 22 nm (**Figure 10C**; $D_h$ (DLS, number) = 22 ± 6 nm; $D_h$ (DLS, volume) = 33 ± 21 nm; $D_h$ (DLS, intensity) = 131 ± 103 nm).

**Figure 10. Characterization of nanoparticles.** DLS histograms of intensity-averaged ($D_h$(intensity)), volume-averaged ($D_h$(volume)), number-averaged ($D_h$(number)) hydrodynamic diameters of A) dual-loaded, B) Ag-loaded, and C). minocycline-loaded SCK nanoparticles. Bright-field, TEM images of D) dual-loaded, E) Ag-loaded, and F) minocycline-loaded SCK nanoparticles. Minocycline-loaded SCKs were stained by uranyl acetate. Scale bar is 100 nm. (Experiments were performed by Fuwu Zhang.) (Reprinted with permission from "Minocycline and Silver Dual-loaded Polyphosphoester-Based Nanoparticles for Treatment of Resistant *Pseudomonas aeruginosa*" Qingquan Chen, Kush N. Shah, Fuwu Zhang, Adam J. Salazar, Parth N. Shah, Richen Li, James C. Sacchettini, Karen L. Wooley, and Carolyn L. Cannon. *Molecular Pharmaceutics* 2019 16 (4), 1606-1619, Copyright 2019 American Chemical Society.)

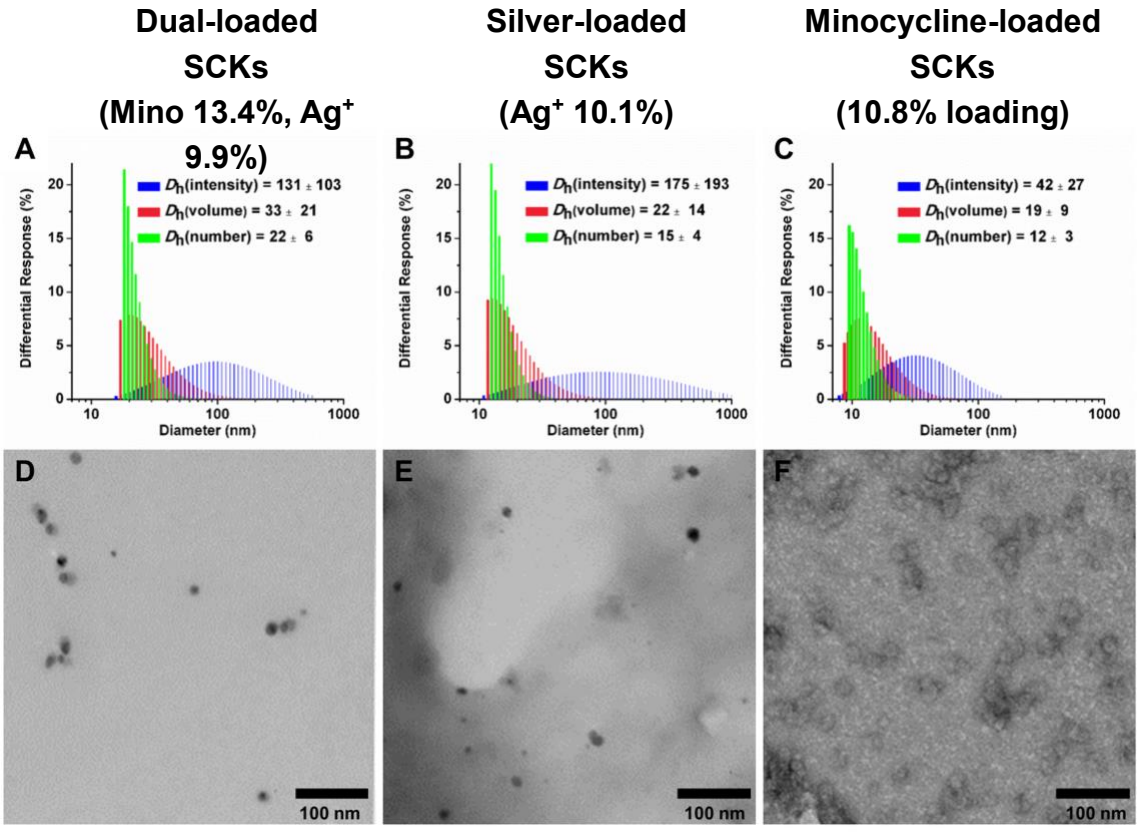

**Table 10. Silver and minocycline hydrochloride loading into aSCKs.** (Experiments were performed by Fuwu Zhang.) (Reprinted with permission from "Minocycline and Silver Dual-loaded Polyphosphoester-Based Nanoparticles for Treatment of Resistant *Pseudomonas aeruginosa*" Qingquan Chen, Kush N. Shah, Fuwu Zhang, Adam J. Salazar, Parth N. Shah, Richen Li, James C. Sacchettini, Karen L. Wooley, and Carolyn L. Cannon. *Molecular Pharmaceutics* 2019 16 (4), 1606-1619, Copyright 2019 American Chemical Society.)

| **Compound/ loading** **Drug-loaded SCKs** | **Silver (mg)** | **Minocycline hydrochloride (mg)** | **SCKs (mg)** | **Drug loading (w/w%)** |
|---|---|---|---|---|
| Silver-loaded | 0.464 | 0 | 4.6 | 10.1 |
| Minocycline-loaded | 0 | 0.175 | 1.63 | 10.8 |
| Dual-loaded | 0.161 | 0.217 | 1.62 | Ag: 9.9; Mino:13.4 |

To investigate the release of minocycline from loaded aSCKs, drug-loaded aSCKs were placed into dialysis tubing containing nanopure water (**Figure 11**). In the absence of SCKs, most (> 99.9%) of the free minocycline hydrochloride was removed after 3 washes. Rapid drug releases were observed for all drug-loaded aSCKs. Minocycline was released from the single-loaded SCK nanoparticles into nanopure water with a release half-life ($t_{1/2}$) of 1.1 hours. The release $t_{1/2}$ of silver from the single-loaded nanoparticles was slightly longer at 1.8 hours. Interestingly, the $t_{1/2}$ of minocycline release from the single-loaded nanoparticles was the same as that from the dual-loaded nanoparticles, but $t_{1/2}$ of silver release increased from 1.8 hours for single loaded nanoparticles to 3.4 hours dual-loaded nanoparticles, respectively (**Figure 11**, **Table 11**). In the absence of SCKs, *ca*. 90% of the free drug is released from the dialysis tubing within one hour.

**Figure 11. Release profiles of silver-loaded, minocycline-loaded or dual-loaded SCK nanoparticles.**

Release profiles of silver and minocycline from dialysis cassettes containing suspensions of silver-loaded, minocycline-loaded or dual-loaded SCK nanoparticles at 37 °C in nanopure water (averages were calculated from triplicate experiments). (Experiments were performed by Fuwu Zhang.) (Reprinted with permission from "Minocycline and Silver Dual-loaded Polyphosphoester-Based Nanoparticles for Treatment of Resistant *Pseudomonas aeruginosa*" Qingquan Chen, Kush N. Shah, Fuwu Zhang, Adam J. Salazar, Parth N. Shah, Richen Li, James C. Sacchettini, Karen L. Wooley, and Carolyn L. Cannon. *Molecular Pharmaceutics* 2019 16 (4), 1606-1619, Copyright 2019 American Chemical Society.)

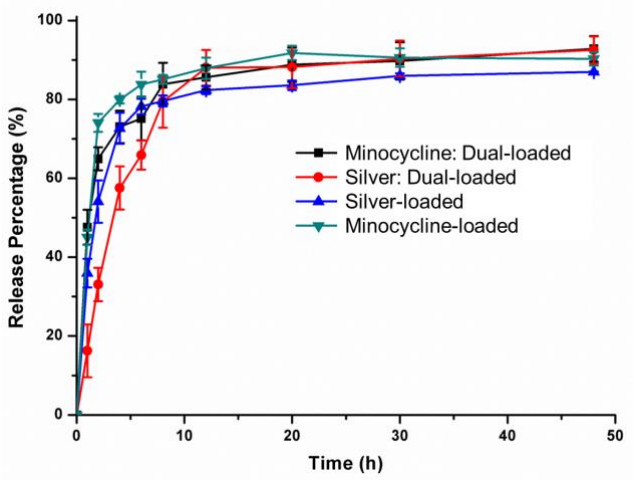

**Table 11. Release kinetics.** Release of minocycline and silver that was single- or dual-loaded into SCK nanoparticles at 37 °C in nanopure water, as measured by either ICP-MS (silver) or UV-Vis (minocycline) in aliquots collected from the cassettes over 2 days. (Reprinted with permission from "Minocycline and Silver Dual-loaded Polyphosphoester-Based Nanoparticles for Treatment of Resistant *Pseudomonas aeruginosa*" Qingquan Chen, Kush N. Shah, Fuwu Zhang, Adam J. Salazar, Parth N. Shah, Richen Li, James C. Sacchettini, Karen L. Wooley, and Carolyn L. Cannon. *Molecular Pharmaceutics* 2019 16 (4), 1606-1619, Copyright 2019 American Chemical Society.)

| **Drug release $t^{1/2}$** / **Drug-loaded SCKs** | **Silver (h)** | **Minocycline (h)** |
|---|---|---|
| Silver-loaded | 1.8 | NA |
| Minocycline-loaded | NA | 1.1 |
| Dual-loaded | 3.4 | 1.1 |

**Silver and minocycline, dual-loaded nanoparticles demonstrated efficacy against PA 0557, and the silver: minocycline ratio demonstrated synergy as free drugs in endpoint CFU studies**

In the previous experiments, silver acetate and minocycline were found to be synergistic as free drugs when the ratio between silver and minocycline was 2:1. However, this first iteration nanoparticle formulation is loaded with a silver:minocycline ratio of 1.15:1, which provides a minocycline concentration of 3.48 μg/mL when the silver cation concentration is 4 μg/mL. The nanoparticles loaded with silver acetate alone or dual-loaded with silver acetate and minocycline demonstrated a 2-$\log_{10}$ or greater reduction in *P. aeruginosa* CFU compared with no treatment or empty nanoparticles, when the silver acetate concentration was 4 μg/mL or higher (**Figure 12A**). Nanoparticles loaded with minocycline alone showed a 2-$\log_{10}$ or greater reduction in CFU compared with no treatment or empty nanoparticles, when the minocycline concentration was 5.22

μg/mL or higher (**Figure 12A**). Both silver and minocycline single-loaded nanoparticles demonstrate antimicrobial activity somewhat comparable to that of the corresponding free drug (**Figure 12 and 13**). In particular, the activity of minocycline-loaded nanoparticles mirrors that of free minocycline against *P. aeruginosa*, but they are less active than free minocycline at the C2 concentration against MRSA. Silver-loaded nanoparticles, however, demonstrate a 5-$\log_{10}$ greater reduction in *P. aeruginosa* CFU compared to free drug at the C3 concentration, which can be attributed to the sustained release and protection of $Ag^+$ cations from chloride ions afforded by the nanoparticles. A similar, but slightly attenuated effect is also observed with MRSA (**Figure 13**). The more potent response of the silver single-loaded nanoparticles against *P. aeruginosa*, compared with MRSA, is likely due to the lower antimicrobial efficacy of silver cations against MRSA. At the C3 concentration, treatment with dual-loaded nanoparticles resulted in a 5-$\log_{10}$ and a half-log reduction in bacterial burden compared to minocycline-loaded and silver-loaded nanoparticles, respectively. In contrast, when *P. aeruginosa* was treated with silver acetate and minocycline as free drugs at the same ratio found in the nanoparticles, the combination of 4 μg/mL silver acetate and 3.48 μg/mL minocycline was found to produce a >2-$\log_{10}$ reduction in CFU compared with either drug added alone and hence, was synergistic (**Figure 12B**). The dual-loaded nanoparticles did not meet the definition of synergy at the C3 concentration because the antimicrobial effects of silver-loaded nanoparticles were significantly enhanced likely due to sustained release of silver. Nevertheless, the dual-loaded nanoparticles demonstrated a 1/3-$\log_{10}$ further bacterial reduction compared to the same C3 concentrations of combined free drugs. For MRSA, dual-loaded nanoparticles at the C2 concentration demonstrate a 2-$\log_{10}$ reduction in the bacterial burden compared with individual drug-loaded nanoparticles meeting the definition for synergy (**Figure 13A**). This activity of the dual-loaded nanoparticles is similar to that of the

combination of free drugs against MRSA, although at the C2 concentration, the antimicrobial activity of free minocycline, the more potent anti-staphylococcal antimicrobial, is greater than that of the nanoparticle formulation (**Figure 13B**).

Taken together, these results suggest that *in vitro* studies of free drugs, either individually or in combination, may not predict the *in vitro* activity of dual-loaded nanoparticles given the complexities of individual drug release from a dual-loaded nanoparticle formulation. Moreover, the advantages of sustained release in an *in vivo* setting cannot be readily replicated in a static, *in vitro* experiment. The *in vitro* advantages of nanoparticles are limited, because the delayed release of encapsulated drugs lead to lower concentrations of free drug available for antimicrobial activity. Additionally, these tests only measure activity against planktonic bacteria. Nevertheless, these results may also suggest that identification of a loading ratio of silver and minocycline that might prove to be synergistic against *P. aeruginosa* in dual-loaded nanoparticles may be achieved by combining silver-loaded nanoparticles with free minocycline, given that the activity of the minocycline in the dual-loaded system mirrored that of the free drug, while the activity of the encapsulated silver was significantly enhanced compared to that of free silver. Ultimately, the ability of these nanoparticles to provide sustained release of two distinct therapeutics, one amphiphilic and one hydrophilic, imparts tremendous potential as delivery devices. The unique design and chemistry of these SCK nanoparticles allow tailoring of the surface characteristics, as well as the relative sizes of the hydrophobic core and hydrophilic shell, which allows tuning of the loading and release rates of both therapeutics. These optimizations to achieve release rates of the two antimicrobials that match synergistic ratios will provide a strong foundation for the next set of experiments, and may realize the full potential of these drug delivery devices as next-generation antimicrobials.

## Conclusions

In summary, we have demonstrated the ability of two known SoC antimicrobials to synergistically eradicate MDR *P. aeruginosa* and *S. aureus*. We have also demonstrated by TEM the ability of both drugs to act in conjunction. Further, we successfully synthesized silver and minocycline dual-loaded nanoparticles and demonstrated improved antibacterial activity compared to the combination of silver and minocycline as free drugs at the same concentrations. The lower concentrations of therapeutics, site-specific delivery, and sustained release achieved with nanoparticle formulations also reduces the possibility of generating drug-resistant mutants and systemic toxicity, and may improve patients' adherence.

**Figure 12. End-point CFU counts for PA0557.** Silver and minocycline, dual-loaded nanoparticles demonstrated efficacy against *P. aeruginosa* (PA) 0557 and the combination of free silver and minocycline demonstrated synergy in endpoint CFU studies. Colony counts of PA 0557 after treating with A) silver nanoparticles, minocycline nanoparticles, and dual-loaded nanoparticles. B) free drug of silver and minocycline or silver combined with minocycline corresponding to the ratio of drugs found in the nanoparticles; The silver: minocycline concentrations tested were C1 1:0.87, C2 2:1.74, C3 4:3.48, C4 6:5.22 and C5 8:6.96 μg/mL. Statistical significance determined by one-way ANOVA followed by Tukey's multiple comparison test (*** $p \leq 0.001$, **** $p \leq 0.0001$). (Reprinted with permission from "Minocycline and Silver Dual-loaded Polyphosphoester-Based Nanoparticles for Treatment of Resistant *Pseudomonas aeruginosa*" Qingquan Chen, Kush N. Shah, Fuwu Zhang, Adam J. Salazar, Parth N. Shah, Richen Li, James C. Sacchettini, Karen L. Wooley, and Carolyn L. Cannon. *Molecular Pharmaceutics* 2019 16 (4), 1606-1619, Copyright 2019 American Chemical Society.)

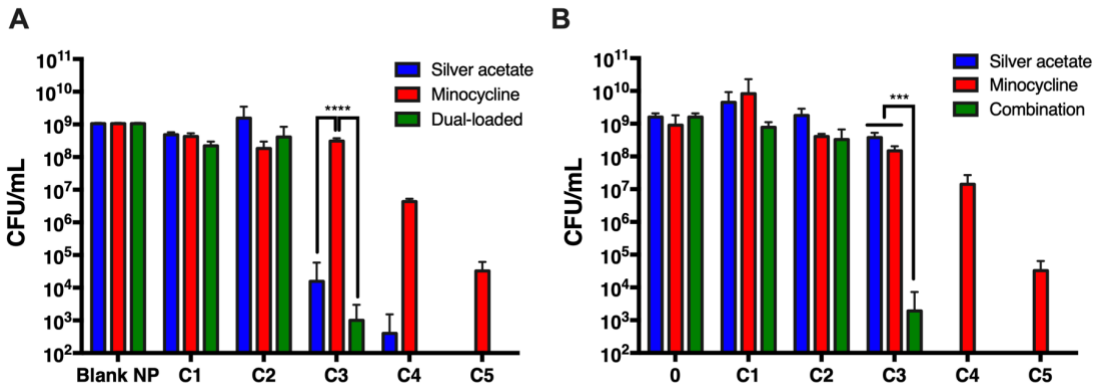

**Figure 13. End-point CFU counts for SAEH05.** End-point CFU counts of *S. aureus* (SA) EH05. A) CFU counts of SAEH 05 treated with drug-loaded nanoparticles. B) CFU counts of SA EH05 treated with free drug; Statistical significance determined by one-way ANOVA followed by Tukey's multiple comparison test (* $p \leq 0.05$, ** $p \leq 0.01$, **** $p \leq 0.0001$) **(**Reprinted with permission from "Minocycline and Silver Dual-loaded Polyphosphoester-Based Nanoparticles for Treatment of Resistant *Pseudomonas aeruginosa*" Qingquan Chen, Kush N. Shah, Fuwu Zhang, Adam J. Salazar, Parth N. Shah, Richen Li, James C. Sacchettini, Karen L. Wooley, and Carolyn L. Cannon. *Molecular Pharmaceutics* 2019 16 (4), 1606-1619, Copyright 2019 American Chemical Society.) (Reprinted with permission from "Minocycline and Silver Dual-loaded Polyphosphoester-Based Nanoparticles for Treatment of Resistant *Pseudomonas aeruginosa*" Qingquan Chen, Kush N. Shah, Fuwu Zhang, Adam J. Salazar, Parth N. Shah, Richen Li, James C. Sacchettini, Karen L. Wooley, and Carolyn L. Cannon. *Molecular Pharmaceutics* 2019 16 (4), 1606-1619, Copyright 2019 American Chemical Society.)

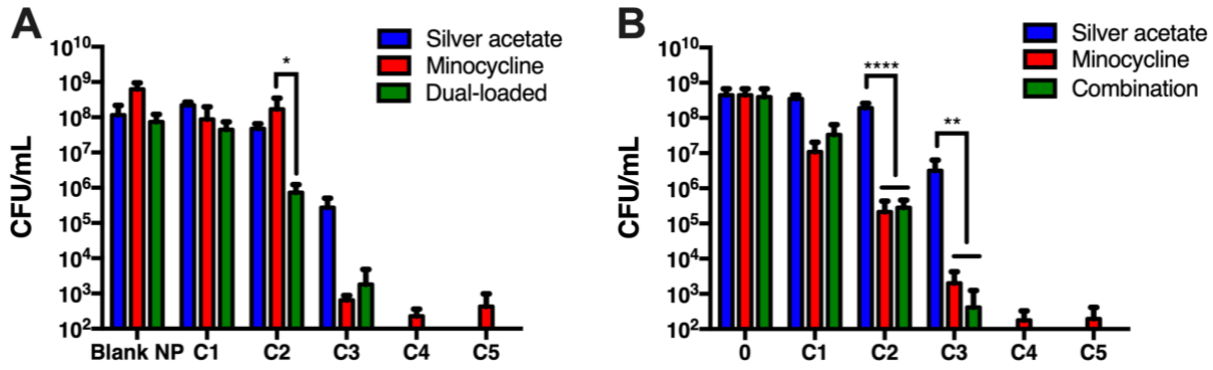

# CHAPTER IV

# ANTIMICROBIAL EFFECTS OF IBUPROFEN (IBU) COMBINED WITH STANDARD OF CARE ANTIMICROBIALS (SOCS) AGAINST CF PATHOGENS

## Introduction

Chronic infection and inflammation are the hallmarks of cystic fibrosis (CF) lung disease, and are responsible for the majority of the morbidity and mortality seen in CF patients (7; 315; 316). Initial airway infection elicits an acute inflammatory response, which is characterized by an excessive neutrophil influx (317). However, due to the distinctly altered lung environment in CF patients, the inflammation fails to clear the infection. The consequent chronic endobronchial infection results in persistently excessive inflammation and mucus secretion with worsening airway obstruction (317; 318). Although clearance of the airway obstruction and underlying endobronchial infection remain the primary foci of CF pulmonary therapies, links between the excessive inflammation and lung destruction have prompted more and more studies investigating therapies aimed at dampening the exuberant inflammatory response (167; 173; 317). Several *in vivo* models and clinical trials have demonstrated appreciable clinical benefit of oral and inhaled corticosteroids, macrolides, and nonsteroidal anti-inflammatory drugs (NSAIDs), such as ibuprofen (163; 168; 319-322).

Due to its effectiveness and safety profile, ibuprofen is advantageous as an anti-inflammatory drug. Compared to corticosteroids that cause growth retardation and cataracts, ibuprofen has fewer safety concerns, mainly GI bleeding and renal toxicity seen with high doses. High-dose ibuprofen reduces the recruitment of neutrophils into the airway in both a mouse model of acute *Pseudomonas* pulmonary infection and a rat model of endotoxin-induced alveolitis (323; 324). In a chronic *Pseudomonas* endobronchial infection study, the agarose bead model, rats

treated orally with high doses of ibuprofen (35 mg/kg twice daily) showed a significant reduction in pulmonary inflammation and improved weight gain compared to rats receiving a control treatment (263). At that concentration, ibuprofen reduced the level of leukotriene B4 production without reducing pulmonary bacterial burden (263). Further, Konstan *et al.* conducted a randomized, double-blind, placebo-controlled clinical trial to evaluate the safety and efficacy of high-dose ibuprofen (50 to 100 μg/mL peak serum concentrations) in CF patients. High-dose ibuprofen reduced the rate of decline of pulmonary function in CF patients (168), particularly those patients from 6 through 17 years old with a baseline forced expiratory volume in 1 second (FEV1) of >60%, compared with patients who received placebo (325). Lands *et al.* also investigated the safety and efficacy of high-dose ibuprofen in CF children between 6 to 18 years old. This randomized, multicenter, double-blinded, placebo-controlled trial did not show a statistically significant difference in the mean annual rate of decline in FEV1. However, the annual rate of decline of the forced vital capacity (FVC) percentage predicted significantly decreased in patients treated with high-dose ibuprofen (163). Recently, Konstan *et al.* assessed the effects of high-dose ibuprofen in CF children. The lung function and survival data of a cohort of 775 high-dose ibuprofen using children and 3665 non-using children were analyzed. Children were treated with high-dose ibuprofen for 2 years and then followed up for 16 years. The study results suggested that high-dose ibuprofen could slow lung function decline as well as increase long-term survival (326). To summarize, these clinical trials suggested the benefits and relative safety of long-term use of high-dose ibuprofen in CF patients, and attributed these benefits to the anti-inflammatory properties of ibuprofen.

Studies have documented the antimicrobial and antifungal activity of ibuprofen. Shah *et al.* demonstrated the direct, dose-dependent antimicrobial effect of high-dose ibuprofen on

bacterial pathogens prevalent in the CF lung including *P. aeruginosa* and *Burkholderia* spp. in both *in vitro* and *in vivo* studies (258). In an acute murine pneumonia model, mice orally administrated high-dose ibuprofen showed a reduced bacterial burden in the lung, and superior survival compared to mice with sham treatment (258). Studies have demonstrated that several NSAIDs, including ibuprofen, and aspirin, are synergistic with cefuroxime and chloramphenicol against MRSA (327). We hypothesized that the remarkable results of the ibuprofen trials in CF patients illustrate that, in addition to its anti-inflammatory properties, ibuprofen prevents lung function decline through inhibition of bacterial growth. Hence, we propose that ibuprofen and other NSAIDs, such as naproxen and aspirin, sensitize drug-resistant bacteria to established antimicrobials, thus exerting a synergistic bactericidal effect. Ibuprofen, and possibly other NSAIDs with dual anti-inflammatory and antimicrobial activity, may prove to be ideal adjunct agents for standard-of-care antibiotics that may be of great treatment benefit to the CF patient. Developing effective combinations comprised of therapeutics already approved for human use will also allow us to rapidly devise novel intervention strategies for the treatment of chronic lung infections with multi-drug resistant pathogens found in the lungs of CF patients.

## Materials and Methods

### Bacterial strains

Both laboratory strains and clinical isolates were studied. *Pseudomonas aeruginosa* laboratory strain PA O1 was generously donated by Gerald Pier (Harvard University, Boston, MA). The CF mucoid *P. aeruginosa* clinical isolate PA M57-15 was graciously donated by Thomas Ferkol (Washington University, St. Louis, MO) (328). The remaining *P. aeruginosa* CF clinical isolates (PA LF05, PA HP3, PA 2-9, PA 2-15, PA 2-22, PA 2-23, PA 2-26, PA 2-45, PA 2-51, and PA 3-39) were isolated from the sputa of cystic fibrosis patients at St. Louis Children's

Hospital. *Achromobacter xylosoxidans* CF clinical isolates (AX 2-79 and AX 3-26), *Elizabethkingia meningoseptica* CF clinical isolates (EM 2-14 and EM 2-18), MRSA (SA EH05 and SA LL06), and *Stenotrophomonas maltophilia* (SM AH06 and SM AH08) were also isolated from the sputa of CF patients at St. Louis Children's Hospital. Similarly, the *Burkholderia* spp., including *Burkholderia dolosa* (CF clinical isolates BD-F, and BD-G), *Burkholderia gladioli* (CF clinical isolate BG5291), and *Burkholderia multivorans* (CF clinical isolate BM 2-6) were isolated from the sputa of CF patients at St. Louis Children's Hospital, while *Burkholderia cenocepacia* J2315 was generously provided by John Lipuma (University of Michigan, Ann Arbor, MI). *Haemophilus influenzae* isolates (HI 4315, HI 2501, and HI 3864) were obtained from CF patients at St. Louis Children's Hopsital and were kindly provided by Joseph St. Geme (University of Pennsylvania, Philadelphia, PA).

**Bacterial culture**

Bacteria were streaked from frozen glycerol stocks onto tryptic soy agar (TSA, BD BBL) or chocolate agar (Hardy Diagnostics) plates and incubated overnight at 37 ℃ with 5% carbon dioxide ($CO_2$) until individual colonies formed. A single colony was inoculated into 5 mL Miller Hinton (MH, BD Difco) or Brain Heart Infusion (BHI, BD Difco) media and grown at 37 ℃ in a shaking incubator at 200 rpm to an $OD_{650}$ of 0.4, which corresponds to ~$5 \times 10^8$ CFU/mL. Bacterial cultures were adjusted to $5 \times 10^8$ CFU/mL to prepare a working stock for all experiments.

**Disc diffusion assay**

MH agar plates were prepared by autoclaving MH with 17g agar per liter of media. After autoclaving, the agar was cooled to 70 ℃ and 100 μg/mL solution of ibuprofen dissolved in DMSO was added to a final concentration of 100 μg/mL. An equivalent amount of DMSO was added to another batch of MH agar to serve as control. Plates were cast from the ibuprofen+DMSO

supplemented MH agar and DMSO supplemented MH agar. 100 µL of bacterial culture was dispensed onto an agar plate and spread evenly, after which antibiotic (amikacin, aztreonam, ceftazidime, colistin, and tobramycin)-infused discs were placed on top of the agar. Plates were incubated between 18-24 hours. Susceptibility was determined by measuring the diameter of the zone of growth inhibition.

***In vitro* antimicrobial activity**

Minimum inhibitory concentrations (MIC) were determined according to the standard Clinical and Laboratory Standards Institute (CLSI) broth-microdilution method and adapted from previous studies (minocycline paper). Briefly, 100 µL working stock of bacterial suspension was added to each well (n=3) containing 100 µL ibuprofen, naproxen, aspirin, ceftazidime, amikacin, or aztreonam solution in a 96 well plate. All solutions were comprised of 95% MH broth and 5% (v/v) DMSO. Bacteria were incubated with 0.06, 0.13, 0.25, 0.5, 1, 2, 4, 8, 16, 32, 64, 128 µg/mL amikacin, aztreonam, or ceftazidime, or 1, 2, 4, 8, 16, 32, 64, 128, 256, 512, and 1024 µg/mL ibuprofen, naproxen, or aspirin at 37 ℃ for 18 - 24 hours under static conditions. The final concentration of DMSO in the assay was 2.5% (v/v). The MIC was determined as the lowest concentration that did not show any signs of bacterial growth upon visual inspection. All experiments were performed in triplicate.

**Determination of synergistic drug combinations**

A *P. aeruginosa* (PA HP3) isolate and *E. meningoseptica* (EM 2-18) isolate were selected for synergy studies based on their susceptibilities in the disc diffusion assay. The final drug concentrations of ibuprofen, naproxen, and aspirin were 0, 50, 75, and 100 µg/mL. Based on the MIC values, a dynamic concentration scale for amikacin, aztreonam, and ceftazidime was used to determine the optimal ratio of synergistic concentrations between the two therapeutic agents. The

final drug concentrations of amikacin against EM 2-18 were 1, 2, 4, 8, 12, and 16 μg/mL. The final drug concentrations of aztreonam against PA HP3 were 0.25, 0.5, 1, 2, and 4 μg/mL. The final drug concentration of ceftazidime against PA HP3 were 1, 2, 4, 8, 12, and 16 μg/mL. The final solutions were comprised of 95% MH broth and 5% DMSO. A 100 μL working stock of bacterial suspension was incubated with a 100 μL solution of therapeutic agents (n = 3) for 18 hours at 37 °C. Wells demonstrating bacterial growth inhibition were identified visually to determine a synergistic MIC. All experiments were performed in duplicate. To evaluate for potential synergy, the fractional inhibitory concentration (FIC) was calculated as shown in **Equation 1** and defined in **Table 1**.

**Determination of bacterial burden for synergistic drug combinations**

Potential synergy between combinations of amikacin, aztreonam, or ceftazidime and ibuprofen, or naproxen against *P. aeruginosa* and *E. meningoseptica* isolates PA HP3 and EM 2-18 at a final concentration of $10^6$ CFU/mL were determined using a 24-hour end point CFU study performed in triplicate. The concentrations of ibuprofen and naproxen tested against PA HP3 and EM 2-18 were 0, 50, 100 μg/mL. The concentrations of aztreonam and ceftazidime in combination with ibuprofen against PA HP3 were 0, 1, 2, 4, and 8 or 0, 2, 4, 8, and 16 μg/mL, respectively. The concentrations of amikacin in combination with ibuprofen tested against EM 2-18 were 2, 4, 8, 12, 16 , and 20 μg/mL. The concentrations of aztreonam and ceftazidime in combination with naproxen against PA HP3 were 0, 1, 2, 4, 8, and 12 or 2, 4, 8, 12, 16, and 20 μg/mL, respectively. The tested concentrations of amikacin in combined naproxen against EM 2-18 were 2, 4, 8, 12, 16, and 20 μg/mL. Synergy was defined as ≥2-$\log_{10}$ CFU/mL reduction between combined agents and the most effective individual agent at 24 hours (293). A 100 μL working stock of bacterial suspension was incubated with 100 μL drug solution (n = 3) in each well of a 96 well plate at 37

°C for 24 hours with constant shaking at 100 RPM. The final solutions were comprised of 97.5% MH broth and 2.5% (v/v) DMSO. Finally, a 10-fold serial dilution was performed in MH broth with the bacterial suspension from each well and 50 µL of each dilution was plated onto a blood agar plate. Plates were incubated for 18 hours and colonies counted to determine the CFU for each condition. The potential synergistic effects were determined as described above. All experiments were performed in duplicate.

**Acute murine *P. aeruginosa* lung infection model**

Male C57BL/6J mice (The Jackson Laboratory, Bar Harbor, ME) aged 5 weeks were used for all acute lung infection studies, which were approved by the Texas A&M University Institutional Animal Care and Use Committee (IACUC). Mice were weighed and randomly assigned into four groups and were housed in a barrier facility under pathogen-free conditions until bacterial inoculation. When necessary, animals were euthanized with an overdose of ketamine:xylazine followed by cardiac puncture for exsanguination, a method approved by our IACUC (TAMU) and consistent with the recommendations of the Panel on Euthanasia of the American Veterinary Medical Association.

*P. aeruginosa* PA HP3 was grown in LB (LB), pelleted, washed with phosphate buffered saline (PBS), and resuspended to an $OD_{650}$ of 2.4 in LB (corresponding ~1.3 x $10^{10}$ CFU/mL, as determined by serial dilution and plating). Following anesthesia via intraperitoneal injection of ketamine (60 mg/kg) and xylazine (8 mg/kg) cocktail, mice were intranasally inoculated with 75 µL of bacteria inoculum in LB broth at an $LD_{100}$ of ~1 x $10^9$ CFU per mouse. To test the efficacy of combinational therapy against PA HP3, mice were treated at 2 h post infection, and every 8 hours subsequently for a maximum of 7 doses. Control mice were intraperitoneally injected with 50 µL saline in water and orally administered with 50 µL of 50:50 strawberry syrup : water mix.

Ibuprofen treated mice were intraperitoneally injected with 50 µL saline in water and orally administrated with 50 µL of 50:50 strawberry syrup : water ibuprofen suspension mix (1.5 mg ibuprofen). Ceftazidime treated mice were intraperitoneally injected with 50 µL of 10 mg/mL ceftazidime and orally administered with 50 µL of 50:50 strawberry syrup : water mix. Combination treated mice were intraperitoneally injected with 50 µL 10 mg/mL ceftazidime and orally administered with 50 µL of 50:50 strawberry syrup : water ibuprofen suspension mix (1.5 mg ibuprofen). Survival of the mice survival was monitored for up to 72 hours.

**Statistical analysis**

All statistics were calculated using JMP pro 13 for Macintosh (SAS Institute, Cary, North Carolina, USA, www.jmp.com). Differences between the treatments were investigated by one-way ANOVA followed by Tukey's multiple comparison test (95% confidence intervals). * indicates $p \leq 0.05$, ** indicates $p \leq 0.01$, *** indicates $p \leq 0.001$, and **** indicates $p \leq 0.0001$. The *in vivo* survival curves in the infection model were compared using a Log-rank Mantel-Cox test. Data were deemed to be significantly different for $p \leq 0.05$.

## Results and Discussion

**The zone of inhibition of antibiotic-infused disc was determined against CF clinical isolates**

We characterized the zone of inhibition of antibiotic-infused disc against 1 *P. aeruginosa* laboratory strain, 10 *P. aeruginosa* CF clinical isolates and 2 *E. meningoseptica* CF isolates (**Table 12**), 1 MRSA laboratory strain and 2 MRSA CF clinical isolates (**Table 13**), and 2 *A. xylosoxidans* CF isolates, 2 *Stenotrophomonas maltophilia* CF isolates, 1 *Burkholderia cenocepacia* laboratory strain and 5 *Burkholderia* spp. CF isolates, and 3 *H. influenzae* CF isolates (**Table 14**). The antimicrobial susceptibility of each drug against the bacterial isolates was determined according to the clinical laboratory standard breakpoints. Green indicates that the bacteria is susceptible;

yellow indicates that the bacteria is intermediate in response; and red indicates that the bacteria is resistant to the tested antimicrobials. Out of 29 isolates tested, 8 of them were multi-drug resistant isolates, as highlighted in orange. After supplementation with high-dose ibuprofen, aztreonam and ceftazidime showed significant zones of inhibition against PA HP3, and amikacin showed a significant increase in the zone of inhibition against EA 2-18 (**Figure 14**). Gentamicin, levofloxacin, and vancomycin demonstrated significant increases in the zones of inhibition against USA300 after adding high-dose ibuprofen. Similarly, gentamicin and vancomycin, with addition of high-dose ibuprofen, showed significant increases in the zones of inhibition against SA LL06 (**Figure 15B**). Amikacin demonstrated a significant zone of inhibition against AX 2-79 with the addition of high-dose ibuprofen (**Figure 15D**). The disc diffusion assay was implemented as a rapid screen with convenient, commercially available drug containing discs. Studies have suggested that the disc diffusion assay might be insensitive, as well inaccurate. However, although the assay may not have identified all synergistic combinations of the tested antibiotics with ibuprofen, this assay provided a rapid means to identify antibiotics with activity that was enhanced in combination with ibuprofen.

**Table 12. The zone of inhibition of antibiotic-infused disc against *P. aeruginosa* and *E. meningoseptica*.**

| Strains | Average zone of inhibition (unit: mm) | | | | |
|---|---|---|---|---|---|
| | Amikacin | Aztreonam | Ceftazidime | Colistin | Tobramycin |
| PA O1 | 21 | 25 | 25 | 11 | 23 |
| PA M57-15 | 22 | 25 | 26 | 11 | 23 |
| PA HP3 | 19 | 18 | 13 | 16 | 6 |
| PA 2-9 | 23 | 24 | 25 | 13 | 24 |
| PA 2-15 | 15 | 23 | 23 | 17 | 20 |
| PA 2-22 | 11 | 25 | 19 | 16 | 17 |
| PA 2-23 | 19 | 33 | 27 | 16 | 22 |
| PA 2-26 | 22 | 34 | 27 | 16 | 24 |
| PA 2-45 | 17 | 20 | 13 | 12 | 6 |
| PA 2-51 | 10 | 19 | 14 | 12 | 15 |
| PA 3-39 | 12 | 7 | 9 | 12 | 17 |
| EM 2-14 | 6 | 6 | 6 | 6 | 6 |
| EM 2-18 | 11 | 6 | 6 | 6 | 6 |

**Table 13. The zone of inhibition of antibiotic-infused disc against MRSA.**

| Strains | Average zone of inhibition (unit: mm) | | |
|---|---|---|---|
| | Gentamicin | Levofloxacin | Vancomycin |
| USA 300 | 18 | 23 | 13 |
| SA EH05 | 20 | 12 | 15 |
| SA LL06 | 22 | 9 | 14 |

**Table 14. The zone of inhibition of antibiotic-infused disc against *A. xylosoxidans*, *S. maltophilia*, *Burkholderia* spp., and *H. influenzae*.**

| Strains | Average zone of inhibition (unit: mm) | | | | | |
|---|---|---|---|---|---|---|
| | Amikacin | Aztreonam | Ceftazidime | Colistin | Levofloxacin | Tobramycin |
| AX 2-79 | 8 | 7 | 23 | 9 | - | 6 |
| AX 3-26 | 8 | 8 | 25 | 9 | - | 13 |
| SM AH06 | 21 | 6 | 8 | 8 | 12 | 20 |
| SM AH08 | 21 | 38 | 7 | 8 | 12 | 21 |
| J 2315 | 37 | 38 | 33 | 13 | 6 | 31 |
| BM 2-6 | 6 | 31 | 33 | 6 | - | 6 |
| BG 5291 | 36 | 9 | 19 | 7 | 28 | 35 |
| BG 5294 | 35 | 8 | 20 | 6 | 29 | 31 |
| BD-F | 6 | 6 | 15 | 6 | 13 | 6 |
| BD-G | 6 | 6 | 6 | 6 | 12 | 6 |
| HI 2501 | 14 | 24 | 24 | 14 | 31 | 15 |
| HI 3864 | 18 | 27 | 24 | 15 | 33 | 17 |
| HI 4315 | 15 | 33 | 25 | 15 | 27 | 14 |

**Figure 14. The zone of inhibition for antibiotic infused discs against *P. aeruginosa* and *Elizabethkingia meningoseptica.***

Supplementing ibuprofen improved the zone of inhibition of antibiotics-infused disc against *P. aeruginosa* (PA) and *E. meningoseptica* (EM). Statistical significance determined by two-way ANOVA followed by Tukey's multiple comparison test (* indicates $p \leq 0.05$, ** indicates $p \leq 0.01$, and **** indicates $p \leq 0.0001$).

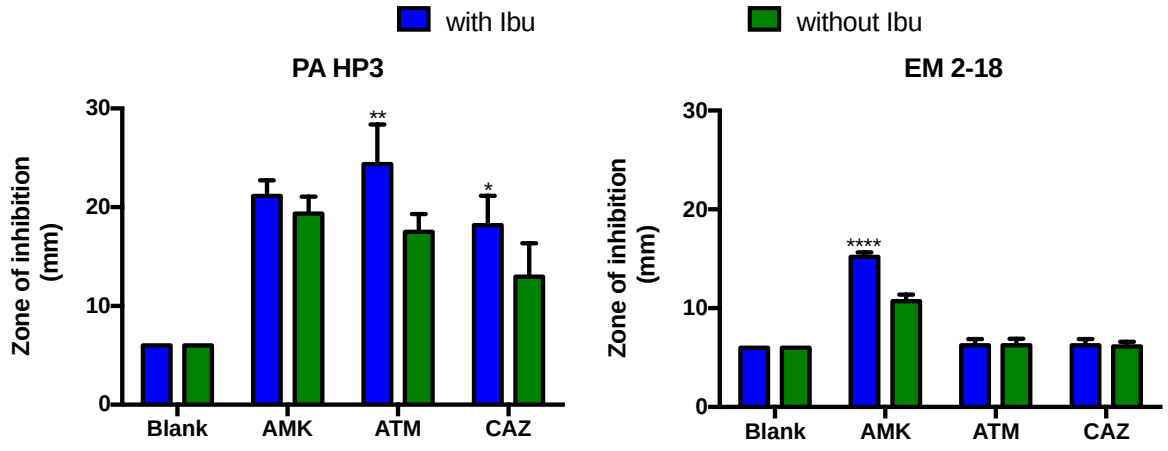

**Figure 15. The zone of inhibition for antibiotic infused discs against other CF pathogens.** The zone of inhibition of antibiotics-infused disc with addition of ibuprofen or equivalent amount DMSO against (A) *P. aeruginosa* (PA), (B) MRSA, (C) *E. meningoseptica* (EM), (D) *A. xylosoxidans* (AX), (E) *S. maltophilia* (SM), (F) *Burkholderia* spp., (G) *H. influenzae* (HI). (* indicates $p \leq 0.05$, ** indicates $p \leq 0.01$, and *** indicates $p \leq 0.001$.

(A)

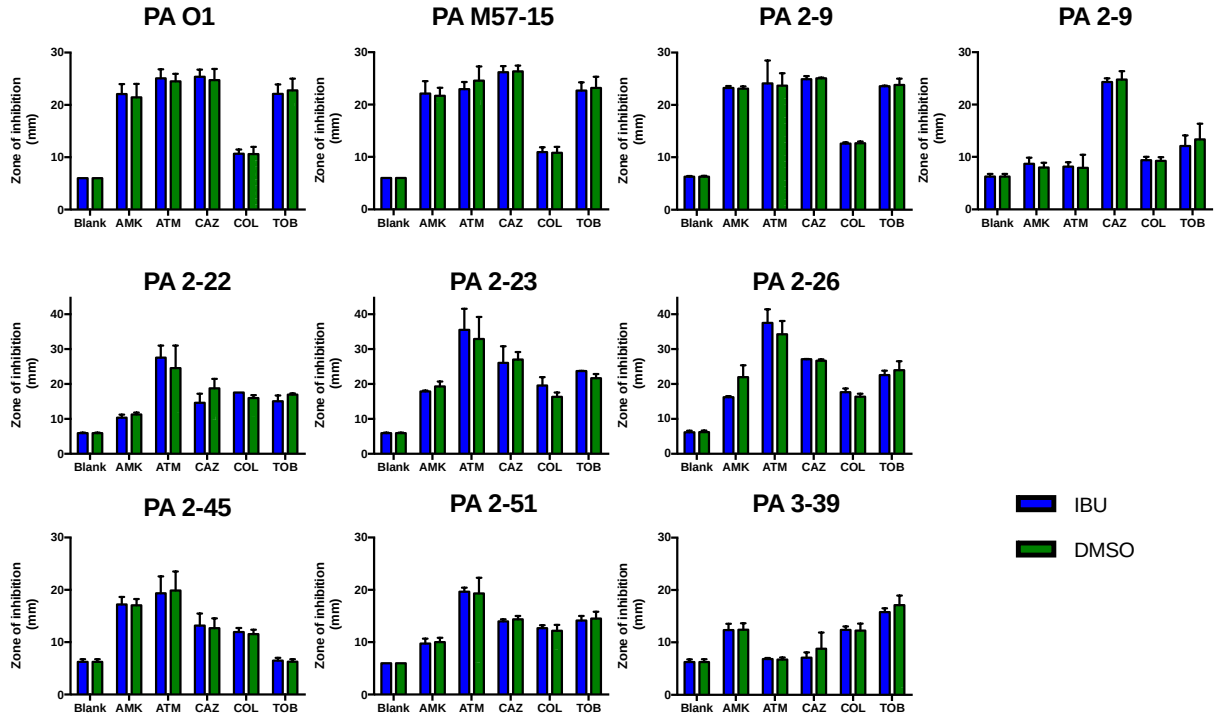


(B)

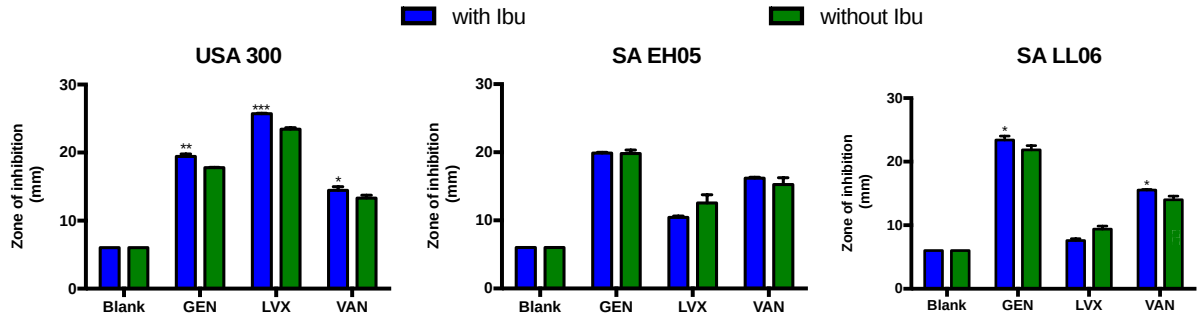

**Figure 15 Continued.**

(C)

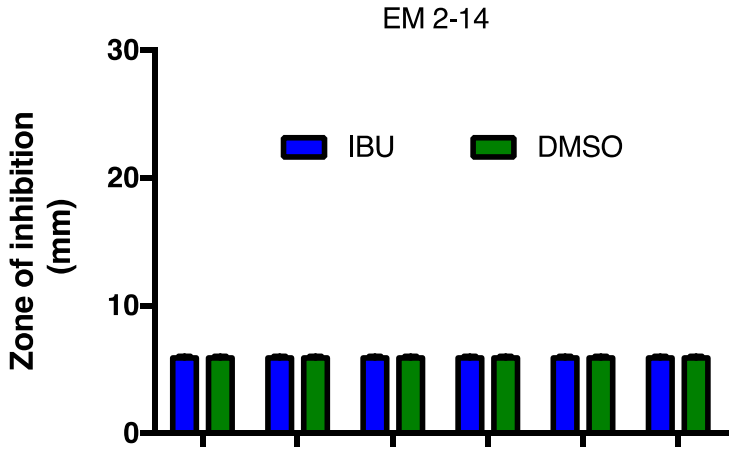


(D)

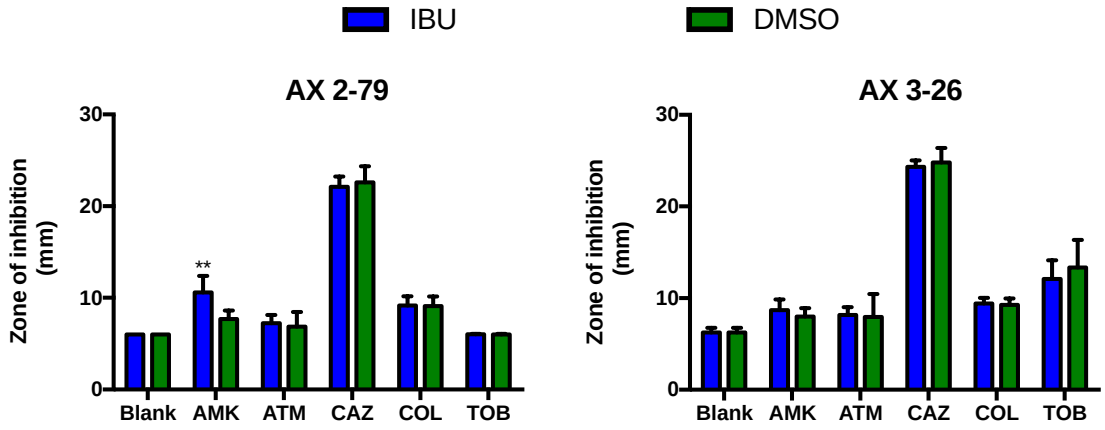


(E)

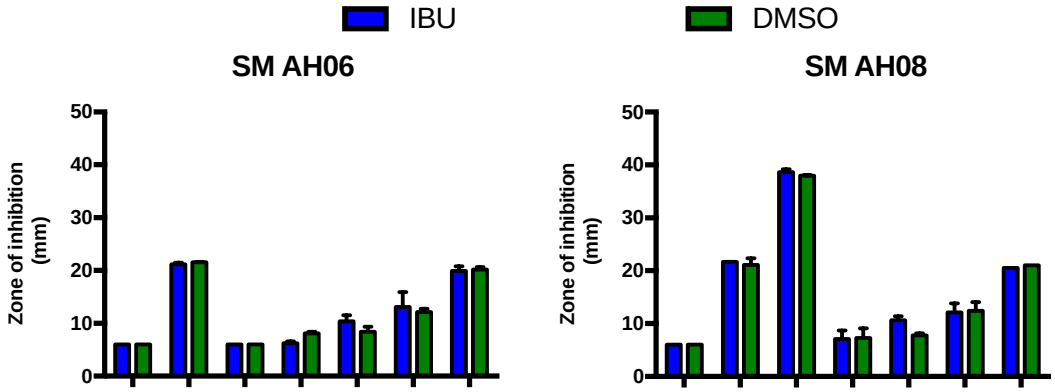

**Figure 15 Continued.**

(F)

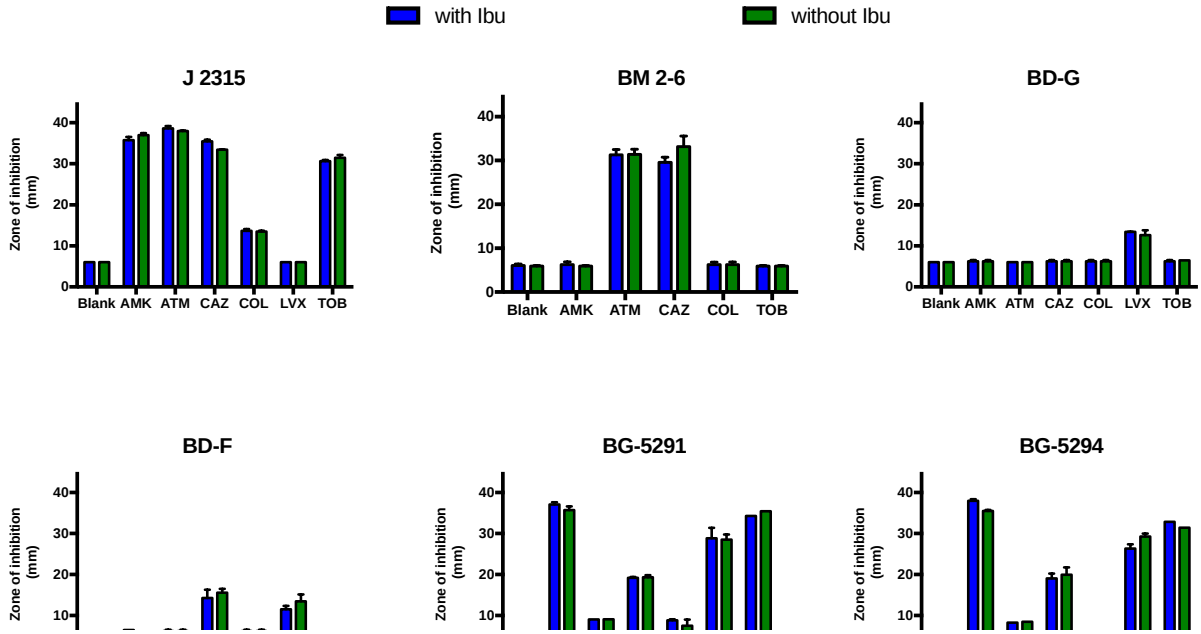


(G)

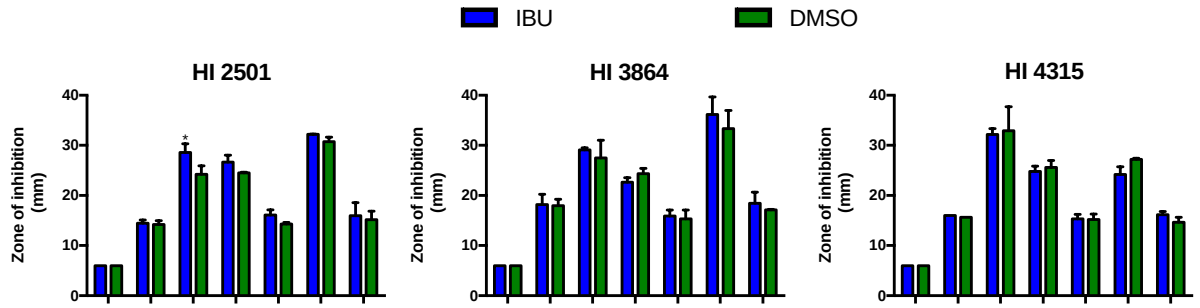

***In vitro* antimicrobial activity of ibuprofen, naproxen, aspirin, amikacin, aztreonam, and ceftazidime against *P. aeruginosa* and *E. meningoseptica***

We characterized the minimum inhibitory concentrations (MICs) of ibuprofen, naproxen, and aspirin against PA HP3 and EM 2-18 (**Table 15)**, amikacin against EM 2-18, and aztreonam and ceftazidime against PA HP3 (**Table 16**). Ibuprofen demonstrated mild antimicrobial activity against PA HP3 and EM 2-18 with MICs of 512 µg/mL and 256 µg/mL, respectively, which are consistent with our previous observations that ibuprofen has mild antimicrobial activity against a *P. aeruginosa* laboratory strain and clinical isolates. The MIC of naproxen is 2048 µg/mL against EM 2-18. However, we were not able to detect an MIC of naproxen against PA HP3, or an MIC of aspirin against PA HP3 or EM 2-18 within our concentration limit, which was 2048 µg/mL. Other studies have observed that the MIC of naproxen and aspirin are above 3 mg/mL against Gram-negative bacteria, which is above our assay detection limit. The MICs of aztreonam and ceftazidime against PA HP3 are 4 and 16 µg/mL, respectively. The MIC of amikacin against EM 2-18 is 16 µg/mL.

**Table 15. The minimum inhibitory concentration of ibuprofen, naproxen, and aspirin against PA HP3 and *E. meningoseptica* isolate EM 2-18**

| | PA HP3 | EM 2-18 |
|---|---|---|
| **Ibuprofen** | 512 | 256 |
| **Naproxen** | >1024 | 2048 |
| **Aspirin** | >1024 | >1024 |

**Table 16. The MIC of aztreonam and ceftazidime against PA HP3, and amikacin against EM 2-18 as well as combining antibiotics with NSAIDs against selected isolates of *Pseudomonas aeruginosa* and *Elizabethkingia meningoseptica*.**

| | MIC µg/mL | MIC ([Ibuprofen]) µg/mL | MIC ([Naproxen]) µg/mL | MIC ([Aspirin]) µg/mL |
|---|---|---|---|---|
| **Aztreonam (PA HP3)** | 4 | 2 (50) | 2 (75) | 4 (100) |
| **Ceftazidime (PA HP3)** | 16 | 4 (50) | 12(50) | 16(100) |
| **Amikacin (EM 2-18)** | 16 | 12(50) | 12(100) | 16(100) |

**Synergistic effect of ibuprofen and ceftazidime against PAHP3 demonstrated by checkerboard assay**

To explore the potential synergistic antimicrobial effects between antibiotics and NSAIDs, we tested combinations of drugs against PA HP3 and EM 2-18 using a checkerboard assay. The MICs of antibiotics were reduced as shown in **Table 16** with the presence of 50 µg/mL ibuprofen and various concentrations of naproxen. However, the MICs of antibiotics did not change with the presence of even the highest concentration of aspirin. Next, we calculated the fractional inhibitory concentration (FIC) to interpret potential drug combination effects. Based on the FIC calculation performed using **Equation 1** and FIC interpretation in **Table 1**, we determined that ceftazidime is synergistic with ibuprofen against PA HP3. Ibuprofen is additive with aztreonam against PA HP3, and with amikacin against EM2-18. Naproxen is additive with all three antibiotics (**Table 16**). Other studies, including our own observations, have demonstrated that NSAIDs are synergistic with antibiotics against Gram-negative and Gram-positive pathogens (327).

**Synergistic effects of NSAIDs and antibiotics demonstrated by endpoint CFU studies.**

Because the combinational MICs in the checkboard assay are determined solely based on turbidity of the liquid in the 96-well plates limiting the sensitivity of the assay, we decided to use the 24-hour endpoint CFU study to further examine potential synergistic drug combinations. For example, even though we observed a synergistic effect between ceftazidime and ibuprofen against PA HP3 using a checkerboard assay, we further performed an end-point CFU study to investigate the effect of the combination of therapeutics on CFU. The concentrations used in the 24-hour end-point CFU study were selected based on the checkerboard assay results. For each 24-hour end-point CFU study, we selected NSAID and antibiotic concentrations at sub-MIC or at individual MIC concentrations, but including the combinational MIC within the testing range.

When treated with 2 μg/mL aztreonam alone, the concentration of PA HP3 is ~$10^9$ CFU/mL. However, following supplementation with 100 μg/mL naproxen, the bacterial burden of PAHP3 is reduced to ~$10^6$ CFU/mL (**Figure 16 A**). Because a synergistic effect in an endpoint CFU study is defined as a $\geq$ 2-$\log_{10}$ reduction in bacterial burden compared with the most efficacious individual treatment, the aforementioned combination of aztreonam and naproxen demonstrated synergy in our endpoint CFU study. When we treated PAHP3 with 8 μg/mL ceftazidime alone, the bacterial concentration of PA HP3 is ~$10^7$ CFU/mL. When we added 100 μg/mL naproxen, the bacterial burden was reduced to ~$10^4$ CFU/mL, which indicated synergy (**Figure 16B**). Furthermore, we verified that ibuprofen was synergistic with all three antibiotics. With the addition of 100 μg/mL ibuprofen, 1 μg/mL aztreonam achieved ~ 6-$\log_{10}$ CFU/mL reduction compared to the individual treatments (**Figure 17A**); 2 μg/mL ceftazidime achieved ~4-$\log_{10}$ bacterial burden reduction compared to individual treatments (**Figure 17B**); and 4 μg/mL amikacin achieved ~3-$\log_{10}$ reduction compared to individual treatments (**Figure 16C**). Thus, both naproxen and ibuprofen demonstrated synergy in combination with aztreonam, ceftazidime, and amikacin. Furthermore, ibuprofen demonstrated a greater reduction of bacterial burden when combined with all three antibiotics compared with the addition of naproxen.

**Ibuprofen in combination with ceftazidime improved mice survival significantly an acute pneumonia infection.**

The high-dose ibuprofen has been used in CF patients as anti-inflammatory drug. Hence, we decided to test the efficacy of antibiotics combined with ibuprofen in a murine pneumonia model. Mice were intranasally infected with PA HP3 and treated with either 1) sham, 2) ceftazidime via intraperitoneal injection only, 3) ibuprofen via oral feeding only, or 4) ceftazidime via intraperitoneal injection combined with ibuprofen via oral feeding, and monitored for the

clinical score described previously and survival. Infected mice were treated every 8 hours for up to 7 doses. The experiment lasted 72 hours. At 72 hours, infected mice treated with combination therapy demonstrated a significant survival advantage over the groups of mice treated with individual drugs or sham (**Figure 18**).

**Figure 16. End-point CFU of naproxen and aztreonam, ceftazidime or amikacin.** Synergy demonstrated between naproxen and (A) aztreonam, (B) ceftazidime, and (C) amikacin against *P. aeruginosa* (PA) HP3 and *E. meningioseptica* (EM) 2-18 by endpoint CFU study after 24-hour incubation with the drug concentration ratios (in μg/mL) indicated under each panel. Data are shown as mean and standard deviation (n = 6). Statistical significance determined by one-way ANOVA followed by Tukey's multiple comparison test (** indicates p≤0.01, *** indicates p≤0.001, and **** indicates p≤0.0001).

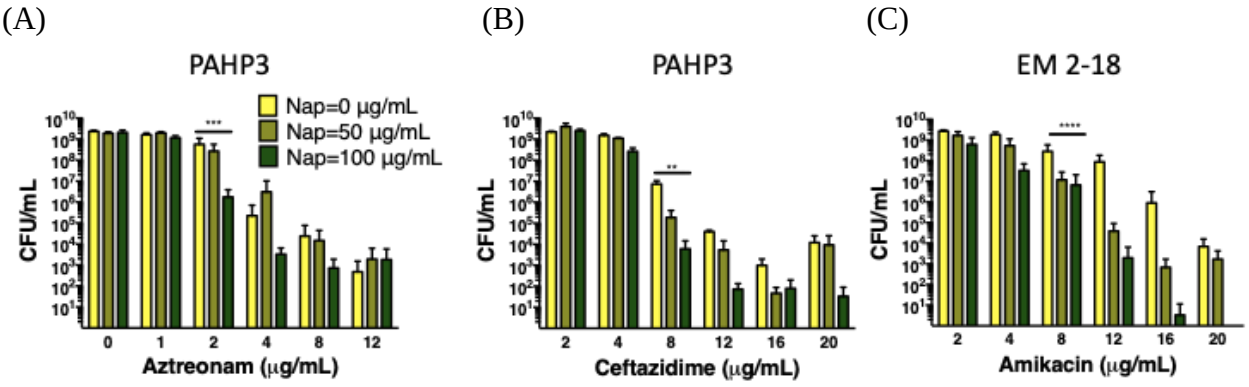

**Figure 17. End-point CFU for ibuprofen and aztreonam, ceftazidime or amikacin.** Synergy demonstrated between ibuprofen and (A) aztreonam, (B) ceftazidime, and (C) amikacin against *P. aeruginosa* (PA) HP3 and *E. meningioseptica* (EM) 2-18 by endpoint CFU study after 24-hour incubation with the drug concentration ratios (in μg/mL) indicated under each panel. Data are shown as mean and standard deviation (n = 6). Statistical significance determined by one-way ANOVA followed by Tukey's multiple comparison test (** indicates p≤0.01, *** indicates p≤0.001, and **** indicates p≤0.0001).

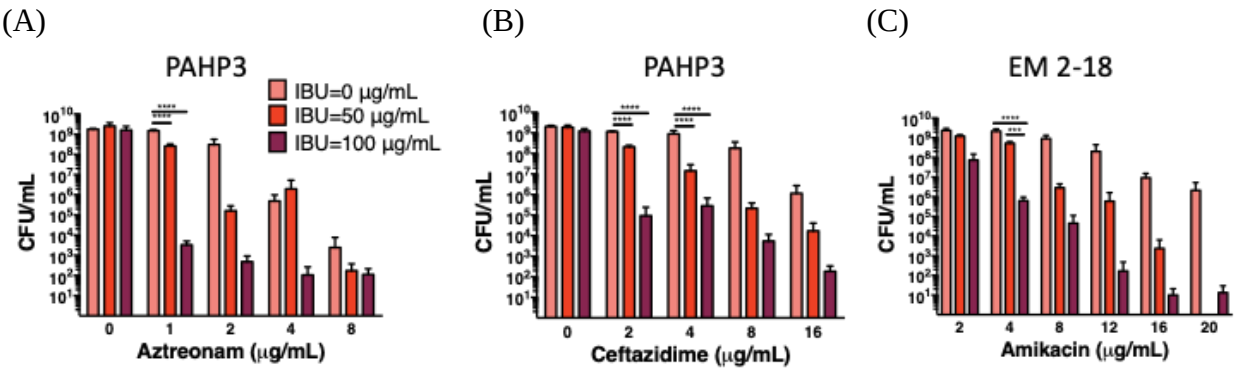

**Figure 18. The survival curve for mice treated with combinational therapy of ibuprofen and ceftazidime.**

The combination therapy of ibuprofen plus ceftazidime demonstrated a significant survival advantage in a murine pneumonia model (n=6). Statistical significance determined by Mantel-Cox test (** indicates $p \leq 0.01$).

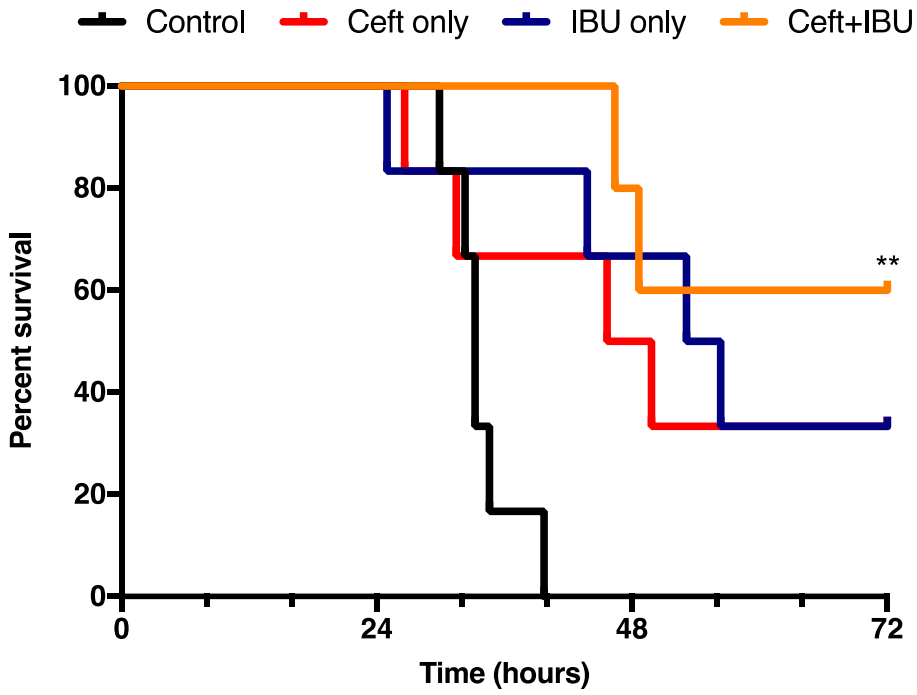

## Conclusions

To summarize, in combination with several standard of care antimicrobials, ibuprofen significantly increases the zone of inhibition against CF clinical isolates. The drug combinations suggestive of synergistic interactions found in the disc diffusion assay provided us candidates to proceed with for detailed microbiological characterization. *In vitro* studies suggested that ibuprofen has antimicrobial activity against CF clinical isolates, which confirmed our previous observation. Although aspirin did not demonstrate either synergy or additive effects, naproxen and ibuprofen showed additive and synergistic effects with selected antibiotics. Further, the 24 hour endpoint CFU study confirmed that naproxen and ibuprofen are synergistic with each of three antibiotics, aztreonam, ceftazidime, and amikacin. Ibuprofen in combination with each of the three antibiotics exerted greater reduction of bacterial burden compared with naproxen combinations. Finally, when intranasally inoculated mice were treated with sub-MIC concentrations of ceftazidime intraperitoneally and ibuprofen orally, they demonstrated improved survival rates compared to mice treated with either drug alone. Our i*n vitro* and *in vivo* experiments suggest that ibuprofen has mild antimicrobial activity in addition to it anti-inflammatory properties, particularly after combining with standard of care antibiotics. Currently, high-does ibuprofen treatment is not widely available in CF centers. It would be worth revisiting ibuprofen to further explore its clinical benefits in CF patients.

# CHAPTER V
# CONCLUSIONS

The chronic bacterial lung infections in cystic fibrosis patients have been problematic to treat. The chronic use of multiple antibiotics increases the possibility of multidrug resistance and limits the treatment options in patients with advanced disease. The exaggerated immune response against the bacterial infection compounds the damage to the lung caused by the bacterial infections. Silver has long been used as a broad-spectrum antimicrobial agent with a low incidence of resistance. Despite low toxicity, poor availability of silver cations mandates a high dosage to effectively eradicate infections. Previously, our group has demonstrated that silver carbene complexes (SCCs) could provide gradual release of bioactive silver cation from a stable silver complex, which sustains silver cation bioavailability, and provides prolonged antimicrobial activity. Meanwhile, several clinical trials have demonstrated that high-dose ibuprofen (peak serum concentrations of 50-100 μg/mL) can reduce the rate of pulmonary function decline in CF patients. This beneficial effect has been attributed to the anti-inflammatory properties of ibuprofen. Our group has confirmed that high-dose ibuprofen reduces the growth rate and bacterial burden of *P. aeruginosa* in a dose-dependent manner, especially at the concentrations studied in the clinical trials. Additionally, our group has demonstrated a significant survival advantage upon treatment with ibuprofen in an acute *P. aeruginosa* murine infection model. Ibuprofen-treated mice also have lower lung and spleen bacterial burdens. Furthermore, studies have demonstrated that synergistic combinations with careful dose calibrations and efficient delivery systems result in superior antimicrobial activity, while avoiding potential side-effects of both therapeutics.

In the current study, we have successfully synthesized silver carbene complex SCC1 conjugated with ibuprofen, SCC1-IBU, or methylated caffeine silver ibuprofen. SCC1-IBU

demonstrated improved *in vitro* antimicrobial activity against CF pathogens compared with SCC1, while preserving the anti-inflammatory activity of ibuprofen as demonstrated through the reduction of IL-8 production after stimulating with LPS. Further, a 24-hour endpoint CFU study suggested that SCC1 has synergistic antimicrobial activity with high-dose ibuprofen.

Meanwhile, 4-epi-minocycline, a metabolite of minocycline, was identified as an active antimicrobial against *P. aeruginosa* using a high-throughput screen. The antimicrobial activities of 4-epi-minocycline, minocycline and silver acetate against clinical isolates of *P. aeruginosa* and MRSA obtained from CF patients were evaluated *in vitro*. Next, the synergistic activity of the silver/minocycline combination against *P. aeruginosa* and MRSA isolates was investigated using checkerboard assays and identified with end-point colony forming unit (CFU) determination assays. Finally, nanoparticles co-loaded with minocycline and silver were evaluated *in vitro* for antimicrobial activity. The results demonstrated that both silver and minocycline are potent antimicrobials alone, and that the combination allows reduced dosage of both therapeutics to achieve the same antimicrobial effect. Furthermore, the proposed synergistic silver/minocycline combination can be co-loaded into nanoparticles as a next-generation antibiotic to combat the threats presented by MDR pathogens.

Lastly, we evaluated possible synergistic activity of combinations of common nonsteroidal anti-inflammatory drugs (NSAIDs), namely, aspirin, naproxen, and ibuprofen, with FDA approved antibiotics. In the presence of 100 μg/mL ibuprofen, antibiotics demonstrated significant increases in the zones of inhibition against the CF pathogens. Fractional Inhibitory Concentrations (FIC) determined using a checkerboard assay demonstrated no synergy with aspirin, additive effects with naproxen, and synergistic effects with ibuprofen. Additionally, in a 24-hour endpoint CFU assay, we verified that in presence of 100 μg/mL ibuprofen or naproxen, PA HP3 and EM 2-18 treated with aztreonam or ceftazidime, and amikacin, respectively, demonstrate a greater than 2-$\log_{10}$ reduction compared with the antibiotic alone, indicating synergy. In particular, combinations of

ibuprofen with amikacin, aztreonam or ceftazidime demonstrate synergistic antimicrobial activity against drug resistant CF isolates *in vitro*. Finally, mice treated with both ceftazidime and ibuprofen demonstrated a significant survival advantage compared to the groups treated with either ceftazidime or ibuprofen alone. Thus, therapy with high-dose ibuprofen in combination with a standard-of-care antibiotic including amikacin, aztreonam or ceftazidime may improve outcomes in CF patients infected with multidrug resistant bacteria.

## REFERENCES


1. Bye MR, Ewig JM, Quittell LM. 1994. Cystic fibrosis. *Lung* 172:251-70
2. Boucher RC. 2004. Relationship of airway epithelial ion transport to chronic bronchitis. *Proc Am Thorac Soc* 1:66-70
3. Lyczak JB, Cannon CL, Pier GB. 2002. Lung Infections Associated with Cystic Fibrosis. *Clinical Microbiology Reviews* 15:194-222
4. Wilschanski M, Zielenski J, Markiewicz D, Tsui LC, Corey M, et al. 1995. Correlation of sweat chloride concentration with classes of the cystic fibrosis transmembrane conductance regulator gene mutations. *J Pediatr* 127:705-10
5. Ramalho AS, Lewandowska MA, Farinha CM, Mendes F, Goncalves J, et al. 2009. Deletion of CFTR translation start site reveals functional isoforms of the protein in CF patients. *Cell Physiol Biochem* 24:335-46
6. Colin AA, Wohl ME. 1994. Cystic fibrosis. *Pediatr Rev* 15:192-200
7. Davis PB, Drumm M, Konstan MW. 1996. Cystic fibrosis. *Am J Respir Crit Care Med* 154:1229-56
8. Chmiel JF, Davis PB. 2003. State of the art: why do the lungs of patients with cystic fibrosis become infected and why can't they clear the infection? *Respir Res* 4:8
9. Armstrong DS, Grimwood K, Carzino R, Carlin JB, Olinsky A, Phelan PD. 1995. Lower respiratory infection and inflammation in infants with newly diagnosed cystic fibrosis. *BMJ* 310:1571-2
10. Armstrong DS, Hook SM, Jamsen KM, Nixon GM, Carzino R, et al. 2005. Lower airway inflammation in infants with cystic fibrosis detected by newborn screening. *Pediatr Pulmonol* 40:500-10

11. Hoiby N, Frederiksen B, Pressler T. 2005. Eradication of early Pseudomonas aeruginosa infection. *J Cyst Fibros* 4 Suppl 2:49-54

12. Foundation CF. 2017. Cystic Fibrosis Foundation Patient Registry Annual Data Report

13. Harrison F. 2007. Microbial ecology of the cystic fibrosis lung. *Microbiology* 153:917-23

14. Folkesson A, Jelsbak L, Yang L, Johansen HK, Ciofu O, et al. 2012. Adaptation of Pseudomonas aeruginosa to the cystic fibrosis airway: an evolutionary perspective. *Nat Rev Microbiol* 10:841-51

15. Hoiby N, Johansen HK. 2007. Isolation measures for prevention of infection with respiratory pathogens in cystic fibrosis: a systematic review? *J Hosp Infect* 65:374-5; author reply 5-6

16. Lowy FD. 1998. Staphylococcus aureus infections. *N Engl J Med* 339:520-32

17. Casewell MW, Hill RL. 1986. The carrier state: methicillin-resistant Staphylococcus aureus. *J Antimicrob Chemother* 18 Suppl A:1-12

18. Noble WC, Valkenburg HA, Wolters CH. 1967. Carriage of Staphylococcus aureus in random samples of a normal population. *J Hyg (Lond)* 65:567-73

19. Chambers HF. 2001. The changing epidemiology of Staphylococcus aureus? *Emerg Infect Dis* 7:178-82

20. Barber M. 1961. Methicillin-resistant staphylococci. *J Clin Pathol* 14:385-93

21. Harkins CP, Pichon B, Doumith M, Parkhill J, Westh H, et al. 2017. Methicillin-resistant Staphylococcus aureus emerged long before the introduction of methicillin into clinical practice. *Genome Biol* 18:130

22. Centers for Disease Control and Prevention. 2013. *Antibiotic resistance threats in the United States*.

23. Moreno F, Crisp C, Jorgensen JH, Patterson JE. 1995. Methicillin-resistant Staphylococcus aureus as a community organism. *Clin Infect Dis* 21:1308-12

24. David MZ, Daum RS. 2010. Community-Associated Methicillin-Resistant Staphylococcus aureus: Epidemiology and Clinical Consequences of an Emerging Epidemic. *Clinical Microbiology Reviews* 23:616-87

25. Goss CH, Muhlebach MS. 2011. Review: Staphylococcus aureus and MRSA in cystic fibrosis. *J Cyst Fibros* 10:298-306

26. ANDERSEN DH. 1938. CYSTIC FIBROSIS OF THE PANCREAS AND ITS RELATION TO CELIAC DISEASE: A CLINICAL AND PATHOLOGIC STUDY. *American Journal of Diseases of Children* 56:344-99

27. Di SAPE, Andersen DH. 1946. Celiac syndrome; chemotherapy in infections of the respiratory tract associated with cystic fibrosis of the pancreas; observations with penicillin and drugs of the sulfonamide group, with special reference to penicillin aerosol. *Am J Dis Child* 72:17-61

28. Huang NN, Van Loon EL, Sheng KT. 1961. The flora of the respiratory tract of patients with cystic fibrosis of the pancreas. *J Pediatr* 59:512-21

29. Miall LS, McGinley NT, Brownlee KG, Conway SP. 2001. Methicillin resistant Staphylococcus aureus (MRSA) infection in cystic fibrosis. *Arch Dis Child* 84:160-2

30. Abman SH, Ogle JW, Harbeck RJ, Butler-Simon N, Hammond KB, Accurso FJ. 1991. Early bacteriologic, immunologic, and clinical courses of young infants with cystic fibrosis identified by neonatal screening. *J Pediatr* 119:211-7

31. Rosenfeld M, Emerson J, Accurso F, Armstrong D, Castile R, et al. 1999. Diagnostic accuracy of oropharyngeal cultures in infants and young children with cystic fibrosis. *Pediatr Pulmonol* 28:321-8

32. Emerson J, McNamara S, Buccat AM, Worrell K, Burns JL. 2010. Changes in cystic fibrosis sputum microbiology in the United States between 1995 and 2008. *Pediatr Pulmonol* 45:363-70

33. Razvi S, Quittell L, Sewall A, Quinton H, Marshall B, Saiman L. 2009. Respiratory microbiology of patients with cystic fibrosis in the United States, 1995 to 2005. *Chest* 136:1554-60

34. Stone A, Saiman L. 2007. Update on the epidemiology and management of Staphylococcus aureus, including methicillin-resistant Staphylococcus aureus, in patients with cystic fibrosis. *Curr Opin Pulm Med* 13:515-21

35. Zhou J, Garber E, Desai M, Saiman L. 2006. Compliance of clinical microbiology laboratories in the United States with current recommendations for processing respiratory tract specimens from patients with cystic fibrosis. *J Clin Microbiol* 44:1547-9

36. Sharp SE, Searcy C. 2006. Comparison of mannitol salt agar and blood agar plates for identification and susceptibility testing of Staphylococcus aureus in specimens from cystic fibrosis patients. *J Clin Microbiol* 44:4545-6

37. Kahl BC, Duebbers A, Lubritz G, Haeberle J, Koch HG, et al. 2003. Population dynamics of persistent Staphylococcus aureus isolated from the airways of cystic fibrosis patients during a 6-year prospective study. *J Clin Microbiol* 41:4424-7

38. Branger C, Gardye C, Lambert-Zechovsky N. 1996. Persistence of Staphylococcus aureus strains among cystic fibrosis patients over extended periods of time. *J Med Microbiol* 45:294-301

39. Dasenbrook EC, Merlo CA, Diener-West M, Lechtzin N, Boyle MP. 2008. Persistent methicillin-resistant Staphylococcus aureus and rate of FEV1 decline in cystic fibrosis. *Am J Respir Crit Care Med* 178:814-21

40. Burns JL, Gibson RL, McNamara S, Yim D, Emerson J, et al. 2001. Longitudinal assessment of Pseudomonas aeruginosa in young children with cystic fibrosis. *J Infect Dis* 183:444-52

41. Govan JR, Nelson JW. 1992. Microbiology of lung infection in cystic fibrosis. *Br Med Bull* 48:912-30

42. Boxerbaum B, Jacobs MR, Cechner RL. 1988. Prevalence and significance of methicillin-resistant Staphylococcus aureus in patients with cystic fibrosis. *Pediatr Pulmonol* 4:159-63

43. Ren CL, Morgan WJ, Konstan MW, Schechter MS, Wagener JS, et al. 2007. Presence of methicillin resistant Staphylococcus aureus in respiratory cultures from cystic fibrosis patients is associated with lower lung function. *Pediatr Pulmonol* 42:513-8

44. Dasenbrook EC, Checkley W, Merlo CA, Konstan MW, Lechtzin N, Boyle MP. 2010. Association between respiratory tract methicillin-resistant Staphylococcus aureus and survival in cystic fibrosis. *JAMA* 303:2386-92

45. Hoiby N, Kilian M. 1976. Haemophilus from the lower respiratory tract of patients with cystic fibrosis. *Scand J Respir Dis* 57:103-7

46. Roman F, Canton R, Perez-Vazquez M, Baquero F, Campos J. 2004. Dynamics of long-term colonization of respiratory tract by Haemophilus influenzae in cystic fibrosis patients shows a marked increase in hypermutable strains. *J Clin Microbiol* 42:1450-9

47. Watson KC, Kerr EJ, Hinks CA. 1985. Distribution of biotypes of Haemophilus influenzae and H parainfluenzae in patients with cystic fibrosis. *J Clin Pathol* 38:750-3

48. Armstrong DS, Grimwood K, Carlin JB, Carzino R, Olinsky A, Phelan PD. 1996. Bronchoalveolar lavage or oropharyngeal cultures to identify lower respiratory pathogens in infants with cystic fibrosis. *Pediatr Pulmonol* 21:267-75

49. Rosenfeld M, Gibson RL, McNamara S, Emerson J, Burns JL, et al. 2001. Early pulmonary infection, inflammation, and clinical outcomes in infants with cystic fibrosis. *Pediatr Pulmonol* 32:356-66

50. Prevaes SM, de Winter-de Groot KM, Janssens HM, de Steenhuijsen Piters WA, Tramper-Stranders GA, et al. 2016. Development of the Nasopharyngeal Microbiota in Infants with Cystic Fibrosis. *Am J Respir Crit Care Med* 193:504-15

51. Navarro J, Rainisio M, Harms HK, Hodson ME, Koch C, et al. 2001. Factors associated with poor pulmonary function: cross-sectional analysis of data from the ERCF. European Epidemiologic Registry of Cystic Fibrosis. *Eur Respir J* 18:298-305

52. Bilton D, Pye A, Johnson MM, Mitchell JL, Dodd M, et al. 1995. The isolation and characterization of non-typeable Haemophilus influenzae from the sputum of adult cystic fibrosis patients. *Eur Respir J* 8:948-53

53. Ramsey KA, Ranganathan S, Park J, Skoric B, Adams AM, et al. 2014. Early respiratory infection is associated with reduced spirometry in children with cystic fibrosis. *Am J Respir Crit Care Med* 190:1111-6

54. Rayner RJ, Hiller EJ, Ispahani P, Baker M. 1990. Haemophilus infection in cystic fibrosis. *Arch Dis Child* 65:255-8

55. Govan JR, Doherty C, Glass S. 1987. Rational parameters for antibiotic therapy in patients with cystic fibrosis. *Infection* 15:300-7

56. Ramsey BW. 1996. Management of pulmonary disease in patients with cystic fibrosis. *N Engl J Med* 335:179-88

57. Isles A, Maclusky I, Corey M, Gold R, Prober C, et al. 1984. Pseudomonas cepacia infection in cystic fibrosis: an emerging problem. *J Pediatr* 104:206-10

58. Biddick R, Spilker T, Martin A, LiPuma JJ. 2003. Evidence of transmission of Burkholderia cepacia, Burkholderia multivorans and Burkholderia dolosa among persons with cystic fibrosis. *FEMS Microbiol Lett* 228:57-62

59. Drevinek P, Mahenthiralingam E. 2010. Burkholderia cenocepacia in cystic fibrosis: epidemiology and molecular mechanisms of virulence. *Clin Microbiol Infect* 16:821-30

60. Roux D, Weatherholt M, Clark B, Gadjeva M, Renaud D, et al. 2017. Immune Recognition of the Epidemic Cystic Fibrosis Pathogen Burkholderia dolosa. *Infect Immun* 85

61. Araque-Calderon Y, Miranda-Contreras L, Rodriguez-Lemoine V, Palacios-Pru EL. 2008. Antibiotic resistance patterns and SDS-PAGE protein profiles of Burkholderia cepacia complex isolates from nosocomial and environmental sources in Venezuela. *Med Sci Monit* 14:BR49-55

62. Kim JM, Ahn Y, LiPuma JJ, Hussong D, Cerniglia CE. 2015. Survival and susceptibility of Burkholderia cepacia complex in chlorhexidine gluconate and benzalkonium chloride. *J Ind Microbiol Biotechnol* 42:905-13

63. Leitao JH, Sousa SA, Cunha MV, Salgado MJ, Melo-Cristino J, et al. 2008. Variation of the antimicrobial susceptibility profiles of Burkholderia cepacia complex clonal isolates obtained from chronically infected cystic fibrosis patients: a five-year survey in the major Portuguese treatment center. *Eur J Clin Microbiol Infect Dis* 27:1101-11

64. Caraher E, Duff C, Mullen T, Mc Keon S, Murphy P, et al. 2007. Invasion and biofilm formation of Burkholderia dolosa is comparable with Burkholderia cenocepacia and Burkholderia multivorans. *J Cyst Fibros* 6:49-56

65. Conway BA, Venu V, Speert DP. 2002. Biofilm formation and acyl homoserine lactone production in the Burkholderia cepacia complex. *J Bacteriol* 184:5678-85

66. Lefebre M, Valvano M. 2001. In vitro resistance of Burkholderia cepacia complex isolates to reactive oxygen species in relation to catalase and superoxide dismutase production. *Microbiology* 147:97-109

67. Lamothe J, Huynh KK, Grinstein S, Valvano MA. 2007. Intracellular survival of Burkholderia cenocepacia in macrophages is associated with a delay in the maturation of bacteria-containing vacuoles. *Cell Microbiol* 9:40-53

68. Lamothe J, Valvano MA. 2008. Burkholderia cenocepacia-induced delay of acidification and phagolysosomal fusion in cystic fibrosis transmembrane conductance regulator (CFTR)-defective macrophages. *Microbiology* 154:3825-34

69. Lewenza S, Sokol PA. 2001. Regulation of ornibactin biosynthesis and N-acyl-L-homoserine lactone production by CepR in Burkholderia cepacia. *J Bacteriol* 183:2212-8

70. Sokol PA, Darling P, Lewenza S, Corbett CR, Kooi CD. 2000. Identification of a siderophore receptor required for ferric ornibactin uptake in Burkholderia cepacia. *Infect Immun* 68:6554-60

71. Sokol PA, Darling P, Woods DE, Mahenthiralingam E, Kooi C. 1999. Role of ornibactin biosynthesis in the virulence of Burkholderia cepacia: characterization of pvdA, the gene encoding L-ornithine N(5)-oxygenase. *Infect Immun* 67:4443-55

72. Sokol PA, Lewis CJ, Dennis JJ. 1992. Isolation of a novel siderophore from Pseudomonas cepacia. *J Med Microbiol* 36:184-9

73. Glendinning KJ, Parsons YN, Duangsonk K, Hales BA, Humphreys D, et al. 2004. Sequence divergence in type III secretion gene clusters of the Burkholderia cepacia complex. *FEMS Microbiol Lett* 235:229-35

74. Parsons YN, Glendinning KJ, Thornton V, Hales BA, Hart CA, Winstanley C. 2001. A putative type III secretion gene cluster is widely distributed in the Burkholderia cepacia complex but absent from genomovar I. *FEMS Microbiol Lett* 203:103-8

75. Tomich M, Griffith A, Herfst CA, Burns JL, Mohr CD. 2003. Attenuated virulence of a Burkholderia cepacia type III secretion mutant in a murine model of infection. *Infect Immun* 71:1405-15

76. Jones AM, Dodd ME, Govan JR, Barcus V, Doherty CJ, et al. 2004. Burkholderia cenocepacia and Burkholderia multivorans: influence on survival in cystic fibrosis. *Thorax* 59:948-51

77. Kalish LA, Waltz DA, Dovey M, Potter-Bynoe G, McAdam AJ, et al. 2006. Impact of Burkholderia dolosa on lung function and survival in cystic fibrosis. *Am J Respir Crit Care Med* 173:421-5

78. Palleroni NJ, Bradbury JF. 1993. Stenotrophomonas, a new bacterial genus for Xanthomonas maltophilia (Hugh 1980) Swings et al. 1983. *Int J Syst Bacteriol* 43:606-9

79. Brooke JS. 2012. Stenotrophomonas maltophilia: an emerging global opportunistic pathogen. *Clin Microbiol Rev* 25:2-41

80. Denton M, Kerr KG. 1998. Microbiological and clinical aspects of infection associated with Stenotrophomonas maltophilia. *Clin Microbiol Rev* 11:57-80

81. Looney WJ, Narita M, Muhlemann K. 2009. Stenotrophomonas maltophilia: an emerging opportunist human pathogen. *Lancet Infect Dis* 9:312-23

82. Denton M, Todd NJ, Kerr KG, Hawkey PM, Littlewood JM. 1998. Molecular epidemiology of Stenotrophomonas maltophilia isolated from clinical specimens from patients with cystic fibrosis and associated environmental samples. *J Clin Microbiol* 36:1953-8

83. Spencer RC. 1995. The emergence of epidemic, multiple-antibiotic-resistant Stenotrophomonas (Xanthomonas) maltophilia and Burkholderia (Pseudomonas) cepacia. *J Hosp Infect* 30 Suppl:453-64

84. Davin-Regli A, Bollet C, Auffray JP, Saux P, De Micco P. 1996. Use of random amplified polymorphic DNA for epidemiological typing of Stenotrophomonas maltophilia. *J Hosp Infect* 32:39-50

85. Laing FP, Ramotar K, Read RR, Alfieri N, Kureishi A, et al. 1995. Molecular epidemiology of Xanthomonas maltophilia colonization and infection in the hospital environment. *J Clin Microbiol* 33:513-8

86. Gerner-Smidt P, Bruun B, Arpi M, Schmidt J. 1995. Diversity of nosocomial Xanthomonas maltophilia (Stenotrophomonas maltophilia) as determined by ribotyping. *Eur J Clin Microbiol Infect Dis* 14:137-40

87. Morrison AJ, Jr., Hoffmann KK, Wenzel RP. 1986. Associated mortality and clinical characteristics of nosocomial Pseudomonas maltophilia in a university hospital. *J Clin Microbiol* 24:52-5

88. Orr K, Gould FK, Sisson PR, Lightfoot NF, Freeman R, Burdess D. 1991. Rapid inter-strain comparison by pyrolysis mass spectrometry in nosocomial infection with Xanthomonas maltophilia. *J Hosp Infect* 17:187-95

89. Hauser AR, Jain M, Bar-Meir M, McColley SA. 2011. Clinical significance of microbial infection and adaptation in cystic fibrosis. *Clin Microbiol Rev* 24:29-70

90. Ballestero S, Virseda I, Escobar H, Suarez L, Baquero F. 1995. Stenotrophomonas maltophilia in cystic fibrosis patients. *Eur J Clin Microbiol Infect Dis* 14:728-9

91. Denton M, Todd NJ, Littlewood JM. 1996. Role of anti-pseudomonal antibiotics in the emergence of Stenotrophomonas maltophilia in cystic fibrosis patients. *Eur J Clin Microbiol Infect Dis* 15:402-5

92. Valdezate S, Vindel A, Maiz L, Baquero F, Escobar H, Canton R. 2001. Persistence and variability of Stenotrophomonas maltophilia in cystic fibrosis patients, Madrid, 1991-1998. *Emerg Infect Dis* 7:113-22

93. Demko CA, Stern RC, Doershuk CF. 1998. Stenotrophomonas maltophilia in cystic fibrosis: incidence and prevalence. *Pediatr Pulmonol* 25:304-8

94. Coutinho HD, Falcao-Silva VS, Goncalves GF. 2008. Pulmonary bacterial pathogens in cystic fibrosis patients and antibiotic therapy: a tool for the health workers. *Int Arch Med* 1:24

95. Barsky EE, Williams KA, Priebe GP, Sawicki GS. 2017. Incident Stenotrophomonas maltophilia infection and lung function decline in cystic fibrosis. *Pediatr Pulmonol* 52:1276-82

96. Waters V, Atenafu EG, Lu A, Yau Y, Tullis E, Ratjen F. 2013. Chronic Stenotrophomonas maltophilia infection and mortality or lung transplantation in cystic fibrosis patients. *J Cyst Fibros* 12:482-6

97. De Baets F, Schelstraete P, Van Daele S, Haerynck F, Vaneechoutte M. 2007. Achromobacter xylosoxidans in cystic fibrosis: prevalence and clinical relevance. *J Cyst Fibros* 6:75-8

98. Tan K, Conway SP, Brownlee KG, Etherington C, Peckham DG. 2002. Alcaligenes infection in cystic fibrosis. *Pediatr Pulmonol* 34:101-4

99. Firmida MC, Pereira RH, Silva EA, Marques EA, Lopes AJ. 2016. Clinical impact of Achromobacter xylosoxidans colonization/infection in patients with cystic fibrosis. *Braz J Med Biol Res* 49:e5097

100. Hansen CR, Pressler T, Nielsen KG, Jensen PO, Bjarnsholt T, Hoiby N. 2010. Inflammation in Achromobacter xylosoxidans infected cystic fibrosis patients. *J Cyst Fibros* 9:51-8

101. Kim KK, Kim MK, Lim JH, Park HY, Lee ST. 2005. Transfer of Chryseobacterium meningosepticum and Chryseobacterium miricola to Elizabethkingia gen. nov. as Elizabethkingia meningoseptica comb. nov. and Elizabethkingia miricola comb. nov. *Int J Syst Evol Microbiol* 55:1287-93

102. King EO. 1959. Studies on a group of previously unclassified bacteria associated with meningitis in infants. *Am J Clin Pathol* 31:241-7

103. Jean SS, Lee WS, Chen FL, Ou TY, Hsueh PR. 2014. Elizabethkingia meningoseptica: an important emerging pathogen causing healthcare-associated infections. *J Hosp Infect* 86:244-9

104. Bloch KC, Nadarajah R, Jacobs R. 1997. Chryseobacterium meningosepticum: an emerging pathogen among immunocompromised adults. Report of 6 cases and literature review. *Medicine (Baltimore)* 76:30-41

105. Hsu MS, Liao CH, Huang YT, Liu CY, Yang CJ, et al. 2011. Clinical features, antimicrobial susceptibilities, and outcomes of Elizabethkingia meningoseptica (Chryseobacterium meningosepticum) bacteremia at a medical center in Taiwan, 1999-2006. *Eur J Clin Microbiol Infect Dis* 30:1271-8

106. Lin YT, Chiu CH, Chan YJ, Lin ML, Yu KW, et al. 2009. Clinical and microbiological analysis of Elizabethkingia meningoseptica bacteremia in adult patients in Taiwan. *Scand J Infect Dis* 41:628-34

107. Hung PP, Lin YH, Lin CF, Liu MF, Shi ZY. 2008. Chryseobacterium meningosepticum infection: antibiotic susceptibility and risk factors for mortality. *J Microbiol Immunol Infect* 41:137-44

108. Lee SH, Yang RL, Su NY. 2008. Surface irregularity induced-tunneling behavior of the formosan subterranean termite. *Behav Processes* 78:473-6

109. Fraser SL, Jorgensen JH. 1997. Reappraisal of the antimicrobial susceptibilities of Chryseobacterium and Flavobacterium species and methods for reliable susceptibility testing. *Antimicrob Agents Chemother* 41:2738-41

110. Kirby JT, Sader HS, Walsh TR, Jones RN. 2004. Antimicrobial susceptibility and epidemiology of a worldwide collection of Chryseobacterium spp: report from the SENTRY Antimicrobial Surveillance Program (1997-2001). *J Clin Microbiol* 42:445-8

111. Lin PY, Chen HL, Huang CT, Su LH, Chiu CH. 2010. Biofilm production, use of intravascular indwelling catheters and inappropriate antimicrobial therapy as predictors of fatality in Chryseobacterium meningosepticum bacteraemia. *Int J Antimicrob Agents* 36:436-40

112. Lin PY, Chu C, Su LH, Huang CT, Chang WY, Chiu CH. 2004. Clinical and microbiological analysis of bloodstream infections caused by Chryseobacterium meningosepticum in nonneonatal patients. *J Clin Microbiol* 42:3353-5

113. Gungor S, Ozen M, Akinci A, Durmaz R. 2003. A Chryseobacterium meningosepticum outbreak in a neonatal ward. *Infect Control Hosp Epidemiol* 24:613-7

114. Tekerekoglu MS, Durmaz R, Ayan M, Cizmeci Z, Akinci A. 2003. Analysis of an outbreak due to Chryseobacterium meningosepticum in a neonatal intensive care unit. *New Microbiol* 26:57-63

115. Tizer KB, Cervia JS, Dunn AM, Stavola JJ, Noel GJ. 1995. Successful combination vancomycin and rifampin therapy in a newborn with community-acquired Flavobacterium meningosepticum neonatal meningitis. *Pediatr Infect Dis J* 14:916-7

116. Lister PD, Wolter DJ, Hanson ND. 2009. Antibacterial-Resistant Pseudomonas aeruginosa: Clinical Impact and Complex Regulation of Chromosomally Encoded Resistance Mechanisms. *Clinical Microbiology Reviews* 22:582-610

117. Curran CS, Bolig T, Torabi-Parizi P. 2018. Mechanisms and Targeted Therapies for Pseudomonas aeruginosa Lung Infection. *Am J Respir Crit Care Med* 197:708-27

118. Singh PK, Schaefer AL, Parsek MR, Moninger TO, Welsh MJ, Greenberg EP. 2000. Quorum-sensing signals indicate that cystic fibrosis lungs are infected with bacterial biofilms. *Nature* 407:762-4

119. Qi L, Li H, Zhang C, Liang B, Li J, et al. 2016. Relationship between Antibiotic Resistance, Biofilm Formation, and Biofilm-Specific Resistance in Acinetobacter baumannii. *Front Microbiol* 7:483

120. Marier JF, Brazier JL, Lavigne J, Ducharme MP. 2003. Liposomal tobramycin against pulmonary infections of Pseudomonas aeruginosa: a pharmacokinetic and efficacy study following single and multiple intratracheal administrations in rats. *Journal of Antimicrobial Chemotherapy* 52:247-52

121. Blaser J, Stone BB, Groner MC, Zinner SH. 1987. Comparative study with enoxacin and netilmicin in a pharmacodynamic model to determine importance of ratio of antibiotic peak concentration to MIC for bactericidal activity and emergence of resistance. *Antimicrobial Agents and Chemotherapy* 31:1054-60

122. Roberts RR, Hota B, Ahmad I, Scott RD, 2nd, Foster SD, et al. 2009. Hospital and societal costs of antimicrobial-resistant infections in a Chicago teaching hospital: implications for antibiotic stewardship. *Clin Infect Dis* 49:1175-84

123. Ventola CL. 2015. The antibiotic resistance crisis: part 1: causes and threats. *P T* 40:277-83

124. Kapoor G, Saigal S, Elongavan A. 2017. Action and resistance mechanisms of antibiotics: A guide for clinicians. *J Anaesthesiol Clin Pharmacol* 33:300-5

125. Magiorakos AP, Srinivasan A, Carey RB, Carmeli Y, Falagas ME, et al. 2012. Multidrug-resistant, extensively drug-resistant and pandrug-resistant bacteria: an international expert

proposal for interim standard definitions for acquired resistance. *Clin Microbiol Infect* 18:268-81

126. Lansdown AB. 1995. Physiological and toxicological changes in the skin resulting from the action and interaction of metal ions. *Crit Rev Toxicol* 25:397-462

127. Wan AT, Conyers RA, Coombs CJ, Masterton JP. 1991. Determination of silver in blood, urine, and tissues of volunteers and burn patients. *Clin Chem* 37:1683-7

128. Russell AD, Hugo WB. 1994. Antimicrobial activity and action of silver. *Prog Med Chem* 31:351-70

129. Albright CF. 1967. Development of an electrolytic silver-ion generator for water sterilization in Apollo spacecraft water systems. Apollo applications program Final report. *Development of an electrolytic silver-ion generator for water sterilization in Apollo spacecraft water systems. Apollo applications program Final report*

130. Conrad AH, Tramp CR, Long CJ, Wells DC, Paulsen AQ, Conrad GW. 1999. Ag+ alters cell growth, neurite extension, cardiomyocyte beating, and fertilized egg constriction. *Aviat Space Environ Med* 70:1096-105

131. Kascatan-Nebioglu A, Panzner MJ, Tessier CA, Cannon CL, Youngs WJ. 2007. N-Heterocyclic carbene–silver complexes: A new class of antibiotics. *Coordination Chemistry Reviews* 251:884-95

132. Klasen HJ. 2000. Historical review of the use of silver in the treatment of burns. I. Early uses. *Burns* 26:117-30

133. Lansdown AB. 2002. Silver. I: Its antibacterial properties and mechanism of action. *J Wound Care* 11:125-30

134. Moyer CA. 1965. Some effects of 0.5 per cent silver nitrate and high humidity upon the illness associated with large burns. *Journal of the National Medical Association* 57:95-100

135. Fox CL, Jr. 1968. Silver sulfadiazine--a new topical therapy for Pseudomonas in burns. Therapy of Pseudomonas infection in burns. *Arch Surg* 96:184-8

136. Melaiye A, Youngs WJ. 2005. Silver and its application as an antimicrobial agent. *Expert Opinion on Therapeutic Patents* 15:125-30

137. Jung WK, Koo HC, Kim KW, Shin S, Kim SH, Park YH. 2008. Antibacterial Activity and Mechanism of Action of the Silver Ion in Staphylococcus aureus and Escherichia coli. *Applied and Environmental Microbiology* 74:2171-8

138. Lansdown AB, Sampson B, Laupattarakasem P, Vuttivirojana A. 1997. Silver aids healing in the sterile skin wound: experimental studies in the laboratory rat. *Br J Dermatol* 137:728-35

139. Wright JB, Lam K, Hansen D, Burrell RE. 1999. Efficacy of topical silver against fungal burn wound pathogens. *Am J Infect Control* 27:344-50

140. Gupta A, Matsui K, Lo J-F, Silver S. 1999. Molecular basis for resistance to silver cations in Salmonella. *Nat Med* 5:183-8

141. Li XZ, Nikaido H, Williams KE. 1997. Silver-resistant mutants of Escherichia coli display active efflux of Ag+ and are deficient in porins. *Journal of Bacteriology* 179:6127-32

142. Pirnay J-P, De Vos D, Cochez C, Bilocq F, Pirson J, et al. 2003. Molecular Epidemiology of Pseudomonas aeruginosa Colonization in a Burn Unit: Persistence of a Multidrug-Resistant Clone and a Silver Sulfadiazine-Resistant Clone. *Journal of Clinical Microbiology* 41:1192-202

143. Silver S. 2003. Bacterial silver resistance: molecular biology and uses and misuses of silver compounds. *FEMS Microbiology Reviews* 27:341-53

144. Kang YO, Jung JY, Cho D, Kwon OH, Cheon JY, Park WH. 2016. Antimicrobial Silver Chloride Nanoparticles Stabilized with Chitosan Oligomer for the Healing of Burns. *Materials (Basel)* 9

145. Kollef MH, Afessa B, Anzueto A, et al. 2008. Silver-coated endotracheal tubes and incidence of ventilator-associated pneumonia: The nascent randomized trial. *JAMA* 300:805-13

146. Silver S, Phung LT, Silver G. 2006. Silver as biocides in burn and wound dressings and bacterial resistance to silver compounds. *Journal of Industrial Microbiology and Biotechnology* 33:627-34

147. Modak S, Fox CL, Jr. 1985. Synergistic action of silver sulfadiazine and sodium piperacillin on resistant Pseudomonas aeruginosa in vitro and in experimental burn wound infections. *J Trauma* 25:27-31

148. Modak SM, Stanford JW, Bradshaw W, Fox CL, Jr. 1983. Silver sulfadiazine (AgSD) resistant pseudomonas infection in experimental burn wounds. *Panminerva Med* 25:181-8

149. Pirnay JP, De Vos D, Cochez C, Bilocq F, Pirson J, et al. 2003. Molecular epidemiology of Pseudomonas aeruginosa colonization in a burn unit: persistence of a multidrug-resistant clone and a silver sulfadiazine-resistant clone. *J Clin Microbiol* 41:1192-202

150. McHugh GL, Moellering RC, Hopkins CC, Swartz MN. 1975. Salmonella typhimurium resistant to silver nitrate, chloramphenicol, and ampicillin. *Lancet* 1:235-40

151. Gupta A, Jain GK, Raghubir R. 1999. A time course study for the development of an immunocompromised wound model, using hydrocortisone. *J Pharmacol Toxicol Methods* 41:183-7

152. Lockhart SP, Rushworth A, Azmy AA, Raine PA. 1983. Topical silver sulphadiazine: side effects and urinary excretion. *Burns Incl Therm Inj* 10:9-12

153. Maitre S, Michel JL, Varlet F, Cambazard F. 2002. [Priapism in the course of generalized atopic dermatitis]. *Ann Dermatol Venereol* 129:1038-41

154. Hidalgo E, Dominguez C. 1998. Study of cytotoxicity mechanisms of silver nitrate in human dermal fibroblasts. *Toxicol Lett* 98:169-79

155. Fraser JF, Cuttle L, Kempf M, Kimble RM. 2004. Cytotoxicity of topical antimicrobial agents used in burn wounds in Australasia. *ANZ J Surg* 74:139-42

156. Hollinger MA. 1996. Toxicological aspects of topical silver pharmaceuticals. *Crit Rev Toxicol* 26:255-60

157. Hussain S, Anner RM, Anner BM. 1992. Cysteine protects Na,K-ATPase and isolated human lymphocytes from silver toxicity. *Biochem Biophys Res Commun* 189:1444-9

158. Trujillo NA, Oldinski RA, Ma H, Bryers JD, Williams JD, Popat KC. 2012. Antibacterial effects of silver-doped hydroxyapatite thin films sputter deposited on titanium. *Materials Science and Engineering: C* 32:2135-44

159. Zahedi P, Rezaeian I, Ranaei-Siadat S-O, Jafari S-H, Supaphol P. 2010. A review on wound dressings with an emphasis on electrospun nanofibrous polymeric bandages. *Polymers for Advanced Technologies* 21:77-95

160. Gupta A, Maynes M, Silver S. 1998. Effects of halides on plasmid-mediated silver resistance in Escherichia coli. *Appl Environ Microbiol* 64:5042-5

161. Liau SY, Read DC, Pugh WJ, Furr JR, Russell AD. 1997. Interaction of silver nitrate with readily identifiable groups: relationship to the antibacterial action of silver ions. *Lett Appl Microbiol* 25:279-83

162. Swathy JR, Sankar MU, Chaudhary A, Aigal S, Anshup, Pradeep T. 2014. Antimicrobial silver: an unprecedented anion effect. *Sci Rep* 4:7161

163. Lands LC, Milner R, Cantin AM, Manson D, Corey M. 2007. High-dose ibuprofen in cystic fibrosis: Canadian safety and effectiveness trial. *J Pediatr* 151:249-54

164. Byrne ST, Denkin SM, Zhang Y. 2007. Aspirin and ibuprofen enhance pyrazinamide treatment of murine tuberculosis. *The Journal of antimicrobial chemotherapy* 59:313-6

165. Dastidar SG, Annadurai S, Kumar KA, Dutta NK, Chakrabarty AN. 2003. Evaluation of a synergistic combination between the non-antibiotic microbicides diclofenac and trifluoperazine. *Int J Antimicrob Agents* 21:599-601

166. Dutta NK, Mazumdar K, Park JH. 2009. In vitro synergistic effect of gentamicin with the anti-inflammatory agent diclofenac against Listeria monocytogenes. *Lett Appl Microbiol* 48:783-5

167. Konstan MW. 2008. Ibuprofen therapy for cystic fibrosis lung disease: revisited. *Curr Opin Pulm Med* 14:567-73

168. Konstan MW, Byard PJ, Hoppel CL, Davis PB. 1995. Effect of high-dose ibuprofen in patients with cystic fibrosis. *The New England journal of medicine* 332:848-54

169. Pina-Vaz C, Sansonetty F, Rodrigues AG, Martinez-De-Oliveira J, Fonseca AF, Mardh PA. 2000. Antifungal activity of ibuprofen alone and in combination with fluconazole against Candida species. *Journal of medical microbiology* 49:831-40

170. Scott EM, Tariq VN, McCrory RM. 1995. Demonstration of synergy with fluconazole and either ibuprofen, sodium salicylate, or propylparaben against Candida albicans in vitro. *Antimicrobial agents and chemotherapy* 39:2610-4

171. Shah PN, Marshall-Batty KR, Smolen JA, Tagaev JA, Chen Q, et al. 2018. Antimicrobial Activity of Ibuprofen against Cystic Fibrosis-Associated Gram-Negative Pathogens. *Antimicrob Agents Chemother* 62

172. Konstan MW, Krenicky JE, Finney MR, Kirchner HL, Hilliard KA, et al. 2003. Effect of ibuprofen on neutrophil migration in vivo in cystic fibrosis and healthy subjects. *J Pharmacol Exp Ther* 306:1086-91

173. Nichols DP, Konstan MW, Chmiel JF. 2008. Anti-inflammatory therapies for cystic fibrosis-related lung disease. *Clin Rev Allergy Immunol* 35:135-53

174. Kohanski MA, Dwyer DJ, Collins JJ. 2010. How antibiotics kill bacteria: from targets to networks. *Nat Rev Microbiol* 8:423-35

175. Kohanski MA, Dwyer DJ, Wierzbowski J, Cottarel G, Collins JJ. 2008. Mistranslation of membrane proteins and two-component system activation trigger antibiotic-mediated cell death. *Cell* 135:679-90

176. Worthington RJ, Melander C. 2013. Combination approaches to combat multidrug-resistant bacteria. *Trends Biotechnol* 31:177-84

177. Leekha S, Terrell CL, Edson RS. 2011. General principles of antimicrobial therapy. *Mayo Clin Proc* 86:156-67

178. Bailey MM, Berkland CJ. 2009. Nanoparticle formulations in pulmonary drug delivery. *Med Res Rev* 29:196-212

179. Sung JC, Pulliam BL, Edwards DA. 2007. Nanoparticles for drug delivery to the lungs. *Trends Biotechnol* 25:563-70

180. Brain JD. 2007. Inhalation, deposition, and fate of insulin and other therapeutic proteins. *Diabetes Technol Ther* 9 Suppl 1:S4-S15

181. Patton JS, Byron PR. 2007. Inhaling medicines: delivering drugs to the body through the lungs. *Nat Rev Drug Discov* 6:67-74

182. Fels AO, Cohn ZA. 1986. The alveolar macrophage. *J Appl Physiol (1985)* 60:353-69

183. Mandal TK. 2005. Inhaled insulin for diabetes mellitus. *Am J Health Syst Pharm* 62:1359-64

184. Patton JS, Bukar JG, Eldon MA. 2004. Clinical pharmacokinetics and pharmacodynamics of inhaled insulin. *Clin Pharmacokinet* 43:781-801

185. Crompton G. 2006. A brief history of inhaled asthma therapy over the last fifty years. *Prim Care Respir J* 15:326-31

186. Shoyele SA, Slowey A. 2006. Prospects of formulating proteins/peptides as aerosols for pulmonary drug delivery. *Int J Pharm* 314:1-8

187. Henry RR, Mudaliar SR, Howland WC, 3rd, Chu N, Kim D, et al. 2003. Inhaled insulin using the AERx Insulin Diabetes Management System in healthy and asthmatic subjects. *Diabetes Care* 26:764-9

188. Dunbar C, Scheuch G, Sommerer K, DeLong M, Verma A, Batycky R. 2002. In vitro and in vivo dose delivery characteristics of large porous particles for inhalation. *Int J Pharm* 245:179-89

189. Edwards DA, Hanes J, Caponetti G, Hrkach J, Ben-Jebria A, et al. 1997. Large porous particles for pulmonary drug delivery. *Science* 276:1868-71

190. Stone KC, Mercer RR, Gehr P, Stockstill B, Crapo JD. 1992. Allometric relationships of cell numbers and size in the mammalian lung. *Am J Respir Cell Mol Biol* 6:235-43

191. Tiano SL, Dalby RN. 1996. Comparison of a respiratory suspension aerosolized by an air-jet and an ultrasonic nebulizer. *Pharm Dev Technol* 1:261-8

192. Siddiqui MA, Plosker GL. 2005. The Novolizer: a multidose dry powder inhaler. *Treat Respir Med* 4:63-9

193. Brocklebank D, Ram F, Wright J, Barry P, Cates C, et al. 2001. Comparison of the effectiveness of inhaler devices in asthma and chronic obstructive airways disease: a systematic review of the literature. *Health Technol Assess* 5:1-149

194. Pauwels R, Newman S, Borgstrom L. 1997. Airway deposition and airway effects of antiasthma drugs delivered from metered-dose inhalers. *Eur Respir J* 10:2127-38

195. Bunnag C, Fuangtong R, Pothirat C, Punyaratabandhu P. 2007. A comparative study of patients' preferences and sensory perceptions of three forms of inhalers among Thai asthma and COPD patients. *Asian Pac J Allergy Immunol* 25:99-109

196. Kohler D. 2003. Novolizer: the new technology for the management of asthma therapy. *Curr Opin Pulm Med* 9 Suppl 1:S11-6

197. Terzano C. 2008. Dry powder inhalers and the risk of error. *Respiration* 75:14-5

198. Edwards DA, Ben-Jebria A, Langer R. 1998. Recent advances in pulmonary drug delivery using large, porous inhaled particles. *J Appl Physiol (1985)* 85:379-85

199. Farokhzad OC, Langer R. 2006. Nanomedicine: developing smarter therapeutic and diagnostic modalities. *Adv Drug Deliv Rev* 58:1456-9

200. Zhang L, Pornpattananangku D, Hu CM, Huang CM. 2010. Development of nanoparticles for antimicrobial drug delivery. *Curr Med Chem* 17:585-94

201. Bangham AD, Standish MM, Watkins JC. 1965. Diffusion of univalent ions across the lamellae of swollen phospholipids. *J Mol Biol* 13:238-52

202. Langer R, Folkman J. 1976. Polymers for the sustained release of proteins and other macromolecules. *Nature* 263:797-800

203. Wagner V, Dullaart A, Bock AK, Zweck A. 2006. The emerging nanomedicine landscape. *Nat Biotechnol* 24:1211-7

204. Gref R, Minamitake Y, Peracchia MT, Trubetskoy V, Torchilin V, Langer R. 1994. Biodegradable long-circulating polymeric nanospheres. *Science* 263:1600-3

205. Bruchez M, Jr., Moronne M, Gin P, Weiss S, Alivisatos AP. 1998. Semiconductor nanocrystals as fluorescent biological labels. *Science* 281:2013-6

206. Namboodiri MA, Bhat SP, Ramasarma T. 1978. Increase in the activity of phenylalanine-4-hydroxylase on hypobaric stress. *Indian J Biochem Biophys* 15:173-7

207. Cui Y, Wei Q, Park H, Lieber CM. 2001. Nanowire nanosensors for highly sensitive and selective detection of biological and chemical species. *Science* 293:1289-92

208. Zhang L, Gu FX, Chan JM, Wang AZ, Langer RS, Farokhzad OC. 2008. Nanoparticles in medicine: therapeutic applications and developments. *Clin Pharmacol Ther* 83:761-9

209. Davis ME, Chen ZG, Shin DM. 2008. Nanoparticle therapeutics: an emerging treatment modality for cancer. *Nat Rev Drug Discov* 7:771-82

210. Peer D, Karp JM, Hong S, Farokhzad OC, Margalit R, Langer R. 2007. Nanocarriers as an emerging platform for cancer therapy. *Nat Nanotechnol* 2:751-60

211. Pison U, Welte T, Giersig M, Groneberg DA. 2006. Nanomedicine for respiratory diseases. *Eur J Pharmacol* 533:341-50

212. Muller RH, Jacobs C, Kayser O. 2001. Nanosuspensions as particulate drug formulations in therapy. Rationale for development and what we can expect for the future. *Adv Drug Deliv Rev* 47:3-19

213. Bhandari KH, Newa M, Yoon SI, Kim JS, Kim DD, et al. 2007. Evaluation of skin permeation and accumulation profiles of ketorolac fatty esters. *J Pharm Pharm Sci* 10:278-87

214. Sandri G, Poggi P, Bonferoni MC, Rossi S, Ferrari F, Caramella C. 2006. Histological evaluation of buccal penetration enhancement properties of chitosan and trimethyl chitosan. *J Pharm Pharmacol* 58:1327-36

215. Bruesewitz C, Funke A, Kuhland U, Wagner T, Lipp R. 2006. Comparison of permeation enhancing strategies for an oral factor Xa inhibitor using the Caco-2 cell monolayer model. *Eur J Pharm Biopharm* 64:229-37

216. Stella VJ, Nti-Addae KW. 2007. Prodrug strategies to overcome poor water solubility. *Adv Drug Deliv Rev* 59:677-94

217. Winkler J, Hochhaus G, Derendorf H. 2004. How the lung handles drugs: pharmacokinetics and pharmacodynamics of inhaled corticosteroids. *Proc Am Thorac Soc* 1:356-63

218. Marier JF, Brazier JL, Lavigne J, Ducharme MP. 2003. Liposomal tobramycin against pulmonary infections of Pseudomonas aeruginosa: a pharmacokinetic and efficacy study following single and multiple intratracheal administrations in rats. *J Antimicrob Chemother* 52:247-52

219. Patton JS, Fishburn CS, Weers JG. 2004. The lungs as a portal of entry for systemic drug delivery. *Proc Am Thorac Soc* 1:338-44

220. Meers P, Neville M, Malinin V, Scotto AW, Sardaryan G, et al. 2008. Biofilm penetration, triggered release and in vivo activity of inhaled liposomal amikacin in chronic Pseudomonas aeruginosa lung infections. *J Antimicrob Chemother* 61:859-68

221. Chambers E, Mitragotri S. 2004. Prolonged circulation of large polymeric nanoparticles by non-covalent adsorption on erythrocytes. *J Control Release* 100:111-9

222. Davda J, Labhasetwar V. 2002. Characterization of nanoparticle uptake by endothelial cells. *Int J Pharm* 233:51-9

223. Koch AM, Reynolds F, Merkle HP, Weissleder R, Josephson L. 2005. Transport of surface-modified nanoparticles through cell monolayers. *Chembiochem* 6:337-45

224. Suh J, Wirtz D, Hanes J. 2003. Efficient active transport of gene nanocarriers to the cell nucleus. *Proc Natl Acad Sci U S A* 100:3878-82

225. Foster KA, Yazdanian M, Audus KL. 2001. Microparticulate uptake mechanisms of in-vitro cell culture models of the respiratory epithelium. *J Pharm Pharmacol* 53:57-66

226. Suk JS, Lai SK, Wang YY, Ensign LM, Zeitlin PL, et al. 2009. The penetration of fresh undiluted sputum expectorated by cystic fibrosis patients by non-adhesive polymer nanoparticles. *Biomaterials* 30:2591-7

227. Dawson M, Wirtz D, Hanes J. 2003. Enhanced viscoelasticity of human cystic fibrotic sputum correlates with increasing microheterogeneity in particle transport. *J Biol Chem* 278:50393-401

228. Panagi Z, Beletsi A, Evangelatos G, Livaniou E, Ithakissios DS, Avgoustakis K. 2001. Effect of dose on the biodistribution and pharmacokinetics of PLGA and PLGA-mPEG nanoparticles. *Int J Pharm* 221:143-52

229. Dhar S, Gu FX, Langer R, Farokhzad OC, Lippard SJ. 2008. Targeted delivery of cisplatin to prostate cancer cells by aptamer functionalized Pt(IV) prodrug-PLGA-PEG nanoparticles. *Proc Natl Acad Sci U S A* 105:17356-61

230. Sinha VR, Aggarwal A, Trehan A. 2004. Biodegradable PEGylated microspheres and nanospheres. *American Journal of Drug Delivery* 2:157-71

231. Yoo HS, Park TG. 2001. Biodegradable polymeric micelles composed of doxorubicin conjugated PLGA-PEG block copolymer. *J Control Release* 70:63-70

232. Peracchia MT, Fattal E, Desmaele D, Besnard M, Noel JP, et al. 1999. Stealth PEGylated polycyanoacrylate nanoparticles for intravenous administration and splenic targeting. *J Control Release* 60:121-8

233. Gu F, Zhang L, Teply BA, Mann N, Wang A, et al. 2008. Precise engineering of targeted nanoparticles by using self-assembled biointegrated block copolymers. *Proc Natl Acad Sci U S A* 105:2586-91

234. Tang BC, Dawson M, Lai SK, Wang YY, Suk JS, et al. 2009. Biodegradable polymer nanoparticles that rapidly penetrate the human mucus barrier. *Proc Natl Acad Sci U S A* 106:19268-73

235. Hostynek JJ, Hinz RS, Lorence CR, Price M, Guy RH. 1993. Metals and the skin. *Crit Rev Toxicol* 23:171-235

236. Klasen HJ. 2000. A historical review of the use of silver in the treatment of burns. II. Renewed interest for silver. *Burns* 26:131-8

237. Silver S. 2003. Bacterial silver resistance: molecular biology and uses and misuses of silver compounds. *FEMS Microbiol Rev* 27:341-53

238. Bridges K, Kidson A, Lowbury EJ, Wilkins MD. 1979. Gentamicin- and silver-resistant pseudomonas in a burns unit. *Br Med J* 1:446-9

239. Gupta A, Matsui K, Lo JF, Silver S. 1999. Molecular basis for resistance to silver cations in Salmonella. *Nat Med* 5:183-8

240. Starodub ME, Trevors JT. 1990. Silver accumulation and resistance in Escherichia coli R1. *J Inorg Biochem* 39:317-25

241. Starodub ME, Trevors JT. 1990. Mobilization of Escherichia coli R1 silver-resistance plasmid pJT1 by Tn5-Mob into Escherichia coli C600. *Biol Met* 3:24-7

242. Lansdown A, Williams A. 2007. Bacterial resistance to silver-based antibiotics. *Nurs Times* 103:48-9

243. Cannon CL, Hogue LA, Vajravelu RK, Capps GH, Ibricevic A, et al. 2009. In Vitro and Murine Efficacy and Toxicity Studies of Nebulized SCC1, a Methylated Caffeine-Silver(I) Complex, for Treatment of Pulmonary Infections. *Antimicrobial Agents and Chemotherapy* 53:3285-93

244. Hindi KM, Siciliano TJ, Durmus S, Panzner MJ, Medvetz DA, et al. 2008. Synthesis, Stability, and Antimicrobial Studies of Electronically Tuned Silver Acetate N-Heterocyclic Carbenes. *Journal of Medicinal Chemistry* 51:1577-83

245. Kascatan-Nebioglu A, Melaiye A, Hindi K, Durmus S, Panzner MJ, et al. 2006. Synthesis from Caffeine of a Mixed N-Heterocyclic Carbene−Silver Acetate Complex Active against Resistant Respiratory Pathogens. *Journal of Medicinal Chemistry* 49:6811-8

246. Hindi KM, Panzner MJ, Tessier CA, Cannon CL, Youngs WJ. 2009. The medicinal applications of imidazolium carbene-metal complexes. *Chem Rev* 109:3859-84

247. Kascatan-Nebioglu A, Panzner MJ, Tessier CA, Cannon CL, Youngs WJ. 2007. N-Heterocyclic carbene-silver complexes: a new class of antibiotics. *Coord Chem Rev* 251:884-95

248. Mercs L, Albrecht M. 2010. Beyond catalysis: N-heterocyclic carbene complexes as components for medicinal, luminescent, and functional materials applications. *Chem Soc Rev* 39:1903-12

249. Teyssot ML, Jarrousse AS, Manin M, Chevry A, Roche S, et al. 2009. Metal-NHC complexes: a survey of anti-cancer properties. *Dalton Trans*:6894-902

250. Hindi KM, Siciliano TJ, Durmus S, Panzner MJ, Medvetz DA, et al. 2008. Synthesis, stability, and antimicrobial studies of electronically tuned silver acetate N-heterocyclic carbenes. *J Med Chem* 51:1577-83

251. Leid JG, Ditto AJ, Knapp A, Shah PN, Wright BD, et al. 2012. In vitro antimicrobial studies of silver carbene complexes: activity of free and nanoparticle carbene formulations against clinical isolates of pathogenic bacteria. *J Antimicrob Chemother* 67:138-48

252. Panzner MJ, Deeraksa A, Smith A, Wright BD, Hindi KM, et al. 2009. Synthesis and in vitro Efficacy Studies of Silver Carbene Complexes on Biosafety Level 3 Bacteria. *Eur J Inorg Chem* 2009:1739-45

253. Patil S, Deally A, Gleeson B, Muller-Bunz H, Paradisi F, Tacke M. 2011. Novel benzyl-substituted N-heterocyclic carbene-silver acetate complexes: synthesis, cytotoxicity and antibacterial studies. *Metallomics* 3:74-88

254. Hindi KM, Ditto AJ, Panzner MJ, Medvetz DA, Han DS, et al. 2009. The antimicrobial efficacy of sustained release silver-carbene complex-loaded L-tyrosine polyphosphate nanoparticles: characterization, in vitro and in vivo studies. *Biomaterials* 30:3771-9

255. Kascatan-Nebioglu A, Melaiye A, Hindi K, Durmus S, Panzner MJ, et al. 2006. Synthesis from caffeine of a mixed N-heterocyclic carbene-silver acetate complex active against resistant respiratory pathogens. *J Med Chem* 49:6811-8

256. Panzner MJ, Hindi KM, Wright BD, Taylor JB, Han DS, et al. 2009. A theobromine derived silver N-heterocyclic carbene: synthesis, characterization, and antimicrobial efficacy studies on cystic fibrosis relevant pathogens. *Dalton Trans*:7308-13

257. Lands LC, Stanojevic S. 2007. Oral non-steroidal anti-inflammatory drug therapy for lung disease in cystic fibrosis. *Cochrane Database of Systematic Reviews*

258. Shah PN, Shah KN, Smolen JA, Tagaev JA, Torrealba J, et al. 2018. A novel in vitro metric predicts in vivo efficacy of inhaled silver-based antimicrobials in a murine Pseudomonas aeruginosa pneumonia model. *Sci Rep* 8:6376

259. del Prado G, Martinez-Marin C, Huelves L, Gracia M, Rodriguez-Cerrato V, et al. 2006. Impact of ibuprofen therapy in the outcome of experimental pneumococcal acute otitis media treated with amoxicillin or erythromycin. *Pediatr Res* 60:555-9

260. Kunkel SL, Standiford T, Kasahara K, Strieter RM. 1991. Interleukin-8 (IL-8): the major neutrophil chemotactic factor in the lung. *Exp Lung Res* 17:17-23

261. Elliott CL, Allport VC, Loudon JA, Wu GD, Bennett PR. 2001. Nuclear factor-kappa B is essential for up-regulation of interleukin-8 expression in human amnion and cervical epithelial cells. *Mol Hum Reprod* 7:787-90

262. Tabary O, Escotte S, Couetil JP, Hubert D, Dusser D, et al. 1999. Genistein inhibits constitutive and inducible NFkappaB activation and decreases IL-8 production by human cystic fibrosis bronchial gland cells. *Am J Pathol* 155:473-81

263. Konstan MW, Vargo KM, Davis PB. 1990. Ibuprofen attenuates the inflammatory response to Pseudomonas aeruginosa in a rat model of chronic pulmonary infection. Implications for antiinflammatory therapy in cystic fibrosis. *The American review of respiratory disease* 141:186-92

264. Scheuren N, Bang H, Munster T, Brune K, Pahl A. 1998. Modulation of transcription factor NF-kappaB by enantiomers of the nonsteroidal drug ibuprofen. *Br J Pharmacol* 123:645-52

265. Ibricevic A, Brody SL, Youngs WJ, Cannon CL. 2010. ATP7B detoxifies silver in ciliated airway epithelial cells. *Toxicol Appl Pharmacol* 243:315-22

266. Cropp GJ. 1996. Effectiveness of bronchodilators in cystic fibrosis. *Am J Med* 100:19S-29S

267. Tilley SL. 2011. Methylxanthines in asthma. *Handb Exp Pharmacol*:439-56

268. Dalabih A, Harris ZL, Bondi SA, Arnold DH. 2012. Contemporary aminophylline use for status asthmaticus in pediatric ICUs. *Chest* 141:1122-3

269. Ford PA, Durham AL, Russell RE, Gordon F, Adcock IM, Barnes PJ. 2010. Treatment effects of low-dose theophylline combined with an inhaled corticosteroid in COPD. *Chest* 137:1338-44

270. Schmidt B, Roberts RS, Davis P, Doyle LW, Barrington KJ, et al. 2006. Caffeine therapy for apnea of prematurity. *N Engl J Med* 354:2112-21

271. Weichelt U, Cay R, Schmitz T, Strauss E, Sifringer M, et al. 2013. Prevention of hyperoxia-mediated pulmonary inflammation in neonatal rats by caffeine. *Eur Respir J* 41:966-73

272. Wang Y, Yang X, Zheng X, Li J, Ye C, Song X. 2010. Theacrine, a purine alkaloid with anti-inflammatory and analgesic activities. *Fitoterapia* 81:627-31

273. Caster JM, Patel AN, Zhang T, Wang A. 2017. Investigational nanomedicines in 2016: a review of nanotherapeutics currently undergoing clinical trials. *Wiley Interdiscip Rev Nanomed Nanobiotechnol* 9

274. Kamaly N, Xiao Z, Valencia PM, Radovic-Moreno AF, Farokhzad OC. 2012. Targeted polymeric therapeutic nanoparticles: design, development and clinical translation. *Chem Soc Rev* 41:2971-3010

275. Lakshminarayanan R, Ye E, Young DJ, Li Z, Loh XJ. 2018. Recent Advances in the Development of Antimicrobial Nanoparticles for Combating Resistant Pathogens. *Adv Healthc Mater*:e1701400

276. Shah PN, Lin LY, Smolen JA, Tagaev JA, Gunsten SP, et al. 2013. Synthesis, Characterization, and In Vivo Efficacy of Shell Cross-Linked Nanoparticle Formulations Carrying Silver Antimicrobials as Aerosolized Therapeutics. *ACS Nano* 7:4977-87

277. Zhang F, Smolen JA, Zhang S, Li R, Shah PN, et al. 2015. Degradable polyphosphoester-based silver-loaded nanoparticles as therapeutics for bacterial lung infections. *Nanoscale* 7:2265-70

278. Li Y, Hindi K, Watts KM, Taylor JB, Zhang K, et al. 2010. Shell crosslinked nanoparticles carrying silver antimicrobials as therapeutics. *Chemical Communications* 46:121-3

279. Thurmond KB, Kowalewski T, Wooley KL. 1996. Water-Soluble Knedel-like Structures: The Preparation of Shell-Cross-Linked Small Particles. *Journal of the American Chemical Society* 118:7239-40

280. Qi K, Ma Q, Remsen E, Clark CG, Wooley K. 2004. Determination of the Bioavailability of Biotin Conjugated onto Shell Cross-Linked (SCK) Nanoparticles. *Journal of the American Chemical Society* 126:6599-607

281. Thurmond KB, Kowalewski T, Wooley K. 1997. Shell Cross-Linked Knedels: A Synthetic Study of the Factors Affecting the Dimensions and Properties of Amphiphilic Core-Shell Nanospheres. *Journal of the American Chemical Society* 119:6656-65

282. Elsabahy M, Wooley K. 2012. Design of polymeric nanoparticles for biomedical delivery applications. *Chemical Society reviews* 41:2545

283. Niemirowicz K, Piktel E, Wilczewska AZ, Markiewicz KH, Durnas B, et al. 2016. Core-shell magnetic nanoparticles display synergistic antibacterial effects against Pseudomonas aeruginosa and Staphylococcus aureus when combined with cathelicidin LL-37 or selected ceragenins. *Int J Nanomedicine* 11:5443-55

284. Habash MB, Goodyear MC, Park AJ, Surette MD, Vis EC, et al. 2017. Potentiation of Tobramycin by Silver Nanoparticles against Pseudomonas aeruginosa Biofilms. *Antimicrob Agents Chemother* 61

285. Kelly RG, Kanegis LA. 1967. Metabolism and tissue distribution of radioisotopically labeled minocycline. *Toxicology and Applied Pharmacology* 11:171-83

286. Nelis HJ, De Leenheer AP. 1982. Metabolism of minocycline in humans. *Drug Metabolism and Disposition* 10:142-6

287. Bradford PA, Jones CH. 2012. Tetracyclines. In *Antibiotic Discovery and Development*, ed. TJ Dougherty, MJ Pucci:147-79. Boston, MA: Springer US. Number of 147-79 pp.

288. Brodersen DE, Clemons WM, Jr., Carter AP, Morgan-Warren RJ, Wimberly BT, Ramakrishnan V. The Structural Basis for the Action of the Antibiotics Tetracycline, Pactamycin, and Hygromycin B on the 30S Ribosomal Subunit. *Cell* 103:1143-54

289. Jonas M. 1982. Minocycline. *Therapeutic drug monitoring* 4:115

290. Colton B, McConeghy K, Schreckenberger P, Danziger L. 2016. I.V. minocycline revisited for infections caused by multidrug-resistant organisms. *American journal of health-system pharmacy* 73:279-85

291. Zhang S, Li A, Zou J, Lin LY, Wooley KL. 2012. Facile Synthesis of Clickable, Water-Soluble, and Degradable Polyphosphoesters. *ACS Macro Letters* 1:328-33

292. Zhang S, Zou J, Zhang F, Elsabahy M, Felder SE, et al. 2012. Rapid and Versatile Construction of Diverse and Functional Nanostructures Derived from a Polyphosphoester-Based Biomimetic Block Copolymer System. *Journal of the American Chemical Society* 134:18467-74

293. Saiman L. 2007. Clinical utility of synergy testing for multidrug-resistant Pseudomonas aeruginosa isolated from patients with cystic fibrosis: 'the motion for'. *Paediatr Respir Rev* 8:249-55

294. Kascatan Nebioglu A, Melaiye A, Hindi K, Durmus S, Panzner M, et al. 2006. Synthesis from Caffeine of a MixedN-Heterocyclic Carbene−Silver Acetate Complex Active against Resistant Respiratory Pathogens. *Journal of medicinal chemistry* 49:6811-8

295. Baugher AH, Goetz JM, McDowell LM, Huang H, Wooley KL, Schaefer J. 1998. Location of Fluorotryptophan Sequestered in an Amphiphilic Nanoparticle by Rotational-Echo Double-Resonance NMR. *Biophysical Journal* 75:2574-6

296. Kao H-M, O'Connor RD, Mehta AK, Huang H, Poliks B, et al. 2001. Location of Cholic Acid Sequestered by Core−Shell Nanoparticles Using REDOR NMR. *Macromolecules* 34:544-6

297. Lim YH, Tiemann KM, Heo GS, Wagers PO, Rezenom YH, et al. 2015. Preparation and in Vitro Antimicrobial Activity of Silver-Bearing Degradable Polymeric Nanoparticles of Polyphosphoester-block-Poly(l-lactide). *ACS Nano* 9:1995-2008

298. Fujita J, Negayama K, Takigawa K, Yamagishi Y, Kubo A, et al. 1992. Activity of antibiotics against resistant Pseudomonas aeruginosa. *Journal of Antimicrobial Chemotherapy* 29:539-46

299. Heggie W. 2010. Topical formulation containing a tetracycline and a method of treating skin infections using the same. Google Patents

300. Naidong W, Hua S, Roets E, Hoogmartens J. 1995. Assay and purity control of minocycline by thin-layer chromatography using UV and fluorescence densitometry — a comparison with liquid chromatography. *Journal of pharmaceutical and biomedical analysis* 13:905-10

301. Sheth NV, Valorose JJ, Ellway KA, Ganesan MG, Mooney KG, Johnson JB. 2002. Pulsatile once-a-day delivery systems for minocycline. Google Patents

302. Nguyen F, Starosta AL, Arenz S, Sohmen D, Donhofer A, Wilson DN. 2014. Tetracycline antibiotics and resistance mechanisms. *Biol Chem* 395:559-75

303. Olson MW, Ruzin A, Feyfant E, Rush TS, 3rd, O'Connell J, Bradford PA. 2006. Functional, biophysical, and structural bases for antibacterial activity of tigecycline. *Antimicrob Agents Chemother* 50:2156-66

304. Feng QL, Wu J, Chen GQ, Cui FZ, Kim TN, Kim JO. 2000. A mechanistic study of the antibacterial effect of silver ions on Escherichia coli and Staphylococcus aureus. *Journal of Biomedical Materials Research* 52:662-8

305. Saivin S, Houin G. 1988. Clinical Pharmacokinetics of Doxycycline and Minocycline. *Clinical Pharmacokinetics* 15:355-66

306. Welling PG, Shaw WR, Uman SJ, Tse FLS, Craig WA. 1975. Pharmacokinetics of Minocycline in Renal Failure. *Antimicrobial Agents and Chemotherapy* 8:532-7

307. Banasiuk R FJ, Krychowiak M, Matuszewska M, Kawiak A, Ziabka M, Lendzion-Bielun Z, Narajczyk M, Krolicka A. 2016. Synthesis of antimicrobial silver nanoparticles through a photomediated reaction in an aqueous environment. *International Journal of Nanomedicine* 2016:11:10

308. Klainer AS, Russell RR. 1974. Effect of the inhibition of protein synthesis on the Escherichia coli cell envelope. *Antimicrob Agents Chemother* 6:216-24

309. Peach KC, Bray WM, Winslow D, Linington PF, Linington RG. 2013. Mechanism of action-based classification of antibiotics using high-content bacterial image analysis. *Mol Biosyst* 9:1837-48

310. Rodgers FG, Tzianabos AO, Elliott TS. 1990. The effect of antibiotics that inhibit cell-wall, protein, and DNA synthesis on the growth and morphology of Legionella pneumophila. *J Med Microbiol* 31:37-44

311. Smith K, Leyden J. 2005. Safety of doxycycline and minocycline: A systematic review. *Clinical Therapeutics* 27:1329-42

312. Lim YH, Tiemann KM, Hunstad DA, Elsabahy M, Wooley KL. 2016. Polymeric nanoparticles in development for treatment of pulmonary infectious diseases. *Wiley Interdisciplinary Reviews: Nanomedicine and Nanobiotechnology* 8:842-71

313. Ensign LM, Schneider C, Suk JS, Cone R, Hanes J. 2012. Mucus Penetrating Nanoparticles: Biophysical Tool and Method of Drug and Gene Delivery. *Advanced Materials* 24:3887-94

314. Günday Türeli N, Türeli AE, Schneider M. 2016. Optimization of ciprofloxacin complex loaded PLGA nanoparticles for pulmonary treatment of cystic fibrosis infections: Design of experiments approach. *International Journal of Pharmaceutics* 515:343-51

315. Chmiel JF, Berger M, Konstan MW. 2002. The role of inflammation in the pathophysiology of CF lung disease. *Clin Rev Allergy Immunol* 23:5-27

316. Dakin CJ, Numa AH, Wang H, Morton JR, Vertzyas CC, Henry RL. 2002. Inflammation, infection, and pulmonary function in infants and young children with cystic fibrosis. *Am J Respir Crit Care Med* 165:904-10

317. Chmiel JF, Konstan MW. 2007. Inflammation and anti-inflammatory therapies for cystic fibrosis. *Clin Chest Med* 28:331-46

318. Dauletbaev N, Lam J, Eklove D, Iskandar M, Lands LC. 2010. Ibuprofen modulates NF-kB activity but not IL-8 production in cystic fibrosis respiratory epithelial cells. *Respiration* 79:234-42

319. Cheng K, Ashby D, Smyth R. 2011. Oral steroids for long-term use in cystic fibrosis. *Cochrane Database of Systematic Reviews*

320. Lai HC, FitzSimmons SC, Allen DB, Kosorok MR, Rosenstein BJ, et al. 2000. Risk of persistent growth impairment after alternate-day prednisone treatment in children with cystic fibrosis. *The New England journal of medicine* 342:851-9

321. Lands LC, Stanojevic S. 2013. Oral non-steroidal anti-inflammatory drug therapy for lung disease in cystic fibrosis. *Cochrane Database Syst Rev* 6:CD001505

322. Saiman L, Marshall BC, Mayer-Hamblett N, Burns JL, Quittner AL, et al. 2003. Azithromycin in patients with cystic fibrosis chronically infected with Pseudomonas aeruginosa: a randomized controlled trial. *JAMA* 290:1749-56

323. Rinaldo JE, Pennock B. 1986. Effects of ibuprofen on endotoxin-induced alveolitis: biphasic dose response and dissociation between inflammation and hypoxemia. *The American journal of the medical sciences* 291:29-38

324. Sordelli DO, Cerquetti MC, el-Tawil G, Ramwell PW, Hooke AM, Bellanti JA. 1985. Ibuprofen modifies the inflammatory response of the murine lung to Pseudomonas aeruginosa. *European journal of respiratory diseases* 67:118-27

325. Konstan MW, Schluchter MD, Xue W, Davis PB. 2007. Clinical use of Ibuprofen is associated with slower FEV1 decline in children with cystic fibrosis. *American journal of respiratory and critical care medicine* 176:1084-9

326. Konstan MW, VanDevanter DR, Sawicki GS, Pasta DJ, Foreman AJ, et al. 2018. Association of High-Dose Ibuprofen Use, Lung Function Decline, and Long-Term Survival in Children with Cystic Fibrosis. *Ann Am Thorac Soc* 15:485-93

327. Chan EWL, Yee ZY, Raja I, Yap JKY. 2017. Synergistic effect of non-steroidal anti-inflammatory drugs (NSAIDs) on antibacterial activity of cefuroxime and chloramphenicol against methicillin-resistant Staphylococcus aureus. *J Glob Antimicrob Resist* 10:70-4

328. van Heeckeren AM, Tscheikuna J, Walenga RW, Konstan MW, Davis PB, et al. 2000. Effect of Pseudomonas infection on weight loss, lung mechanics, and cytokines in mice. *Am J Respir Crit Care Med* 161:271-9